EFFECTS OF BIOREACTOR OPERATION PARAMETERS ON INTRACELLULAR REACTION RATE DISTRIBUTION IN BETA-LACTAMASE PRODUCTION BY *Bacillus* SPECIES

A THESIS SUBMITTED TO
THE GRADUATE SCHOOL OF NATURAL AND APPLIED SCIENCES
OF
THE MIDDLE EAST TECHNICAL UNIVERSITY

BY

MÜGE ARİFOĞLU

IN PARTIAL FULFILLMENT OF THE REQUIREMENTS
FOR
THE DEGREE OF MASTER OF SCIENCE
IN
CHEMICAL ENGINEERING

AUGUST 2004

Approval of the Graduate School of Natural and Applied Sciences

Prof. Dr. Canan Özgen
Director

I certify that this thesis satisfies all the requirements as a thesis for the degree of Master of Science.

Prof. Dr. Timur Doğu
Head of Department

This is to certify that we have read this thesis and that in our opinion it is fully adequate, in scope and quality, as a thesis and for the degree of Master of Science.

Prof. Dr. Güzide Çalık
Co-Supervisor

Assoc. Prof. Dr. Pınar Çalık
Supervisor

Examining Committee Members

Prof. Dr. Türker Gürkan	(METU, CHE)	
Assoc. Prof. Dr. Pınar Çalık	(METU, CHE)	
Prof. Dr. Güzide Çalık	(Ankara Univ., CHE)	
Prof. Dr. H. Tunçer Özdamar	(Ankara Univ., CHE)	
Assoc. Prof. Dr. Nihal Aydoğan	(Hacettepe Univ., CHE)	

I hereby declare that all information in this document has been obtained and presented in accordance with academic rules and ethical conduct. I also declare that, as required by these rules and conduct, I have fully cited and referenced all material and results that are not original to this work.

Name, Last name : Müge Arifoğlu

Signature :

ABSTRACT

EFFECTS OF BIOREACTOR OPERATION PARAMETERS ON INTRACELLULAR REACTION RATE DISTRIBUTION IN BETA-LACTAMASE PRODUCTION BY *Bacillus* SPECIES

Arifoğlu, Müge
M.S., Department of Chemical Engineering
Supervisor: Assoc. Dr. Pınar Çalık
Co-Supervisor: Prof. Dr. Güzide Çalık

August 2004, 120 pages

In this study, the effects of oxygen transfer (OT) on β-lactamase production and on intracellular reaction rates were investigated with *Bacillus licheniformis* ATCC 2597. In order to clarify the oxygen transfer effects on the production of β-lactamase, firstly a glucose based defined medium was designed and using this medium, the effects of bioreactor operation parameters, i.e., pH and temperature, on β-lactamase activity and cell formation were investigated in laboratory scale batch-bioreactors using shake bioreactors having V=33 ml working volumes. Among the investigated bioprocess conditions, the highest β-lactamase activity was obtained as A=115 U cm^{-3}, in the medium with 7.0 kg m^{-3} glucose, 7.1 kg m^{-3} $(NH_4)_2HPO_4$ and the salt solution, at pH_0=7.5, T=37°C, N=200 min^{-1}. At the optimum conditions found in laboratory scale the effects of OT on cell generation, substrate consumption, product (β-lactamase) and by-products formations were investigated at three different air inlet (Q_0/ V_R = 0.2, 0.5 and 1 vvm) and at three agitation rates (N=250, 500, 750 min^{-1}) in V = 3.0 dm^3 batch bioreactors consisting of temperature, pH, foam, stirring rate and dissolved oxygen controls. Along with the fermentation, cell, substrate and by-product concentrations, β-lactamase activity, yield coefficients, specific rates,

oxygen uptake rates and the liquid phase mass transfer coefficient values were determined. The highest β-lactamase activity was obtained at 0.5 vvm 500 min^{-1} and at 0.2 vvm 500 min^{-1} conditions as ca. A=90 U cm^{-3} while the highest cell concentration was obtained as C_x=0.67 kg m^{-3} at 0.5 vvm 750 min^{-1} and at 0.2 vvm 750 min^{-1} conditions. K_La, increased with the increase in the agitation and aeration rates and its values varied between 0.007-0.044 s^{-1} and oxygen uptake rate varied between 0.4-1.6 mol m^{-3} s^{-1}. Finally, the influence of OT conditions on the intracellular reaction rates was investigated using metabolic flux analysis to evaluate the effects of oxygen on the metabolism.

Keywords: β-lactamase, production, *Bacillus*, oxygen transfer, metabolic flux analysis

ÖZ

Bacillus TÜRLERİ İLE BETA-LAKTAMAZ ÜRETİMİNDE BİYOREAKTÖR İŞLETİM PARAMETRELERİNİN HÜCRE İÇİ TEPKİME HIZ DAĞILIMLARINA ETKİLERİ

Arifoğlu, Müge
Yüksek Lisans, Kimya Mühendisliği Bölümü
Tez Yöneticisi: Doç. Dr. Pınar Çalık
Ortak Tez Yöneticisi: Prof. Dr. Güzide Çalık

Ağustos 2004, 120 sayfa

Bu çalışmada, *Bacillus licheniformis* ATCC 25972 ile oksijen aktarımının β-laktamaz üretimine ve hücreiçi tepkime hızlarına etkisi araştırılmıştır. Bu amaçla önce glukoz temelli tanımlanmış ortam tasarımı yapılmış ve tasarlanan bu üretim ortamı kullanılarak biyoproses işletim parametrelerinden pH ve sıcaklığın β-laktamaz üretimine ve hücre oluşumuna etkileri, laboratuvar ölçekli, V=33 ml çalışma hacımlı kesikli biyoreaktörler kullanılarak araştırılmıştır. En yüksek aktivite, 7.0 kg m^{-3} glukoz, 7.1 kg m^{-3} $(NH_4)_2HPO_4$, ve tuz çözeltisini içeren ortamda, pH_0=7.5, T=37°C, N=200 dk^{-1} koşullarında, A=115 U cm^{-3} olarak bulunmuştur. Laboratuvar ölçekte bulunan en uygun koşullar kullanılarak, oksijen aktarımının substrat tüketimine, mikroorganizma derişimine, ürün (β-laktamaz) ve yan-ürün oluşumuna etkileri üç farklı hava giriş (Q_0/ V_R = 0.2, 0.5 and 1 vvm) ve karıştırma hızlarında (N=250, 500, 750 dk^{-1}) V= 3.0 dm^3 hacımlı, sıcaklık, pH, köpük, karıştırma ve çözünmüş oksijen derişimi kontrollü kesikli biyoreaktörde araştırılmıştır. Proses sürecince, farklı oksijen aktarım koşullarında hücre, substrat ve yan-ürün derişimleri, β-laktamaz aktivitesi, verim katsayıları, spesifik hızlar, oksijen tüketim hızları ve sıvı faz kütle aktarım katsayıları (K_La) bulunmuştur. En yüksek enzim aktivitesine A=90 U cm^{-3} olarak 0.5 vvm, 500 dk^{-1} ve 0.2 vvm 500 dk^{-1} koşullarında ulaşılırken, en yüksek hücre derişimine

C_x=0.67 kg m^{-3} olarak 0.5 vvm 750 dk^{-1} ve 0.2 vvm 750 dk^{-1} koşullarında ulaşılmıştır. K_La, havalandırma ve karıştırma hızları artıkça artmış ve değeri 0.007-0.044 s^{-1} aralığında değişmiştir. Oksijen tüketim hızı ise 0.4-1.6 mol m^{-3} s^{-1} aralığında değişmiştir. Son olarak *B.licheniformis* ile β-laktamaz üretiminde oksijen aktarım koşullarının hücreiçi tepkime hızlarına etkisi metabolik akı analizi ile bulunmuştur.

Anahtar Kelimeler: β-laktamaz, üretim, *Bacillus*, oksijen aktarımı, metabolik akı analizi

To My Family

ACKNOWLEDGEMENTS

I wish to express my sincere gratitude to my supervisor Assoc. Prof. Dr. Pınar Çalık and my co-supervisor Prof. Dr. Güzide Çalık for their guidance, advice, criticism, encouragements and insight throughout the research.

I would also like to express my appreciation to Prof. H. Tunçer Özdamar for giving me every opportunity to use the laboratories in Ankara University. And I wish to thank all the members of his research group for their guidance, patience and friendship during the experiments I performed in Ankara University.

I also wish to give my special thanks to all my friends in our research group in Industrial Biotechnology Laboratory. I am especially grateful to Pınar Yılgör, Pınar Kocabaş, İlkin Ece Telli, Peruze Ayhan, Eda Çelik and Ceren Oktar for their valuable help, cooperation and friendship.

Financial Support provided by TUBITAK through project MISAG-258 and METU-Research Fund are gratefully acknowledged.

Finally, I would like to express my deepest thanks to my family for supporting, encouraging and loving me all through my life.

TABLE OF CONTENTS

LIST OF TABLES

TABLE

LIST OF FIGURES

FIGURE

NOMENCLATURE

a	The gas liquid interfacial area per unit liquid volume, $m^2\ m^{-3}$
A	Beta-lactamase activity, U cm^{-3}
A_λ	Absorbance
Ae	Aeration number ($=Q / ND_I^3$)
c (t)	Metabolite accumulation vector
c_1 (t)	Extracellular metabolite accumulation vectors
c_2 (t)	Intracellular metabolite accumulation vectors
C_{AA}	Amino acid concentration, kg m^{-3}
C_B	β-lactamase concentration, kg m^{-3}
C_C	Citric Acid concentration, kg m^{-3}
C_G	Glucose concentration, kg m^{-3}
C_G^0	Initial glucose concentration, kg m^{-3}
C_N	Nitrogen concentration, kg m^{-3}
C_N^0	Initial nitrogen concentration, kg m^{-3}
C_{OA}	Organic acid concentration, kg m^{-3}
C_O	Dissolved oxygen concentration, mol m^{-3}; kg m^{-3}
Co_0	Initial dissolved oxygen concentration, mol m^{-3}; kg m^{-3}
C_O^*	Oxygen saturation concentration, mol m^{-3}; kg m^{-3}
C_{SAP}	Serine alkaline protease concentration, kg m^{-3}
C_X	Cell concentration, kg dry cell m^{-3}
Da	Damköhler number ($=OD / OTR_{max}$; Maximum possible oxygen utilization rate per maximum mass transfer rate)
D	Bioreactor diameter, m
D_I	Impeller diameter, m
E	Enhancement factor ($=K_La / K_La_o$); mass transfer coefficient with chemical reaction per physical mass transfer coefficient
Fr	Froude number, ($=N^2D_I/g$)
K_La_0	Physical overall liquid phase mass transfer coefficient; s^{-1}
K_La	Overall liquid phase mass transfer coefficient; s^{-1}

N	Agitation or shaking rate, min^{-1}
N_p	Power number
P	Power input in gas-free stirred liquid, W
P_G	Power input in aerated stirred liquid, W
pH_0	Initial pH
Qo	Volumetric air feed rate, $m^3\ min^{-1}$
q_o	Specific oxygen uptake rate, kg kg $^{-1}$ DW h^{-1}
q_s	Specific substrate consumption rate, kg kg $^{-1}$ DW h^{-1}
r	Volumetric rate of reaction, mol $m^{-3}\ s^{-1}$
r(t)	Vector of reaction fluxes
Re	Reynolds number, ($=ND_I^2\rho/\mu$)
r_0	Oxygen uptake rate, mol $m^{-3}\ s^{-1}$; kg $m^{-3}\ h^{-1}$
r_P	Product formation rate, kg $m^{-3}\ h^{-1}$
r_S	Substrate consumption rate, kg $m^{-3}\ h^{-1}$
r_X	Rate of cell growth, kg $m^{-3}\ h^{-1}$
t	Bioreactor cultivation time, h
T	Bioreaction medium temperature, °C
T_{AA}	Total amino acid concentration, kg m^{-3}
T_{OA}	Total organic acid concentration, kg m^{-3}
U	One unit of an enzyme
V	Volume of the bioreactor, m^3
V_R	Volume of the bioreaction medium, m^3
V_S	Superficial gas velocity, m s^{-1}
$Y_{X/S}$	Yield of cell on substrate, kg kg^{-1}
$Y_{X/O}$	Yield of cell on oxygen, kg kg^{-1}
$Y_{S/O}$	Yield of substrate on oxygen, kg kg^{-1}
$Y_{P/X}$	Yield of product on cell, kg kg^{-1}
$Y_{P/S}$	Yield of product on substrate, kg kg^{-1}
$Y_{P/O}$	Yield of product on oxygen, kg kg^{-1}
Z	Objective function

Greek Letters

η	Effectiveness factor (=OUR/OD; the oxygen uptake rate per maximum possible oxygen utilization rate)
μ	Specific cell growth rate, h^{-1}
μ_{max}	Maximum specific cell growth rate, h^{-1}

λ	Wavelength, nm
α_i	Stoichiometric coefficient of the fluxes
ρ_l	Liquid phase density, kg m^{-3}

Abbreviations

Ac	Acetic acid
AcCoA	Acetyl coenzyme A
ADEPT	Antibody-Directed Enzyme Prodrug Therapy
ADP	Adenosine 5’-diphosphate
ADPHep	ADP-D-glycerol-D-mannoheptose
Ala	Alanine
AMP	Adenosine 5’-monophosphate
Arg	Arginine
Asn	Asparagine
Asp	Aspartic acid
AspSa	Aspartate semialdehyde
ATP	Adenosine 5’-triphosphate
ATCC	American Type Culture Collection
But	Butyric acid
C14:0	Myristic acid
C14:1	Hydroxymyristic acid
CaP	Carbamoyl-phosphate
CDP	Cytidine 5’-diphosphate
CDPEtN	CDP-ethanolamine
Cit	Citrate
Citr	Citruline
Chor	Chorismate
CMP	Cytidine 5’-monophosphate
CMPKDO	CMP-3-deoxy-D-manno-octulosonic acid
CO_2	Carbondioxide
CTP	Cytidine 5’-triphosphate
Cys	Cysteine
dATP	2’-Deoxy-ATP
dCTP	2’-Deoxy-CTP
dGTP	2’-Deoxy-GTP
dTTP	2’-Deoxy-TTP

DC	L-2,3 dihyrodipicolinate
DHF	7,8-Dihydrofolate
DNS	Dinitrosalisylic acid
DO	Dissolved oxygen
E4P	Erythrose 4-phosphate
EC	Enzyme Commission
F10THF	N^{10}-Formyl-THF
F6P	Fructose 6-phosphate
FA	Fatty acids
FADH	Flavine adeninedinucleotide (reduced)
Frc	Fructose
Fum	Fumarate
G1P	Glucose 1-phosphate
G6P	Glucose 6-phosphate
GDP	Guanosine 5'-diphosphate
GL3P	Glycerol 3-phosphate
Glc	Glucose
Gln	Glutamine
Glu	Glutamate
Gluc	Gluconate
Gluc6P	Gluconate 6-phosphate
Glx	Glyoxylate
Gly	Glycine
GMP	Guanosine 5'-monophosphate
GTP	Guanosine 5'-triphosphate
H_2S	Hydrogen sulfide
His	Histidine
HOT_1	High-oxygen transfer (Q_0/V_R = 1.0 vvm, N =500 min^{-1} condition)
HOT_2	High-oxygen transfer (Q_0/V_R = 0.5 vvm, N =750 min^{-1} condition)
HSer	Homoserine
ICit	Isocitrate
IGP	Indoleglycerolphosphate
Ile	Isoleucine
IMP	Inosinemonophosphate
αKG	α-ketoglutarate
Kval	Ketovaline
Lac	Lactate

Leu	Leucine
LimOT	Limited-oxygen transfer (Q_0/V_R =0.2 vvm, N =250 min^{-1} condition)
LOT_1	Low-oxygen transfer (Q_0/V_R = 0.5 vvm, N =250 min^{-1} condition)
LOT_2	Low-oxygen transfer (Q_0/V_R = 0.2 vvm, N =500 min^{-1} condition)
Lys	Lysine
Mal	Malate
Man	Mannose
Man6P	Mannose 6-phosphate
mDAP	meso-Diaminopimelate
Met	Methionine
MeTHF	N^5- N^{10}-methenyl-THF
MetTHF	N^5- N^{10}-methylene-THF
MFA	Metabolic Flux Analysis
MOT_1	Medium-oxygen transfer (Q_0/V_R=0.5 vvm, N=500 min^{-1} condition)
MOT_2	Medium-oxygen transfer (Q_0/V_R=0.2 vvm, N=750 min^{-1} condition)
MTHF	N^5- methyl-THF
NADH	Nicotinamide-adeninedinucleotide (reduced)
NADPH	Nicotinamide-adeninedinucleotide phosphate (reduced)
NH_3	Ammonia
OA	Oxaloacetic acid
Orn	Ornithine
OD	Oxygen demand (=μ_{max} C_X / $Y_{X/O}$; mol m^{-3} s^{-1})
OUR	Oxygen uptake rate, mol m^{-3} s^{-1}
OTR	Oxygen transfer rate, mol m^{-3} s^{-1}
OTR_{max}	Maximum possible mass transfer rate (=$K_La C_O$*; mol m^{-3} s^{-1})
PEP	Phosphoenolpyruvate
PG3	Glycerate 3-phosphate
Phe	Phenylalanine
Pi	Inorganic ortophosphate
PPi	Inorganic pyrophosphate
PRAIC	5'-Phosphoribosyl-4-carboxamide-5-aminoimidazole
Pro	Proline
PRPP	5-Phospho-D-ribosylpyrophosphate
Pyr	Pyruvate
R5P	Ribulose 5-phosphate
Rib5P	Ribose 5-phosphate
RPM	Reference production medium

S7P	Sedoheptulose-7-phosphate
SAP	Serine Alkaline Protease
Ser	Serine
Suc	Succinate
SucCoA	Succinate coenzyme A
Xyl5P	Xylulose 5-phosphate
TCA	Tricarboxylic acid
Tet	L-2,3,4,5 Tetrahydrodipicolinate
T3P	Triose 3-phosphate
THF	Tetrahydrofolate
Thr	Threonine
Trp	Tyrptophan
Tyr	Tyrosine
UDP	Uridine 5’-diphosphate
UDPGlc	UDP-glucose
UDPNAG	UDP-N-Acetyl-glucosamine
UDPNAM	UDP-N-Acetyl-muramic acid
UMP	Uridine 5’-monophosphate
UTP	Uridine 5’-triphosphate
Val	Valine

CHAPTER 1

INTRODUCTION

Biotechnology is the integrated use of natural sciences (biology, biochemistry, molecular biology, chemistry and physics) and engineering sciences (chemical reaction engineering, electronics) to the processing of materials by biological agents to provide goods and services (Moser, 1988). Biotechnology has produced new products and processes in a number of economic sectors including agriculture, food processing, chemical and pharmaceutical industries, pesticides, detergents, feed stocks, recycling, and waste treatment.

Enzymes are one of the most important products of biotechnological processes. Industrial biotechnology companies develop new enzymes, biocatalysts, to be used in manufacturing processes of other industries. Enzymes are proteins produced by all living organisms. They are characterized according to the compounds they act upon.

Industrial biotechnology companies look for biocatalysts with industrial value in the natural environment; improve the biocatalysts to meet very specific needs and manufacture them in commercial quantities using fermentation systems. In some cases, genetically altered microbes (bacteria, yeast, etc.), in others, naturally occurring microbes carry out the fermentation.

Some industrial enzymes are extracted from animal or plant tissues. Plant derived commercial enzymes include proteolytic enzymes papain, bromelain and ficin and some other specialty enzymes like lipoxygenase from soybeans. Animal derived enzymes include proteinases like pepsin and rennin (Leisola et al., 2001). Most of the enzymes are, however, produced by microorganisms in submerged cultures. The use of microorganisms as a source material for enzyme production has developed for several important reasons. These are the:

- Short operation time,

- Cheap production medium,

- High specific activity per unit dry weight of product,

- Nonoccurrence of seasonal fluctuations of raw materials and possible shortages due to climatic changes or political upheaval (Goel et al., 1994),

- Availability of a wide spectrum of enzyme characteristics, such as pH range and temperature resistance for selection,

- Possibility of increasing enzyme production by modifying the medium composition or by genetic manipulation of the microorganism.

Presently the industrial enzyme companies sell enzymes for a wide variety of applications. Detergents, textiles, starch, baking, animal feed, and pharmaceuticals are the main industries using these industrially produced enzymes. The estimated value of world enzyme market was about US $ 1.3 billion in 2000 and it has been forecasted to grow to almost US $ 2 billion by 2005 (Leisola et al., 2001).

β-lactamases, which are one of the most important industrial enzymes, catalyze the hydrolysis of the β-lactam ring in the β-lactam antibiotics, i.e., penicillins and cephalosporins and antibiotically inactive products are formed. Actually β-lactamases are the primary agents of bacterial resistance to antibiotics. They are manufactured for the specific assay of penicillins, destruction of residual penicillins / cephalosporins in body fluids and culture media, sterility tests of penicillins, treatment of penicillin sensitivity reactions, penicillin electrodes and for drug design (White and White, 1997). Recently, the development of β-lactamase dependent prodrugs with the applications in antibody-directed enzyme prodrug therapy (ADEPT) has been an area of particular interest (Tang et al., 2003).

In enzyme production by bioprocesses, there are some important factors that must be taken into account in order to get high yield, selectivity and productivity. These are the microorganism, medium design and bioreactor operation conditions, i.e., oxygen transfer rate, pH and temperature.

Selection of a proper microorganism is very important in bioprocesses since microorganisms act as microbioreactors in the bioreactor operation systems. Therefore the microorganisms used should be stable, should not produce toxins and its enzyme production capacity should be high. Beta-lactamases, like most of the commercial enzymes, are industrially produced mostly by *Bacillus* species due to their ability to secrete high amounts of extracellular enzymes.

In bioprocesses besides the selection of the most potential producer, the medium composition is indeed important. Carbon and energy sources and their concentrations are important as they are the tools for bioprocess medium design (Çalık et al., 2001).

Oxygen transfer, pH, and temperature that are the major bioreactor operation conditions show diverse effects on product formation in aerobic fermentation processes by influencing metabolic pathways and changing metabolic fluxes (Çalık et al., 1999). In general, according to cell growth conditions and metabolic pathway analysis, some bioprocesses require high oxygen transfer rate conditions, while others require controlled oxygen transfer rates in order to regulate oxygen uptake rates (Çalık et al., 1998).

In *Bacillus*, substrate and medium design, and bioreactor operation conditions, e.g. oxygen transfer rate and pH, regulate enzyme formation throughout the bioprocess. In this context, the regulation of the intracellular reaction network towards the synthesis of the desired enzyme in a well designed medium is indeed important in order to increase the yield and selectivity within the ultimate limit of the production capacity of the cell (Çalık et al., 2001).

Because metabolic reactions are intimately coupled with bioreactor-operation conditions, metabolic flux analysis, in addition to the successful application of metabolic engineering, is helpful in describing the interactions between the cell and the bioreactor for the purpose of fine tuning the bioreactor performance. Therefore, knowing the distribution of the metabolic fluxes during the growth, product, and by-product formations in the bioreactor provides new information for understanding physiological characteristics of the microorganism and reveals important features of the regulation of the bioprocess for enzyme production (Çalık et al., 1998).

Because of the medical implications of β-lactamase, it has been focus of intense research over the last half century, however, mostly from the point of view of enzyme induction, secretion and purification.

Related with medium design, the effect of glucose was investigated for improving β-lactamase production (Hemila et al., 1992). Among the bioreactor operation parameters, the effects of pH (Sargent et al., 1968; Hemila et al., 1992), temperature (Bernstein et al., 1967; Kuennen et al.,1980; Hemila et al., 1992) and dissolved oxygen (Sargantanis and Karim, 1996; 1998) on β-lactamase production are reported (Çelik, 2003). In the recent study of Çelik and Çalık (2004) bioprocess design parameters for β-lactamase production by *Bacillus* species were investigated. However in the literature there are no studies related with the metabolic flux analysis for β-lactamase production and the influence of oxygen-transfer conditions on the intracellular metabolic flux distributions.

In this study, the defined medium was designed in terms of its carbon and nitrogen sources concentration. Thereafter, by using the designed medium, the effects of bioprocess operation parameters, i.e., pH and temperature, on β-lactamase activity were investigated in laboratory scale bioreactors. Then, using the optimum bioprocess parameters, the effects of oxygen transfer on the β-lactamase production and variations in the by-product concentration were investigated. Finally, metabolic flux analysis for β-lactamase production was made and the influence of oxygen transfer conditions on the intracellular metabolic flux distributions in *B.licheniformis* under well-defined batch bioreactor conditions was investigated to evaluate the effects on the metabolism of the bacilli in the β-lactamase fermentation process.

CHAPTER 2

LITERATURE SURVEY

2.1 Enzymes

2.1.1 General Characteristics

Enzymes are usually proteins of high molecular weight (15,000 < MW< several million daltons) that act as catalysts. Some RNA molecules are also catalytic, but the vast majority of cellular reactions are mediated by protein catalysts (Shuler and Kargi, 1992).

Similar to chemical catalyst, enzymes lower the activation energy of the reaction catalyzed without undergoing a permanent chemical change. While a catalyst influences the rate of a chemical reaction, it does not affect reaction equilibrium. Catalytic activity of enzymes differs from that of other catalysts as follows:

1) Enzymes are highly efficient, with turnover numbers (N, i.e. the number of molecules associated with a site per second) frequently higher than those of inorganic catalysts, especially when considering reactions carried out within the physiological temperature range 25-37°C.

2) Enzyme reactions are specific in the nature of the reaction catalyzed and the substrate utilized.

3) Enzymes are extremely versatile catalysts.

4) Enzymes are subject to cellular control. For example, genetic control can influence the rate of synthesis and final cellular concentration of an enzyme. Using gene manipulation techniques, it is possible to produce microbial mutants that are capable of producing large amounts of an enzyme, resulting in high product formation from readily available substrate. Furthermore, the presence of

a certain substrate may induce the conversion of an enzyme from an inactive to active form (Atkinson and Mavituna, 1991).

Another distinguishing characteristic of enzymes is their frequent need for cofactors. A cofactor is a nonprotein compound which combines with an otherwise inactive protein to give a catalytically active complex. The simplest cofactors are metal ions like Ca^{2+}, Zn^{2+}, Co^{2+}, etc (Bailey, 1986).

2.1.2 Nomenclature and Classification

Individual enzymes selectively catalyze specific reactions. Because of the high degree of specificity, a system has been established by the Commission on Enzymes of the International Union of Biochemistry. In this system, as given in Table 2.1 enzymes are divided into six major classes.

Each of the major classes is further divided into numerical subclasses and sub-subclasses according to the individual reactions involved (Atkinson and Mavituna, 1991). Each enzyme has a classification number proposed by the Enzyme Commission (EC numbers). These classification numbers, prefixed by EC, which are now widely in use, contain four elements separated by points, with the following meaning: (i) the first number shows to which of the six main divisions (classes) the enzyme belongs, (ii) the second figure indicates the subclass, (iii) the third figure gives the sub-subclass, (iv) the fourth figure is the serial number of the enzyme in its sub-subclass. For example, the EC number of β-lactamase is EC 3.5.2.6, which catalyzes the hydrolysis of C-N bond in β-lactam ring.

2.1.3 Enzyme Activity

The qualitative description of the chemical reactions they catalyze forms the basis for their classification, while their catalytic activity is quantitatively expressed in terms of units of activity. The quantitative activity of enzymes give indication of how much enzyme should be used to achieve a required effect (product yield) and forms the basis for comparison of several similar enzyme products (Godfrey and West, 1996). However, a comparison of the activity of different enzyme preparations is only possible if the assay procedure is performed exactly in the same way (Faber, 2000). The Commission on Enzymes

suggested that a standard unit definition of enzyme activity should be as (Çelik, 2003):

> One unit (U) of any enzyme is defined as that amount which will catalyze the transformation of one micromole of substrate per minute under defined conditions.

Table 2.1 International classification of enzymes.

No	Class	Type of reaction catalyzed
1	Oxidoreductases	Transfer of electrons
2	Transferases	Group-transfer reactions
3	Hydrolases	Transfer of functional groups to water
4	Lyases	Addition of groups to double bonds or the reverse
5	Isomerases	Transfer of groups within molecules to yield isomeric forms
6	Ligases	Formation of C-C, C-S, C-O, and C-N bonds by condensation reactions coupled to ATP cleavage

2.2 Beta-Lactamases

Bacteria have developed several strategies for escaping the activity of lethal compounds: enzymatic destruction, decrease of the target sensitivity, modification of the diffusion barrier(s) and active efflux systems. They utilise them all to fight beta-lactams but the most common of these resistance mechanisms is the synthesis of beta-lactamases, enzymes which are usually secreted into the outer medium by Gram-positive species and into the periplasm by their Gram-negative counterparts (Matagne et al., 1998). They catalyze the hydrolysis of β-lactam ring in β-lactam antibiotics, i.e. penicillins and cephalosporins (Figure 2.1). The products of this hydrolysis reaction are antibiotically inactive biomolecules.

The synthesis of β-lactamases is observed in a wide range of bacteria in varying amounts. It has also been found in blue-green algae (Kushner and

Breuil, 1977) and yeast (Mehta and Nash, 1978). The presence of this enzyme in non-bacterial systems suggests that it may have a more widespread role (Çelik, 2003).

Beta-lactamases consist of a single polypeptide chain with the complete absence of cysteine residue. Specifically β-lactamase from *Bacillus licheniformis* consists of 265 amino acids (Çelik, 2003).

In most cases the reported molecular weight for β-lactamases from gram-positive bacteria is within the range of 28000 – 30000 Da. With benzylpenicillin as the substrate, typical pH-activity and temperature-activity curves obtained with β-lactamases from gram-positive bacteria shows maxima in the range of pH 6.0-7.0 and 30°-40°C respectively. The enzyme from *Bacillus* species are reasonably stable between pH 3.0-10.0 and are quite thermostable (Çelik, 2003).

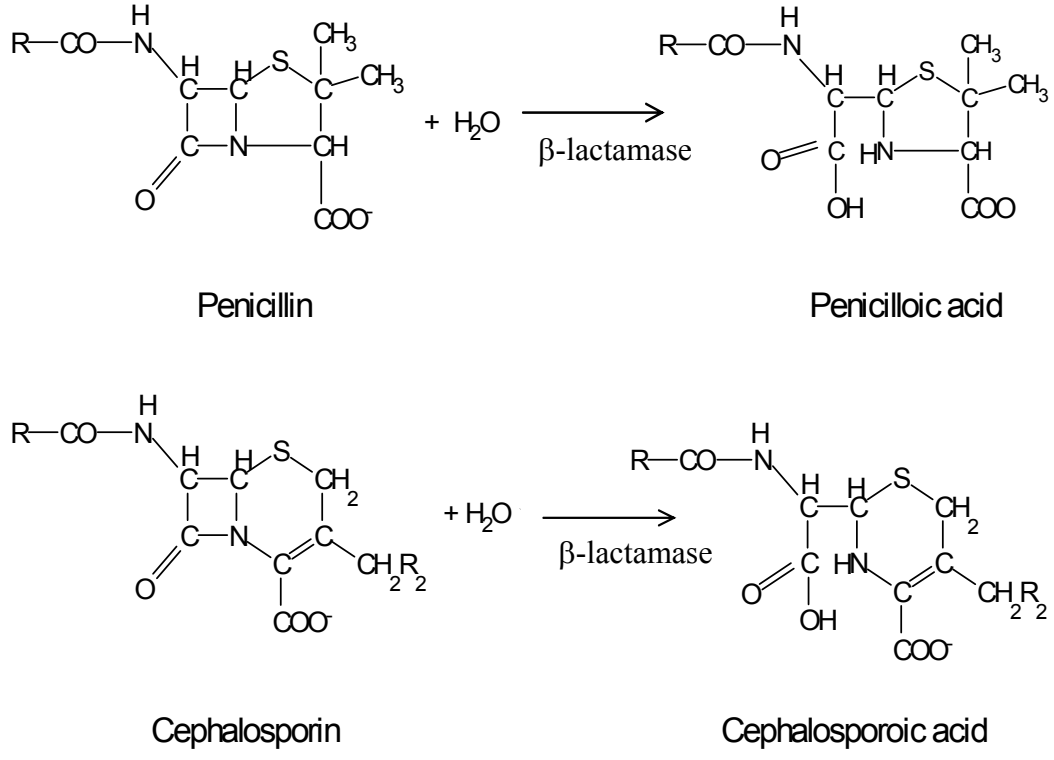

Figure 2.1 Hydrolysis of penicillins and cephalosporins by β-lactamase.

Beta-lactamases are manufactured for the specific assay of penicillins, destruction of residual penicillins/ cephalosporins in body fluids and culture media, sterility tests of penicillins, treatment of penicillin sensitivity reactions and for drug design (White and White, 1997).

2.3 Bioprocess Parameters in Enzyme Production

Any operation involving the transformation of some raw material (biological or non-biological) into some product by means of microorganisms, animal or plant cell cultures, or by materials (e.g. enzymes, organelles) derived from them, may be termed as a "bioprocess" (Moses and Cape, 1991).

In aerobic bioprocesses, there are some important factors that must be taken into account in order to have high product yield. These are:

1. Microorganism
2. Medium design
3. Bioreactor operation parameters
    i. Oxygen transfer rate
        * Air inlet rate (Q_0/ V)
        * Agitation rate (N)
    ii. pH and temperature.

2.3.1 Microorganism

In bioprocesses selecting the proper microorganism is very important in order to obtain the desired product. In choosing the production strain several aspects have to be considered. Ideally the enzyme is secreted from the cell. This makes the recovery and purification process much simpler compared to production of intracellular enzymes, which must be purified from thousands of different cell proteins and other components. Secondly, the production host should have a GRAS-status, which means that it is Generally Regarded As Safe. Thirdly, the organism should be able to produce high amount of the desired enzyme in a reasonable time frame (Leisola et al., 2001). Traditionally, identification of the most suitable enzyme source involves screening a wide range of candidate microorganisms. After screening, most of the industrially used microorganisms have been genetically modified to overproduce the desired activity and not to produce undesired side activities.

Beta-lactamases are produced by most, if not all, bacterial species, blue green algae and yeasts. Among many species, *Bacillus* strains, which fulfill all the above criteria, are attractive as microbioreactors under well-designed bioreactor operation conditions due to their secretion ability of large amounts of enzyme into the bioreactor medium (Çalık et al., 2003b), and this makes the genus *Bacillus* more favorable than the others for β-lactamase production.

In the literature concerning β-lactamase production, Sargent et al. (1968) and Çelik and Çalık (2004) used *B. licheniformis*; Bernstein et al. (1967), Kuennen et al. (1980) and Wase and Patel (1987) used *B. cereus;* whereas, Hemila et al. (1992), and Sargantanis and Karim (1996, 1998) used *B.subtilis*.

2.3.1.1 The Genus *Bacillus*

The rod-shaped bacteria that aerobically form refractile endospores are assigned to the genus *Bacillus*. The endospores of the bacilli are resistant to heat, drying, disinfectants and other destructive agents, and thus may remain viable for centuries.

The genus *Bacillus* encompasses a great diversity of strains. Some species are strictly aerobic, others are facultatively aerobic. Although the majority are mesophobic, there are also psycrophilic and thermophilic species. Some are acidophiles while others are alkalophiles. Specifically, *B.licheniformis* produces oval endospores that do not swell the mother cell. It is gram positive, is motile by peritrichous flagella, and produces acids from a range of sugars. It is listed by the American Food and Drug Administration (FDA) as a GRAS organism. *B.licheniformis* is a facultative anaerobe, having pH and temperature tolerance in the range of 5.0-7.5 and 15°C-50°C respectively. (Priest, 1993; and Laskin and Lechevalier, 1973).

2.3.1.2 Major Metabolic Pathways and Regulations

A living cell is a complex chemical reactor in which more than 1000 independent enzyme-catalyzed reactions occur. The metabolic reactions tend to be organized into sequences called metabolic pathways, and that there is some connection between the pathways by virtue of circular, closed pathways feeding back on themselves and because of pathway branches which connect one reaction sequence with another. In this sequence of steps (the pathway), a

precursors is converted into a product through series of metabolic intermediates (metabolites) (Bailey and Ollis 1986). Catabolism is the degradative phase of metabolism, in which organic nutrient molecules (carbohydrates, fats, and proteins) are converted into smaller, simpler end products (e.g., lactic acid CO_2, NH_3). Catabolic pathways release free energy some of which is converted in the formation of ATP and reduced electron carriers (NADH and NADPH). In anabolism, also called biosynthesis, small, simple precursors are built up into larger and more complex molecules, including lipids, polysaccharides, proteins, and nucleic acids. Anabolic reactions require the input of energy, generally in the forms of the free energy of hydrolysis of ATP and the reducing power of NADH and NADPH (Lehninger, Nelson and Cox, 1993).

Glycolysis and tricarboxylic acid are two central catabolic pathways by which cells obtain energy from various fuels. Furthermore, the synthesis of carbohydrates, proteins, lipids and nucleotides are the major anabolic pathways taking place in the microorganism.

In cell metabolism, groups of enzymes work together in sequential pathways to carry out a given metabolic process, such as the multi-reaction synthesis of an amino acid from simpler precursors in a bacterial cell. In such enzyme systems, the reaction product of the first enzyme becomes the substrate of the next and so on. In each enzyme system, there is at least one enzyme that sets the rate of the overall sequence because it catalyzes the slowest or rate-limiting reaction. These regulatory enzymes exhibit increased or decreased catalytic activity in response to certain signals. By the action of such regulatory enzymes, the rate of each metabolic sequence is constantly adjusted to meet changes in the cell's demands for energy and for biomolecules required in cell growth and repair. In most multi-enzyme systems the first enzyme of the sequence is a regulatory enzyme. The activity of regulatory enzymes is modulated through various types of signal molecules, which are generally small metabolites or cofactors. There are two major classes of regulatory enzymes in metabolic pathways. Allosteric enzymes function through reversible, non covalent binding of a regulatory metabolite called a modulator. The modulators for allosteric enzymes may be either inhibitory or stimulatory. An activator is often the substrate itself, and regulatory enzymes for which substrate and modulator are identical are called homotropic. When the modulator is a molecule other than the substrate the enzyme is heterotropic. Allosteric enzymes are

significantly different from those of simple non-regulatory enzymes. Some of the differences are structural. In addition to active or catalytic sites, allosteric enzymes generally have one or more regulatory or allosteric sites for its substrate, the allosteric site is specific for its modulator (Lehninger, Nelson and Cox, 1993).

The second class includes enzymes regulated by reversible covalent modification. Modifying groups include phosphate, adenosine monophosphate, adenosine diphosphate ribose, and methyl groups. These are generally covalently linked to and removed from the regulatory enzyme by separate enzymes (Lehninger, Nelson and Cox, 1993).

In some multi-enzyme systems the regulatory enzyme is specifically inhibited by the end product of the pathway, whenever the end product increases in excess of the cell's needs. When the regulatory enzyme reaction is slowed, all subsequent enzymes operate at reduced rates because their substrates are depleted by mass action. The rate of production of the pathway's end product is thereby brought into balance with the cell's needs. This type of regulation is called feedback inhibition (Lehninger, Nelson and Cox, 1993).

a) Glycolysis Pathway

In glycolysis a molecule of glucose is degraded in a series of enzyme-catalyzed reactions to yield two molecules of pyruvate. The breakdown of six-carbon glucose into two molecules of the three-carbon pyruvate occurs in ten steps, the first five of which constitute the preparatory phase. In these reactions glucose is first phosphorylated at the hydroxyl group on C-6. The glucose-6-phosphate (G6P) thus formed is converted to fructose-6-phosphate (F6P), which is again phosphorylated, this time at C-1, to yield fructose-1,6-bisphosphate. For both phosphorylations, ATP is the phosphate donor. Fructose-1,6-bisphosphate is next split to yield two three-carbon molecules, dihydroxyacetone phosphate and glyceraldehyde-3-phosphate. The dihydroxyacetone phosphate is isomerized to a second molecule of glyceraldehyde-3-phosphate; this ends the first phase of glycolysis. The energy gain comes in the payoff phase of glycolysis. Each molecule of glyceraldehyde-3-phosphate is oxidized and phosphorylated by inorganic phosphate to form 1,3-bisphosphoglycerate. Energy is released as two molecules of 1,3-bisphosphoglycerate are converted into two molecules of pyruvate (Lehninger, Nelson and Cox, 1993).

The flux of glucose through the glycolytic pathway is regulated to achieve constant ATP levels as well as adequate supplies of glycolytic intermediates that serve biosynthetic roles. The required adjustment in the rate of glycolysis is achieved by the regulation of three enzymes: Hexokinase, phosphofructokinase-1 and pyruvate kinase. Hexokinase which catalyze the conversion of glucose to G6P is one of the regulatory enzyme in glycolytic pathway, whenever the concentration of G6P in the cell rises above its normal level, hexokinase is temporarily and reversible inhibited, bringing the rate of G6P formation balance with the rate of its utilization and reestablishing the steady-state (Lehninger, Nelson and Cox, 1993).

The irreversible reaction of F6P to fructose-1,6-bisphosphate catalyzes by phosphofructokinase-1 (PFK-1) which has several regulatory sites where allosteric activators or inhibitors bind. ATP is not only a substrate for PFK-1 but also the end product of the glycolytic pathway. When high ATP levels signal that the cell is producing ATP faster than it is consuming it, ATP inhibits PFK-1 by binding to an allosteric site and lowering the affinity of the enzyme for its substrate fructose-6-phosphate. ADP and AMP, which rise in concentration when the consumption of ATP outpaces its production, act allosterically to relieve this inhibition by ATP. These effects combine to produce higher enzyme activity when F6P, ADP, or AMP builds up, and lower activity when ATP accumulates. Citrate, a key intermediate in the aerobic oxidation of pyruvate, also serves as an allosteric regulator of PFK-1; high citrate concentration increases the inhibitory effect of ATP, further reducing the flow of glucose through glycolysis (Lehninger, Nelson and Cox, 1993).

The reaction of phosphoenolpyruvate to pyruvate catalyzes by pyruvate kinase. High concentrations of ATP inhibit pyruvate kinase allosterically, by decreasing the affinity of the enzyme for its substrate phosphoenolpyruvate (PEP). Pyruvate kinase is also inhibited by acetyl-CoA and by long-chain fatty acids. Thus whenever the cell has a high concentration of ATP, or whenever ample fuels are already available for energy-yielding respiration, glycolysis is inhibited by the slowed action of pyruvate kinase (Lehninger, Nelson and Cox, 1993).

b) Tricarboxylic Acid Cycle

In aerobic organisms, glucose and other sugars, fatty acids, and most of the amino acids are ultimately oxidized to CO_2 and H_2O via the tricarboxylic acid cycle (citric acid cycle). Before they can enter the cycle, the carbon skeletons of sugars and fatty acids must be degraded to the acetyl group of acetyl-CoA, the form in which the citric acid cycle accepts most of its fuel input.

To begin a turn of the cycle, acetyl-CoA donates its acetyl group to the four-carbon compound oxaloacetate to form the six-carbon citrate. Citrate is then transformed into isocitrate, also six-carbon molecule, which is dehydrogenated with loss of CO_2 to yield the five-carbon compound α-ketoglutarate. The latter undergoes loss of CO_2 and ultimately yields the four-carbon compound succinate and a second molecule of CO_2. Succinate is then enzymatically converted in three steps into the four-carbon oxaloacetate, with which the cycle began; thus, oxaloacetate is ready to react with another molecule of acetyl-CoA to start a second turn. In each turn of the cycle, one acetyl group enters as acetyl-CoA and two molecules of CO_2 leave. Four of the eight steps in this process are oxidations, in which the energy of oxidation is conserved, with high efficiency, in the formation of reduced cofactors (NADH and $FADH_2$) (Lehninger, Nelson and Cox, 1993).

The flow of carbon atoms from pyruvate into and through the citric acid cycle is under tight regulation at two levels: the conversion of pyruvate into acetyl-CoA, the starting material for the cycle, and the entry of acetyl-CoA into the cycle. The cycle is also regulated at the isocitrate dehydrogenase and α-ketoglutarate dehydrogenase reactions (Lehninger, Nelson and Cox, 1993).

The combined dehydrogenation and de-carboxylation of pyruvate to acetyl-CoA catalyzes by pyruvate dehydrogenase complex contains three different enzymes which are pyruvate dehydrogenase (E_1), dihydrolipoyl transacetylase (E_2) and dihydrolipoyl dehydrogenase (E_3) as well as five different coenzymes or prosthetic groups- thiamine pyrophosphate (TPP), flavin adenine dinucleotide (FAD), coenzyme A (CoA), nicotinamide adenine dinucleotide (NAD), and lipoate. Furthermore, thiamin (in TPP), riboflavin (in FAD), niacin (in NAD), and pantothenate (in coenzyme A) are vital vitamins of this system. The complex is strongly inhibited by ATP, as well as by acetyl-CoA and NADH, the products of

the reaction. The allosteric inhibition of pyruvate oxidation is greatly enhanced when long-chain fatty acids are available. AMP, CoA, and NAD^+, all of which accumulate when too little acetate flows into the citric acid cycle, allosterically activate the pyruvate dehydrogenase complex. Thus this enzyme activity is turned off when sufficient fuel is available in the form of fatty acids and acetyl-CoA and when the cell's ATP concentration and [NADH]/[NAD^+] ratio are high, and turned on when energy demands are high and greater flux of acetyl-CoA into the citric acid cycle is required (Lehninger, Nelson and Cox, 1993).

There are three strongly exergonic steps in the cycle, those catalyzed by citrate synthase, isocitrate dehydrogenase, and α-ketoglutarate dehydrogenase. Each can become the rate-limiting step under some circumstances. The availability of the substrates for citrate synthase (acetyl-CoA and oxaloacetate) varies with the metabolic circumstances and sometimes limits the rate of citrate formation. NADH, a product of the oxidation of isocitrate and α-ketoglutarate, accumulates under some conditions, and when the [NADH]/[NAD^+] ratio becomes large, both dehydrogenase reactions are severely inhibited by mass action. Similarly, the malate dehydrogenase reaction is essentially at equilibrium in the cell, and when [NADH]/[NAD^+] ratio is large, the concentration of oxaloacetate is low, slowing the first step in the cycle. Product accumulation inhibits all three of the limiting steps of the cycle. The inhibition of citrate synthase by ATP is relieved by ADP, an allosteric activator of this enzyme. In short, the concentrations of substrates and intermediates of the citric acid cycle set the flux through this pathway at a rate that provides optimal concentrations of ATP and NADH (Lehninger, Nelson and Cox, 1993).

In some organisms acetate can serve both as an energy-rich fuel and as a source of phosphoenolpyruvate for carbohydrate synthesis. These organisms have a pathway, the glyoxylate cycle, that allows the net conversion of acetate to oxaloacetate. In the glyoxylate cycle, acetyl-CoA condenses with oxaloacetate to form citrate exactly as in the citric acid cycle. The breakdown of isocitrate does not occur via the isocitrate dehydrogenase reaction, however, but through a cleavage catalyzed by the enzyme isocitrate lyase, to form isocitrate and glyoxylate. The glyoxylate then condenses with acetyl-CoA to yield malate in a reaction catalyzed by malate synthase. The malate subsequently oxidized to oxaloacetate, which can condense with another molecule of acetyl-CoA to start another turn of the cycle. The accumulation of intermediates of the central

energy-yielding pathways, or energy depletion, results in the activation of isocitrate dehydrogenase. When the concentration of these regulators falls, signaling enough flux through the energy yielding citric acid cycle, isocitrate dehydrogenase is inactivated.

The tricarboxylic cycle and glycolysis are critical catabolic pathways and also provide important precursors for the biosynthesis of amino acids, nucleic acids, lipids and polysaccharides. There are, however, other catabolic pathways taken by glucose that lead to specialized products needed by the cell, and these pathways constitute part of the secondary metabolism of glucose. One such pathway is pentose-phosphate pathway which produces NADPH and ribose-5-phosphate. NADPH is a carrier of chemical energy in the form of reducing power. The biosynthesis of fatty acids requires reducing power in the form of NADPH to reduce the double bounds and carbonyl groups of intermediates in this process. A second function of the pentose phosphate pathway is to generate essential pentoses, particularly ribose, used in the biosynthesis of nucleic acids (Lehninger, Nelson and Cox, 1993).

In cells that require primarily NADPH rather than ribose-5-phosphate, pentose phosphates are recycled into glucose-6-phosphate in a series of reactions. First, ribulose-5-phosphate (R5P) is epimerized to xylulose-5-phosphate. Then, in series of rearrangements of the carbon skeletons of sugar phosphate intermediates, six five-carbon sugar phosphates are converted into five six-carbon sugar phosphates, completing the cycle and allowing continued oxidation of glucose-6-phosphate with the production of NADPH. In non-oxidative reactions of the pentose phosphate pathway convert pentose phosphates back into hexose phosphates, allowing the oxidative reactions to continue (Lehninger, Nelson and Cox, 1993).

2.3.1.3 Cell Growth, Kinetics and Yield Factors

Cellular growth is the result of a very large number of chemical reactions that occur inside individual cells. These reactions include formation of Gibbs free energy, which is used to fuel all the other reactions, biosynthesis of building blocks from substrates, polymerization of the building blocks into macromolecules, and assembly of macromolecules into organelles. In order to ensure orderly and energy-efficient growth, most of these reactions have to be

tightly coupled, and the flux through the various pathways inside the cell is therefore carefully controlled (Nielsen and Villadsen, 1994).

The rates of formation of biomass and metabolic products can be determined from measurements of the corresponding concentrations. It is therefore possible to determine what flows into the total pool of cells and what flows out of this pool. Volumetric rates can be obtained from the direct measurements of the concentrations. Often it is convenient to normalize the rates with respect to the amount of biomass present, since the rates hereby easily can be compared between fermentation experiments, even when the amount of biomass changes. Such normalized rates are referred to as specific rates. The specific growth rate of the total biomass, μ, is also a very important variable, which is defined as:

$$\mu = \frac{1}{C_x}\frac{dC_x}{dt} \tag{2.1}$$

where C_X is the cell mass concentration (kg m^{-3}), and t is time (h). The specific growth rate, μ has the units h^{-1} (Ratledge and Kristiansen, 2001).

Several phases of cell growth are observed in batch culture. Table 2.2 provides a summary of batch cell growth and metabolic activity during the phases of batch culture.

Table 2.2 Summary of batch cell growth.

Phase	Description	Specific growth rate
Lag	Cells adapt to the new environment	$\mu \approx 0$
Acceleration	Growth starts	$\mu < \mu_{max}$
Growth	Growth achieves its maximum rate	$\mu \approx \mu_{max}$
Decline	Growth slows due to nutrient exhaustion or build-up of inhibitory products	$\mu < \mu_{max}$
Stationary	Growth ceases	$\mu = 0$
Death	Cells lose viability and lyse	$\mu < 0$

During the exponential growth period –including lag, acceleration, and growth phases in batch growth, rate of cell growth, r_X, is described by the following equation:

$$r_X = \frac{dC_X}{dt} = \mu C_X \tag{2.2}$$

Similarly, substrate consumption rate, $-r_S$ and product formation rate, r_P, is described by the following equations respectively:

$$-r_S = \frac{dC_S}{dt} \tag{2.3}$$

$$r_P = \frac{dC_P}{dt} \tag{2.4}$$

Specific substrate consumption and product formation rates are described as follows:

$$q_S = \frac{-r_S}{C_X} \tag{2.5}$$

$$q_P = \frac{r_P}{C_X} \tag{2.6}$$

Another class of very important design parameters is the yield coefficients, which quantify the amount of substrate recovered in biomass and metabolic products. A list of frequently used yield coefficients is given in Table 2.3.

Yield coefficients are defined based on the amount of consumption of another material. For example, the yield coefficient of a metabolic product on a substrate is:

$$Y_{P/S} = -\frac{\Delta P}{\Delta S} \tag{2.7}$$

where, $Y_{P/S}$ is the yield coefficient, P and S are product and substrate, respectively, involved in metabolism. ΔP is the mass or moles of P produced, and ΔS is the mass or moles of S consumed. This definition gives an overall yield representing some sort of average value for the entire culture period. However, in batch processes, the yield coefficients may show variations throughout the process for a given microorganism in a given medium, due to the growth rate and metabolic functions of the microorganism. Therefore, it is sometimes necessary to evaluate the instantaneous yield at a particular point in time. Instantaneous yield can be calculated as follows:

$$Y_{P/S} = -\frac{dP}{dS} = -\frac{dP/dt}{dS/dt} = \frac{r_P}{r_S} \tag{2.8}$$

When yields for fermentation are reported, the time or time period to which they refer should be stated (Doran, 1995).

Table 2.3 Definition of yield coefficients.

Symbol	Definition	Unit
$Y_{X/S}$	Mass of cells produced per unit mass of substrate consumed	kg cell kg^{-1} substrate
$Y_{X/O}$	Mass of cells produced per unit mass of oxygen consumed	kg cell kg^{-1} oxygen
$Y_{S/O}$	Mass of substrate consumed per unit mass of oxygen consumed	kg substrate kg^{-1} oxygen
$Y_{P/X}$	Mass of product formed per unit mass of cells produced	kg product kg^{-1} cell
$Y_{P/S}$	Mass of product formed per unit mass of substrate consumed	kg product kg^{-1} substrate
$Y_{P/O}$	Mass of product formed per unit mass of oxygen consumed	kg product kg^{-1} oxygen

2.3.2 Medium Design

The general goal in making a medium is to support good growth and/or high rates of product synthesis. Contrary to intuitive expectation, this does not necessarily mean that all nutrients should be supplied in great excess.

Most of the products formed by organisms are produced as a result of their response to environmental conditions, such as nutrients, growth hormones, and ions. The qualitative and quantitative nutritional requirements of cells need to be determined to optimize growth and product formation (Shuler and Kargi, 1992). Nutrients required by cells can be classified in two categories:

1. *Macronutrients* are needed in concentrations larger than 10^{-4}M. Carbon, nitrogen, oxygen, hydrogen, sulfur, phosphorus, Mg^{2+}, and K^{+} are major macronutrients.
2. *Micronutrients* are needed in concentrations of less than 10^{-4}M. Trace elements such as Mo^{2+}, Zn^{2+}, Cu^{2+}, Mn^{2+}, Fe^{2+}, Ca^{2+}, Na^{2+}, vitamins, growth hormones, and metabolic precursors are micronutrients.

Table 2.4 lists the eight major macronutrients, their physiological functions, typical amount required in fermentation broth, and common sources.

For any bacterium to be propagated for any purpose it is necessary to provide the appropriate biochemical and biophysical environment. The biochemical (nutritional) environment is made available as a culture medium, and depending upon the special needs of particular bacteria a large variety and types of culture media have been developed with different purposes and uses (Todar, 2000). There are two major types of growth media, defined and complex, depending on their composition. A chemically defined (synthetic) medium is one in which chemical composition is well known. Such media can be constructed by supplementing a mineral base with the necessary carbon, nitrogen, and energy sources as well as any necessary vitamins. The primary advantage of defined media is that the results are more reproducible and the operator has better control of the fermentation. Complex media contain natural compounds whose chemical composition is not exactly known. A complex medium usually can provide the necessary growth factors, vitamins, hormones, and trace elements.

Table 2.4 The major macronutrient elements, their physiological functions, growth requirements and common sources.

Element	Physiological Function	Required Concentration (mol l^{-1})	Common Source
Carbon	Constituent of organic cellular material. Often the energy source.	> 10^{-2}	Glucose, sucrose fructose (for defined medium)
Nitrogen	Constituent of proteins, nucleic acids, and coenzymes.	10^{-3}	Ammonia, ammonia salts, proteins, amino acids
Hydrogen	Constituent of organic cellular material and water.		Carbon compounds such as carbohydrates
Oxygen	Constituent of organic cellular material and water. Required for aerobic respiration.		Sparging air or surface aeration
Sulfur	Constituent of proteins and certain coenzymes.	10^{-4}	Sulphate salts
Phosphorus	Constituent of nucleic acids, phospholipids, nucleotides and certain coenzymes.	10^{-4} to 10^{-3}	Inorganic phosphate salts (KH_2PO_4, K_2HPO_4)
Potassium	Principal inorganic cation in the cell and cofactor for some enzymes.	10^{-4} to 10^{-3}	Inorganic potassium salts (KH_2PO_4, K_2HPO_4, K_3PO_4)
Magnesium	Cofactor for many enzymes and chlorophylls and present in the cell walls and membranes.	10^{-4} to 10^{-3}	$MgSO_47H_2O$, $MgCl_2$

In the study of Çelik and Çalık (2004), the effects of medium components for β-lactamase production by *Bacillus* species were investigated and medium containing 1.2 kg m^{-3} $(NH_4)_2HPO_4$, 8.0 kg m^{-3} yeast extract, 10 kg m^{-3} glucose and salt solution gave maximum β-lactamase production. In the study of Hemila et al. (1992), the effect of glucose was investigated for improving β-lactamase production in a strain of *B.subtilis*, and the addition of 60 kg m^{-3} glucose and 100 mM potassium phosphate was defined as the favorable condition for higher yields and stability, but with the disadvantage of retardation of growth in the exponential phase.

2.3.3 Bioreactor Operation Parameters

Bioreactor operation parameters i.e., oxygen transfer rate, pH, and temperature influences the patterns of microbial growth and product formation.

2.3.3.1 Temperature

Temperature is an important factor affecting the performance of cells. As the temperature is increased toward optimal growth temperature, the growth rate approximately doubles for every 10°C increase in the temperature. Above the optimal temperature range, the growth rate decreases and thermal death may occur. Temperature also affects product formation. However, the temperature optimum for growth and product formation may be different. When temperature is increased above the optimum value, the maintenance requirements of cells increase. The yield coefficient is also affected by temperature (Shuler and Kargi, 1992).

In the literature concerning β-lactamase production, Wase and Patel (1987) and Sargent et al. (1968) conducted β-lactamase production at T=30°C and Sargantanis and Karim (1996, 1998) at T=37°C, without investigating the effect of temperature. Bernstein et al. (1967) investigated the effect of temperature on β-lactamase production in the range T=18°C-46°C, and reported that the basal level of β-lactamase production in an inducible strain of *B. cereus* reaches a maximum at T=42°C. They have also proposed that culturing at 42°C and lowering the temperature to 37°C leads to an increase in β-lactamase production. Kuennen et al. (1980) also investigated the effect of temperature, and reported that β-lactamase activity was relatively constant when a constitutive strain of *B.*

cereus was grown at a temperature range of 33°C to 42°C, above which a rapid decrease in activity was observed. In the study with *B.subtilis* β-lactamase by Hemila et al. (1992), it was concluded that in the range 27°C to 40°C, 30°C was the optimum cultivation temperature for β-lactamase production. In a more recent study, Çelik and Çalık (2004) investigated the effects of temperature in the range T=29°C-37°C, and T=32°C was found to be the most favorable condition for β-lactamase production by *B.licheniformis*.

2.3.3.2 pH

Microbial cells have a remarkable ability to maintain the intracellular pH at a constant level even with large variations in the pH of the extracellular medium, but only at the expense of a significant increase in the maintenance demands, since Gibbs free energy has to be used for maintaining the proton gradient across the cell membrane (Nielsen and Villadsen, 1994).

In most fermentation processes, pH can vary substantially. Often the nature of the nitrogen source can be important. Also, pH can change due to the production of organic acids, utilization of acids (particularly amino acids). Thus, pH control by means of a buffer or an active pH control system can be important depending on the nature of the bioprocess, since , some bioprocesses require controlled pH conditions, while others might require uncontrolled pH operations, in order to increase the product yield and selectivity (Çalık et al.,2002).

In the study by Sargent et al. (1968), specific β-lactamase activity of cells was shown to be constant irrespective of pH over the range of pH 5.5 to 7.5. However, the fraction of the total enzyme secreted into the extracellular medium was favorable around pH 7.5. In the study with *B.subtilis* β-lactamase by Hemila et al. (1992), it was concluded that in the pH range 5.8 to 7.4, pH 6.0 was the optimum cultivation pH for β-lactamase production. Sargantanis and Karim (1996) stated that pH control was not beneficial for β-lactamase productivity, and conducted their experiments at an initial pH of 7.0, without investigating its effect (Çelik, 2003). In a more recent study, Çelik and Çalık (2004) investigated the effects of pH in the range of 5.8 - 7.2 in media with NaH_2PO_4 - Na_2HPO_4 buffer having a buffering capacity of 0.02 M, and in media without buffer, where the initial pH was set by the addition of either NaH_2PO_4 or Na_2HPO_4. The

uncontrolled pH operation with an initial pH of 6.25 was found to be the most favorable condition for β-lactamase production by *B.licheniformis*.

2.3.3.3 Oxygen Transfer Rate

Oxygen is an essential element for aerobic growth and product formation. The transfer of oxygen into the microbial cell in aerobic fermentation processes affects product formation by influencing metabolic pathways and changing metabolic fluxes (Çalık et al., 1999). In general, according to cell growth conditions and metabolic pathway analysis, some bioprocesses require high oxygen transfer rate conditions while others require controlled oxygen transfer rates in order to regulate oxygen uptake rates (Çalık et al., 1998). Oxygen transfer rate can be adjusted by either changing the air inlet rate or agitation rate.

In aerobic processes, oxygen is a key substrate and because of its low solubility in aqueous solutions a continuous transfer of oxygen from the gas phase to the liquid phase is decisive for maintaining the oxidative metabolism of the cells. An overview of mass transfer phenomena in a fermentation process is given in Figure 2.2, which summarizes all the individual steps involved in oxygen transport from a gas bubble to the reaction site inside the individual cells (Bailey and Ollis, 1986). The steps are:

1. Diffusion of oxygen from the bulk gas to the gas-liquid interface.

2. Transport across the gas-liquid interface.

3. Diffusion of oxygen through a relatively stagnant liquid region adjacent to the gas bubble, i.e., from the gas-liquid interface to the well-mixed bulk liquid.

4. Transport of oxygen through the well-mixed liquid to a relatively unmixed liquid region surrounding the cells.

5. Diffusion through the stagnant region surrounding the cells

6. Transport from the liquid to the pellet, cell aggregate, etc.

7. Diffusive transport of oxygen into the pellet, etc.

8. Transport across the cell envelope

9. Transport from the cell envelope to the intracellular reaction site, e.g., the mitochondria.

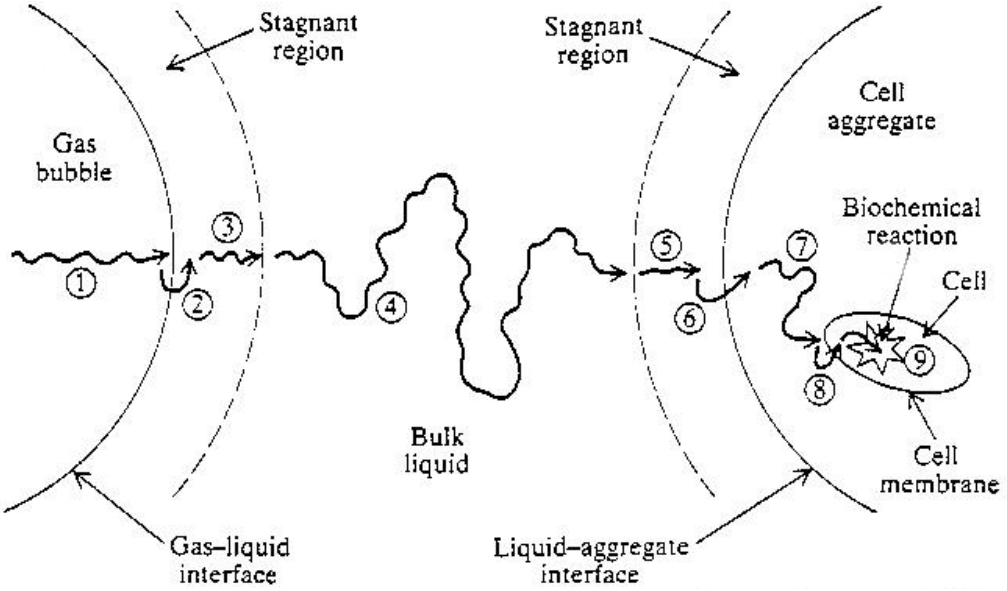

Figure 2.2 Overview of steps in the overall mass transfer of oxygen from a gas buble to the reaction site inside the individual cells.

When cells are dispersed in the liquid, and the bulk fermentation broth is well mixed, the transport through the well-mixed liquid is normally very rapid. Furthermore steps five, six and seven are relevant only for processes in which pellets or cell aggregates appear. Transport resistance within the cell is normally also neglected, because of the small size of most cells (Nielsen and Villadsen 1994). Therefore mass transfer of gas to liquid, normally modeled by the two-film theory, is of prime importance. An expression for oxygen transfer rate (OTR) from gas to liquid is given by the following equation:

$$OTR = K_L a(C_O^* - C_O) \quad (2.9)$$

Since solubility of oxygen in aqueous solutions is very low, the liquid phase mass transfer resistance dominates, and the overall mass transfer coefficient, K_L, is approximately equal to liquid phase mass transfer coefficient, k_L.

The rate of oxygen transfer in fermentation broth is influenced by several physical and chemical factors. These are bubble characteristics, rheological properties of the medium, air inlet rate, agitation rate, antifoam agents, temperature and the presence of cells and solutes that change either the value of K_La, or the oxygen uptake rate of the cell. Therefore, oxygen uptake rate (OUR) and volumetric mass transfer coefficient (K_La) are known as the oxygen transfer characteristics.

a) Oxygen Uptake Rate

The rate at which oxygen is consumed by cells in fermenters determines the rate at which it must be transferred from the gas to liquid. Many factors can influence the total microbial oxygen demand. The more important of these are cell species, culture growth phase, carbon nutrients, pH, and the nature of the desired microbial process, i.e., substrate utilization, biomass production, or product yield. The carbon nutrient affects oxygen demand in a major way. For example, glucose is generally metabolized more rapidly than other carbohydrate substances. The component parts of oxygen utilization by the cell include cell maintenance, respiratory oxidation for further growth, and oxidation of substrates into related metabolic end products. In examining metabolic stoichiometry, oxygen utilization for growth is typically coupled directly to the amount of carbon-source substrate consumed (Bailey and Ollis 1986). Oxygen uptake rate (OUR), $-r_0$, per unit volume of broth is given by

$$-r_0 = q_0 C_X \quad (2.10)$$

where qo is the specific oxygen uptake rate, kg kg^{-1} DW h^{-1}, C_x is the cell concentration, kg DW m^{-3}.

For the design of aerobic biological reactors correlations of data more or less approximating the situation of interest are frequently used to establish whether the slowest process step is the oxygen transfer rate or the rate of cellular utilization of oxygen (or other limiting substrate). The maximum possible mass-transfer rate is simply that found by setting $C_0 = 0$ in equation (2.9): all oxygen entering the bulk solution is assumed to be rapidly consumed. The maximum possible oxygen utilization rate can be found by the following equation:

$$-r_{0\max} = C_x \mu_{\max} / Y_{X/0} \tag{2.11}$$

Evidently, if maximum possible oxygen transfer rate is much larger than maximum possible oxygen utilization rate, the main resistance to increased oxygen consumption is microbial metabolism and the reaction appears to be biochemically limited. Conversely, the reverse inequality apparently leads to C_0 near zero, and the reactor seems to be in the mass-transfer-limited mode. The situation is actually slightly more complicated. In general above some critical bulk oxygen concentration the cell metabolic machinery is saturated with oxygen. In this case, sufficient oxygen is available to accept immediately all electron pairs which pass through the respiratory chain, so that some other biochemical process within the cell is rate-limiting (Bailey and Ollis 1986).

b) Volumetric Mass Transfer Coefficient

The product of the overall mass transfer coefficient K_L and the specific interfacial area a is called the volumetric mass transfer coefficient K_La. Due to the difficulties in the determination of K_L and a individually, their product is normally used to specify the gas-liquid mass transfer.

A large number of different empirical correlations for the volumetric mass transfer coefficient K_La have been presented in the literature. Most of these correlations can be written in the form:

$$K_L a = k\left(\frac{P_G}{V_R}\right)^{\beta} V_s^{\alpha} \tag{2.12}$$

where the parameters are specific for the considered system, i.e. for the bioreactor design. Thus for different stirrers and different tank geometry the parameter values may change significantly, and a certain set of parameters can be reasonably used only when studying a system which the parameters were originally derived. Some of the parameter values reported in the literature for stirred tanks are listed in Table 2.5.

Table 2.5 Parameter values for the empirical correlation of K_La.

Medium	Eq #	k	α	β	Agitator	Reference
Coalescing	1	0.025	0.5	0.4	Six-bladed Rushton turbines	Moo-Young and Blanch (1981)
	2	0.00495	0.4	0.593	Six-bladed Rushton turbines	Linek et al. (1987)
	3	0.01	0.4	0.475	Various agitators	Moo-Young and Blanch (1981)
	4	0.026	0.5	0.4	Not specified	van't Riet (1979)
Noncoalescing	5	0.0018	0.3	0.7	Six-bladed Rushton turbines	Moo-Young and Blanch (1981)
	6	0.02	0.4	0.475	Various agitators	Moo-Young and Blanch (1981)
	7	0.002	0.2	0.7	Not specified	van't Riet (1979)
	8	0.00525	0.2	0.7	Not specified	Çalık et al. (1998)

Although K_La is difficult to predict, it is a measurable parameter. There are several methods for measuring the volumetric mass transfer coefficient K_La for oxygen. A few of the best known methods are Sulphite Method, Gas Analysis Method and Dynamic Method.

Dynamic Method is a widely used simple method that can be applied during a fermentation process to determine the value of K_La experimentally. The method is based on an unsteady state mass balance for oxygen given by the following equation:

$$\frac{dC_O}{dt} = K_L a(C_O^* - C_O) - q_0 C_X \tag{2.13}$$

As shown in Figure 2.3, at some time t_0, the broth is de-oxygenated by stopping the air flow. During this period, dissolved oxygen concentration, Co_0, drops, and since there is no oxygen transfer, equation (2.13) becomes:

$$\frac{dC_O}{dt} = r_0 \tag{2.14}$$

Using equation (2.14) in region-II of Figure 2.3, oxygen uptake rate, $-r_0$, can be determined.

Air inlet is then turned back on, and the increase in C_O is monitored as a function of time. In this period, region-III, equation (2.13) is valid. Combining equations (2.10) and (2.13) and rearranging,

$$C_O = -\frac{1}{K_L a}(\frac{dC_O}{dt} - r_0) + C_O^* \tag{2.15}$$

From the slope of a plot of C_O versus ($dC_O/dt - r_0$), K_La can be determined (Figure 2.4).

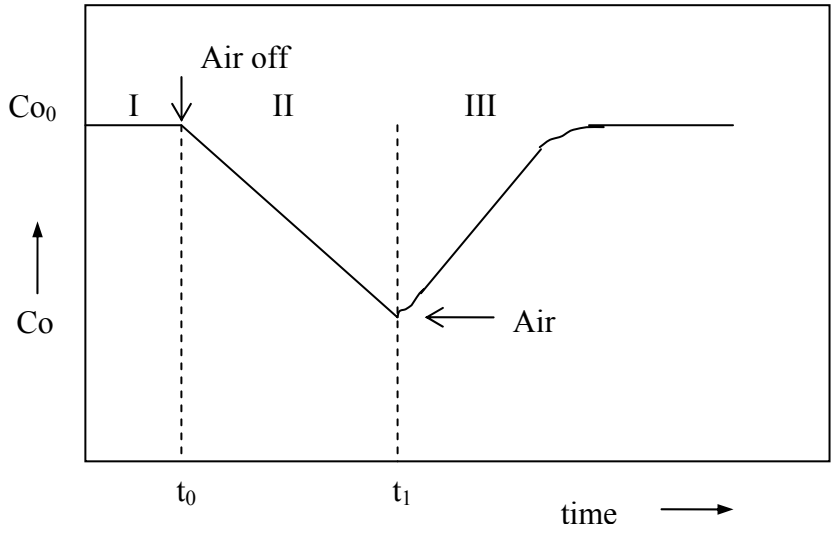

Figure 2.3 Variation of dissolved oxygen concentration with time in dynamic measurement of K_La.

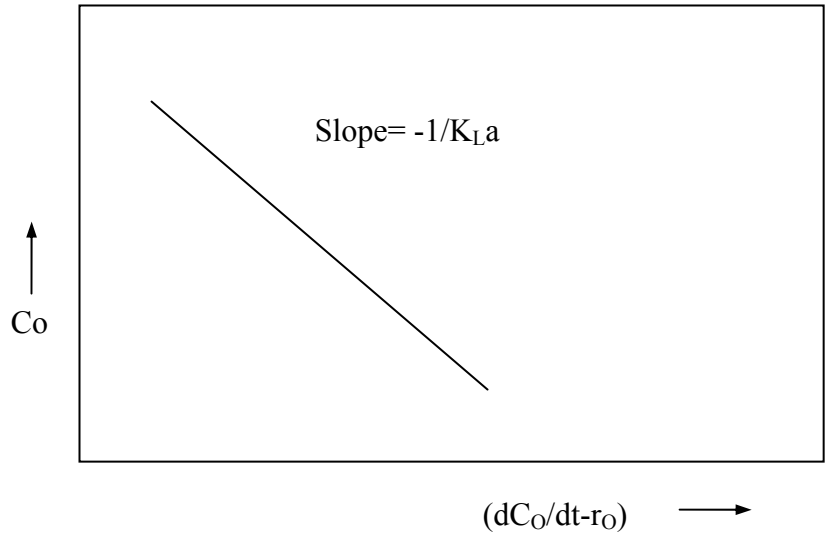

Figure 2.4 Evaluating K_La using the Dynamic Method

The Dynamic Method can also be applied to conditions under which there is no reaction, i.e., r_0=0 (Nielsen and Villadsen, 1994). In this case, the broth is de-oxygenated by sparging nitrogen into the vessel. Air inlet is turned back on and again the increase in Co is monitored as a function of time. Modifying equation (2.15)

$$C_O = -\frac{1}{K_L a}\frac{dC_O}{dt} + C_O^* \qquad (2.16)$$

From the slope of a plot of C_O versus dC_O/dt, the physical mass transfer coefficient, $K_L a_0$, can be determined.

The effect of oxygen transfer conditions on β-lactamase production by *Bacillus* species was investigated by Sargantanis and Karim (1996, 1998). They mainly focused on the performance of dissolved oxygen (DO) control strategy, and compared β-lactamase activities observed at different dissolved oxygen levels, which were kept constant during the bioprocess using an adaptive pole placement control algorithm. They performed the experiments at 3%, 5%, 8% and 15% constant dissolved oxygen levels and reported the highest productivity of β-lactamase at the highest DO level (15%), but that the rate of β-lactamase degradation by proteases was the highest at this level also, without giving the protease activities. Therefore, they concluded that β-lactamase production was much higher at low DO levels (3%), although it occurred at a later stage of the fermentation, and that limited growth conditions favored long-term β-lactamase production.

In the recent study of Çelik and Çalık (2004), oxygen transfer characteristics ($-r_0$, $K_L a$) of the bioprocess for β-lactamase production by *B.licheniformis* were investigated in a semi-defined medium containing glucose, $(NH_4)_2HPO_4$, yeast extract and the salt solution, at pH_0 = 6.0, T= 32°C at Q_0/V=0.5 vvm and N=500 min^{-1} oxygen transfer conditions and found that throughout the bioprocess, overall oxygen transfer coefficient ($K_L a$) varied between 0.008-0.016 s^{-1}; oxygen uptake rate varied between 0.001-0.003 mol m^{-3} s^{-1}.

Related with the production of other biomolecules using *Bacillus licheniformis*, effects of oxygen transfer were investigated in the production of

serine alkaline protease by Çalık et al. (1999) at nine different oxygen transfer conditions by forming a 3x3 matrix using three agitation rates N=150, 500, 750 min^{-1} and three air inlet rates Q_O/V_R=0.2, 0.5, 1.0 vvm with the initial substrate concentration C_C=9.0 kg m^{-3} by using a laboratory-scale 3.5 dm^3 batch bioreactor consisted of a system of working volume 2.0 dm^3 equipped with two four-blade Rushton turbines, and dissolved oxygen, temperature, pH, foam, air–inlet and stirring rate measurements and control. In the bioreactor the oxygen uptake rate (OUR) values as well as the oxygen transfer rate (OTR) increased with the increasing oxygen transfer, i.e. Q_O/V_R and N, up to the medium oxygen transfer condition, Q_O/V_R= 0.5 vvm and N=750 min^{-1}. Nevertheless, at higher oxygen transfer conditions the cell growth, and consequently the OUR and OTR decreased. The impact of the further increase in Q_O/V_R and/or N after Q_O/V_R= 0.5 vvm and N=750 min^{-1} condition increases the shear fields in the bioreactor; and the exposure of the bacilli to higher shear fields at high oxygen transfer conditions causes considerable dynamic influences that decrease the OUR as well as the OTR and consequently perturbs the metabolism of *B.licheniformis.* With the carbon source citrate, the consumption rate of the substrate increases with increasing agitation rate and air inlet rate, and cell concentration was the highest at low oxygen transfer condition.

2.4 Metabolic Flux Analysis

Metabolic flux analysis (MFA) is based on calculation of intracellular reaction network rates through various reaction pathways -either theoretical or by using elaborate experimental data on uptake, excretion, secretion rates, biosynthetic requirements with metabolic stoichiometry- by solving the mass-balance-based mathematical model developed for the bioreaction network components, either at pseudo-steady state or at steady-state. MFA describes the interactions between the cell and the bioreactor with proper emphasis on the metabolic state and the metabolic process in order to fine-tune the bioreactor performance. This analysis can be used to find the critical branch points and bottlenecks in the overall flux distributions, for modifying the medium composition, for improving the bioreactor operation conditions, moreover for calculating the theoretical metabolic capacities of the microorganism, and for selecting the host microorganism (Çalık et al., 2002).

2.4.1 Modelling of Bioreaction Network for Metabolic Flux Analysis

Conceptually, the cell functions as the semibatch micro-bioreactor with volume V wherein the biochemical reactions take place; and, a small number of compounds of the intracellular biochemical reaction network (e.g substrates, oxygen, H^+, H_2O, CO_2, amino acids, organic acids of the glycolysis or gluconeogenesis pathways and the tricarboxylic acid (TCA) cycle, and extracellular proteins) is exchanged or transferred with facilitated and active transport mechanisms between the metabolic system, and the bioreactor medium which is defined as the environment. Therefore, the reactions that represent the specific properties of the microorganism used should be studied; consequently, an idea of the main biochemical processes that occur inside the organism and an idea about the chemical reactants which are involved are indeed needed. In order to describe the intracellular metabolic reaction network in chemical detail by an increased number of reactions, of which the stoichiometry is precisely known, the biochemical reactions of the biochemical reaction network need to be determined and studied one-by-one. Consequently, the biochemical reaction network, including the cell synthesis reaction using the complete chemical composition data of the cell and the product synthesis reaction, must be set up. Thus, starting from the site that the substrate(s) enters into the carbon mechanism, the biochemical reaction network should consider all the relevant bioreactions of the central carbon metabolism, i.e., the glycolysis and the gluconeogenesis pathways, the pentose phosphate pathway (PPP), the TCA cycle including the glyoxylate shunt, and the anaplerotic reactions. The overall pathway can be simplified based on a comparison of the extracellular growth compounds and the intracellular chemical compounds by lumping some reactions into single ones without loosing representation accuracy. Moreover, some major assumptions can also be incorporated in the model. In this context in the second step, for the each metabolite of the intracellular reaction network one equation is obtained which is defined as the algebraic sum of all the conversions in the defined reactions and transport equals to the accumulation of the intracellular metabolite in the micro-bioreactor (cell), as follows (Çalık et al., 2002):

$$r_{Ri} \pm r_{Ti} = d(C_i)/dt \tag{2.17}$$

where, r_{Ri} is the net-reaction and r_{Ti} is the net-transfer rate; and $d(C_i)/dt$ is the accumulation rate of the intracellular metabolite within cell. In the mass flux balance-based analysis, equation (2.17) can be written in a vector form as follows:

$$A * r(t) = c(t) \tag{2.18}$$

where, A is the stochiometric coefficients matrix of the metabolic network, r(t) is the vector of reaction fluxes and c(t) is the metabolite accumulation vector. The elements of c(t) are divided into two subvectors.

$$c(t) = c_1(t) + c_2(t) \tag{2.19}$$

where $c_1(t)$ and $c_2(t)$ corresponding to extracellular and intracellular metabolite accumulation vectors, respectively. Due to the very high turnover of the pools of most metabolites, the concentrations of the different metabolites pools rapidly adjusted to new levels, even after large perturbations in the fermentation broth. Therefore, it is reasonable to use the pseudo-steady state (PSS) approximation for the intracellular metabolites, $c_2(t)=0$. Thus, equation (2.18) can be written as (Çalık et al., 2001):

$$A * r(t) = c_1(t) \tag{2.20}$$

For the corresponding vector equation (2.20), the stoichiometric coefficients matrix of *m* x *n* need to be constructed, where *m* is the number of the metabolites in the bioreaction network and *n* is the number of the reactions.

2.4.2 Solution of the Mathematical Model

The A matrix can be determined on the basis of the biochemistry of the microorganism. If $m > n$ the solution of the model gives the approximate exact solution. The solution of equation 2.20 can be determined by a constrained least-squares approach with the objective of minimising the sum of squares of residuals from the stoichiometric mass balance. Nevertheless, if $m<n$, metabolic flux distributions can be obtained by minimising or maximising the objective function, whereupon the best metabolic pathway utilisation that would fulfill the

stated objective is obtained. If *m*<*n,* the mathematical formulation for the objective function Z is:

$$Z = \sum \alpha_i r_i \qquad (2.21)$$

where, Z is a linear combination of the fluxes r_i , and α_i is the coefficient of the component-i in the stoichiometric equation of the corresponding reaction. In least-squares method matrix is solved and a unique solution is obtained (Çalık et al., 2002).

Metabolic flux analysis has been successfully applied to a number of fermentation processes. In general, the literature reports on the metabolic flux analysis for four enzymes, serine alkaline protease (SAP) (Çalık et al., 1999, 2001) , neutral protease (Çalık et al., 2001), amylase (Amy) (Çalık et al., 2001; Nielsen et al., 1999), and glucoamylase (Nielsen et al., 1996).

Related with an enzyme production by *Bacillus* species, *Bacillus licheniformis* (Çalık and Özdamar, 1999; Çalık et al., 1999, 2000, 2001), was the only microorganism studied for the metabolic flux analysis. Çalık and Özdamar (1999) investigated the biochemistry of *Bacillus licheniformis* and developed a detailed mass flux balance-based stoichiometric model that contains *m*=105 metabolites and *n*=148 reaction fluxes to obtain the intracellular metabolic flux distributions for serine alkaline protease production by using batch experimental data in which citrate was used as the carbon source. The model was solved by using simplex optimization algorithm in which the objective function was defined as the difference between protease synthesis rate and protease secretion rate. The results indicated that the intracellular amino acid fluxes played an important role in the serine alkaline protease fermentation process. Çalık et al. (1999) reported the influence of bioreactor operation conditions, i.e. the effects of oxygen-transfer rate on the intracellular metabolic flux distributions, in *B.licheniformis* under well-defined batch bioreactor conditions to evaluate the effects on the metabolism of the bacilli in serine alkaline protease fermentation process. They reported that the flux partitioning in the TCA cycle at α-ketoglutarate towards glutamate group and at oxaloacetate towards aspartate group amino acids were dependent mainly on the oxygen transfer rate, moreover, the flux of the anaplerotic reactions that connects the TCA cycle either

from malate or oxaloacetate to the gluconeogenesis pathway via the main branch point pyruvate was also influenced by the oxygen transfer rate. Further, with the decrease in the oxygen transfer rate, the intracellular flux values after glycerate 3-phosphate in the gluconeogenesis pathway and the specific growth rate decreased and the total ATP generation rate increased with the increase in oxygen transfer rate. Lastly they mentioned that the pathway towards the aspartic acid family amino acids which is important for sporulation that precedes the serine alkaline protease synthesis were all active throughout the bioprocess.

CHAPTER 3

MATERIALS AND METHODS

3.1 Chemicals

Benzylpenicillin (penicillin G) was purchased from Sigma Chemical Company, St. Louis, Missouri, USA. All other chemicals were analytical grade, and obtained either from Sigma Ltd., Difco Laboratories, or Merck Ltd.

3.2 The Microorganism

Bacillus licheniformis 749/C (ATCC 25972) was used as the microbial source of β-lactamase (EC 3.5.2.6). The microorganisms, which were freeze dried when received, were kept at -20ºC, and brought to an active state by incubating for 30 min, at 30ºC, in a liquid medium, V=0.3ml, that contained (kg m^{-3}): soytryptone, 5; peptone, 5; $MnSO_4.2H_2O$, 0.010. Afterwards, the microorganisms were inoculated onto a solid medium, and stored at 4ºC.

3.3 The Solid Medium

The microorganisms, stored on agar slants at 4ºC, were inoculated onto the newly prepared agar slants under sterile conditions, and they were incubated at 30ºC for 24h. The composition of the solid medium for β-lactamase production by *Bacillus* sp. is given in Table3.1 (Çelik, 2003).

Table 3.1 The composition of the solid medium for *Bacillus* sp.

Compound	Concentration, kg m^{-3}
Soytryptone	5.00
Peptone	5.00
$MnSO_4.2H_2O$	0.01
Agar	15.00

3.4 The Precultivation Medium

Microorganisms grown in the solid medium for 24 h, were inoculated into precultivation medium, and incubated at 37ºC and N=200 min^{-1} for 3.5 h. Microorganism growth was conducted in orbital shakers under agitation and heating rate control, using air-filtered Erlenmeyer flasks 150 ml in size that had working volume capacities of 33 ml. The composition of the precultivation medium for cell growth and β-lactamase production is given in Table 3.2 (Çelik, 2003).

Table 3.2 The composition of the precultivation medium.

Compound	Concentration, kg m^{-3}
Soytryptone	15.0
Peptone	5.00
Na_2HPO_4	0.25
$CaCl_2$	0.10
$MnSO_4.2H_2O$	0.01

3.5 The Production Medium

When the microorganism concentration in the precultivation medium reached to 0.30 kg m^{-3}, the microorganisms were inoculated to the production medium, contained either in the laboratory scale bioreactor (V=150 ml) or pilot scale bioreactor (V=3.0 dm^3), with an inoculation ratio of 1/10.

Laboratory scale batch fermentations were conducted in agitation and heating rate controlled orbital shakers at an agitation rate of 200 min^{-1} and a cultivation temperature of 37ºC, using air filtered 150 cm^3 shake bioreactor that contained V_R = 33 cm^3 reference medium whose composition is given in Table 3.3 (Çelik, 2003), unless otherwise stated.

The laboratory scale experiment results enabled the design of the defined medium for the β-lactamase production in terms of the initial carbon and nitrogen source concentrations and bioreactor operation conditions. Pilot scale β-lactamase fermentation were accomplished using this optimized medium in 3.0

dm^3 batch bioreactor (Braun CT2-2), having a working volume of 0.5-2.0 dm^3 and a diameter of 12.1 cm, and consisting of temperature, pH, foam, stirring rate and dissolved oxygen controls. The bioreactor utilized an external cooler, steam generator and a jacket around the bioreactor for sterilization and temperature control. The bioreactor was stirred with two four-blade Rushton turbines with a diameter of 5.4 cm, and consisted of four baffles and a sparger.

All the medium components except the salt solution were steam sterilized at 121°C for 20 min, glucose being sterilized separately. The micronutrients all together, referred to as the salt solution, was filter sterilized with a sterile filter of 0.2 μm pore size.

Table 3.3 The composition of the reference production medium.

Macronutrients	Concentration, kg m^{-3}
Glucose	8.0
$(NH_4)_2HPO_4$	4.7
Micronutrients (salt solution)	Concentration, kg m^{-3}
$MgSO_4.7H_2O$	0.25
$FeSO_4.7H_2O$	1.0×10^{-3}
$ZnSO_4.7H_2O$	1.0×10^{-3}
$MnSO_4.H_2O$	7.5×10^{-5}
$CuSO_4.5H_2O$	1.0×10^{-5}

3.6 Analysis

Throughout the bioprocess, samples were taken at different cultivation times. After determining the cell concentration, the medium was centrifuged at 13500 min^{-1} for 10 min to separate the cells. Supernatant was used for the determination of β-lactamase activity. In pilot scale experiments, besides β-lactamase activity, cell, glucose, β-lactamase and SAP concentrations; amino acid and organic acid concentrations were determined.

3.6.1 Cell Concentration

Cell concentrations based on dry weights were measured with a UV-Vis spectrophotometer (Thermo Spectronic, Heλios α) using a calibration curve (Appendix A) obtained at 600 nm.

3.6.2 Beta-Lactamase Activity

Beta-lactamase activity was determined by measuring the hydrolysis of benzylpenicillin. Samples from the culture broth was harvested by centrifugation (Sigma 1-15) at 13,500 g for 10 min. Fresh substrate solutions were prepared daily and maintained at 30°C, by dissolving 0.25 kg m^{-3} benzylpenicillin in 0.1 M phosphate buffer, pH 7.0. 0.1 cm^3 sample of centrifuged culture supernatant, diluted properly, was added to 3 cm^3 of substrate solution and immediately analyzed, by following the change in absorbance in one minute at 232 nm with a UV spectrophotometer (Thermo Spectronic, Heλios α) (Wase and Patel, 1987). One unit of β-lactamase activity was defined as the amount of enzyme that could hydrolyze 1μmol of benzylpenicillin at 30°C and pH 7.0 in one minute (Çelik, 2003), (Appendix B).

3.6.3 Beta-Lactamase and Serine Alkaline Protease Concentrations

β-lactamase and serine alkaline protease concentrations were determined with a high performance capillary electrophoresis at 214 nm (Waters HPCE, Quanta 4000E). The samples were analyzed at 12kV and 15°C with a negative power supply by hydrostatic pressure injection, using an electrolyte containing Z1-Methyl (Waters) salt in 100 mM borate buffer (Çalık et al., 1998). The enzyme concentrations were calculated from the chromatogram, based on the chromatogram of the standard enzyme solutions. The calibration curves for β-lactamase and serine alkaline protease concentrations are given in Appendix C and Appendix D respectively.

3.6.4 Reduced Sugar Concentration

Reduced sugar, glucose, concentration was determined by the DNS (dinitrosalisylic acid) method (Miller, 1959) at 550 nm with a UV spectrophotometer. The calibration curve and the preparation method of the DNS solution are given in Appendix E and F, respectively. The method used in analysis of samples and preparation of the calibration curve is given below:

1. 3 cm^3 of DNS solution was added into test tubes containing 1 cm^3 of sample at different glucose concentrations.
2. The test tubes were put into boiling water for 5 min and then into ice for another 5 min.
3. The sample passing through the same steps but do not contain any reducing sugar is used as blank and the absorbance values of the samples were measured by a UV spectrophotometer at 550 nm (Çelik, 2003).

3.6.5 Amino Acid Concentrations

Amino acid concentrations were measured with an amino acid analysis system (Waters, HPLC), using the Pico Tag method (Cohen, 1983). The method is based on reversed phase HPLC, using a precolumn derivation technique with a gradient program developed for amino acids. The amino acid concentrations were calculated from the chromatogram, based on the chromatogram of the standard amino acids solution. The analysis was performed under the conditions specified below:

Column	:Amino acid analysis column (Nova-Pak C18, Millipore)
Column dimensions	:3.9 mm x 30 cm
System	:Reversed phase chromatography
Mobile phase flow rate	:1 ml/min
Column temperature	:38 °C
Detector and wavelength	:UV/VIS, 254 nm
Injection volume	:4 µl
Analysis period	:20 min

3.6.6 Organic Acid Concentrations

Organic acid concentrations were determined with a high performance capillary electrophoresis at 254 nm (Waters HPCE, Quanta 4000E). The samples were analyzed at 20kV and 15°C with a negative power supply by hydrostatic pressure

injection, using an electrolyte containing 5mM potassium hydrogen phtalate and 0.5mM OFM Anion Bt (Waters) as the flow modifier at pH=5.6 (for α-ketoglutaric acid, acetic acid, malic acid, fumaric acid, succinic acid, lactic acid, oxalacetate and gluconic acid) and at pH=7.0 (for, pyruvic acid, citric acid, lactic acid, gluconic acid) (Çalık et al., 1998).

3.6.7 Liquid Phase Mass Transfer Coefficient and Oxygen Uptake Rate

In order to determine the liquid phase mass transfer coefficient and oxygen uptake rate in the β-lactamase production process, the Dynamic Method (Rainer 1990), as explained in section 2.3.3.3, was used.

Prior to inoculation of the microorganism to the production medium in the bioreactor, the physical mass transfer coefficient (K_La_0) was determined. After inoculation of the microorganism to the bioreactor, the dynamic oxygen transfer experiments were carried out at certain cultivation times for a short period of time, so that the biological activities of the microorganisms are unaffected. During this period, while the air inlet was totally ceased, the agitation rate was lowered to N=100 min^{-1} in order to lower the effect of surface aeration (Çelik, 2003).

3.7 Mass Flux Balance-Based Analysis

Effects of the oxygen transfer conditions on the intracellular carbon flux distributions were investigated by the metabolic flux analysis. The reaction network of *Bacillus licheniformis* given in Appendix G represented by the metabolic system sums up to a total of 105 metabolites and 149 reaction fluxes. The optimized program GAMS 2.25 (General Algebraic Modeling System, GAMS Development Corp., Washington, DC) was used to solve mass-flux balance equation (Eq 2.20) given in Section 2.4. Using the mathematical programming, optimum flux distributions were obtained by minimizing the objective function Z (Eq 2.21). The model variables that are the reaction fluxes of metabolites were expressed in mmol g^{-1} DW h^{-1}; and the flux towards biomass represented the specific growth rate, μ in h^{-1} (Çalık, 1998).

CHAPTER 4

RESULTS AND DISCUSSION

This study focuses on the effects of oxygen transfer on β-lactamase production by *Bacillus licheniformis* on a defined medium. In order to clarify the oxygen transfer effects on the production of β-lactamase, firstly a glucose based defined medium was designed and using this medium, the effects of bioreactor operation parameters, i.e., pH and temperature, on β-lactamase activity and cell formation were investigated in laboratory scale bioreactors. Thereafter, using the optimized medium the effects of oxygen transfer on cell generation, substrate consumption, product (β-lactamase) and by-products formation were investigated in the pilot scale bioreactor. Finally, the influence of oxygen transfer conditions on the intracellular reaction rates in β-lactamase production by *B.licheniformis* under well-defined batch bioreactor conditions was investigated using metabolic flux analysis to evaluate the effects of oxygen on the metabolism.

4.1 Medium Design

In order to design a defined medium firstly yeast extract was omitted from the medium found in the study of Çalık and Çelik (2004), and medium, that contained (kg m^{-3}): glucose, 8; $(NH_4)_2HPO_4$, 4.7 and the salt solution in which the β-lactamase activity was obtained as 60 U cm^{-3} was considered as the starting point for the medium design experiments and the medium was named as the reference production medium (RPM).

In this context, the effects of $(NH_4)_2HPO_4$ concentration was investigated in agitation and heating rate controlled laboratory scale bioreactors as it was found as the optimum nitrogen source in the study of Çalık and Çelik (2004).

4.1.1 Effect of Nitrogen Source Concentration

Firstly, the effect of $(NH_4)_2HPO_4$ concentration on β- lactamase activity was investigated within the range corresponding to the initial nitrogen

concentrations of C_N^0=0.0 – 4.0 kg m^{-3} at 37°C with an initial pH of pH_0=7.2. As can be seen from Figure 4.1 the medium containing initial nitrogen concentration of 1.5 kg m^{-3} gave the maximum β-lactamase activity as A=76 U cm^{-3}. Furthermore, it was observed that higher nitrogen content had an inhibitory effect on both cell formation and beta-lactamase activity.

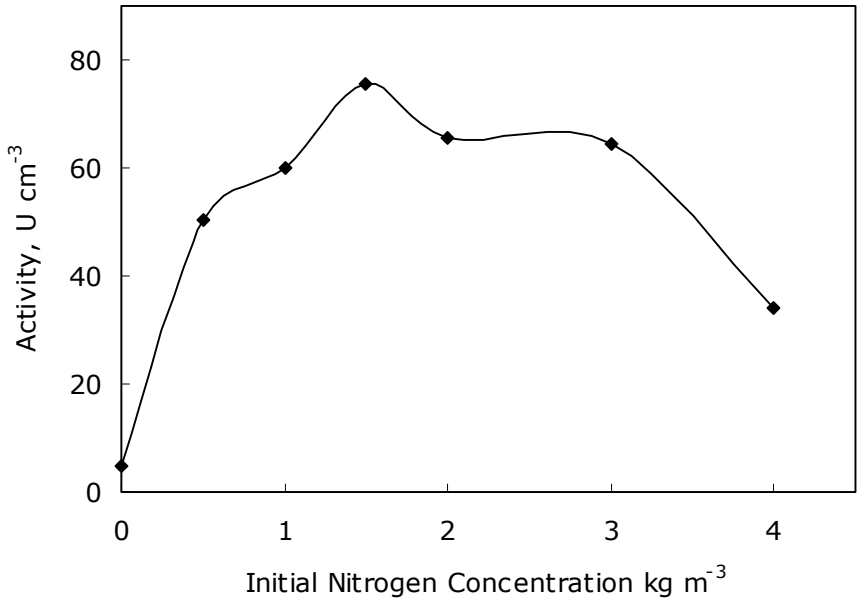

Figure 4.1 The variations in β-lactamase activity with the initial nitrogen concentration. t=32 h, V=33 cm^3, T=37°C, pH_0=7.2, N=200 min^{-1}.

4.2 Bioreactor Operation Parameters

By using *B.licheniformis* 749/C and the medium containing 8 kg m^{-3} glucose, 7.1 kg m^{-3} $(NH_4)_2HPO_4$ and the salt solution, the bioreactor operation parameters, i.e., pH and temperature were investigated in the laboratory scale bioreactors. Thereafter the effect of the initial glucose concentration was investigated.

4.2.1 Effect of pH and Temperature

The medium design experiments were conducted with an initial pH of 7.2 in media without buffer. Under the scope of determining the most favorable bioreactor operation conditions, the effect of pH control was investigated first, since some bioprocesses require controlled pH conditions, while others might require uncontrolled pH operations (Çalık et al.,2002).

The effect of pH control was investigated in an initial pH range of 5.8-8.0, in media with NaH_2PO_4 - Na_2HPO_4 buffer, and in media without buffer, where the initial pH was adjusted by the addition of either 5M KOH or 10M H_3PO_4. Comparing the controlled and uncontrolled-pH operations; it can be observed at pH_0= 7.2-7.6 uncontrolled-pH operation favors β-lactamase production (Figure 4.2). As seen in Figure 4.2, the highest β-lactamase activity was obtained at pH_0=7.5 uncontrolled-pH operation, the activity value (A=113 U cm^{-3}) obtained was approximately 1.5-fold higher than that of pH_0=7.2. Çalık and Çelik (2004); and Sargantanis and Karim (1996) stated that controlled-pH operation was not beneficial for β-lactamase productivity.

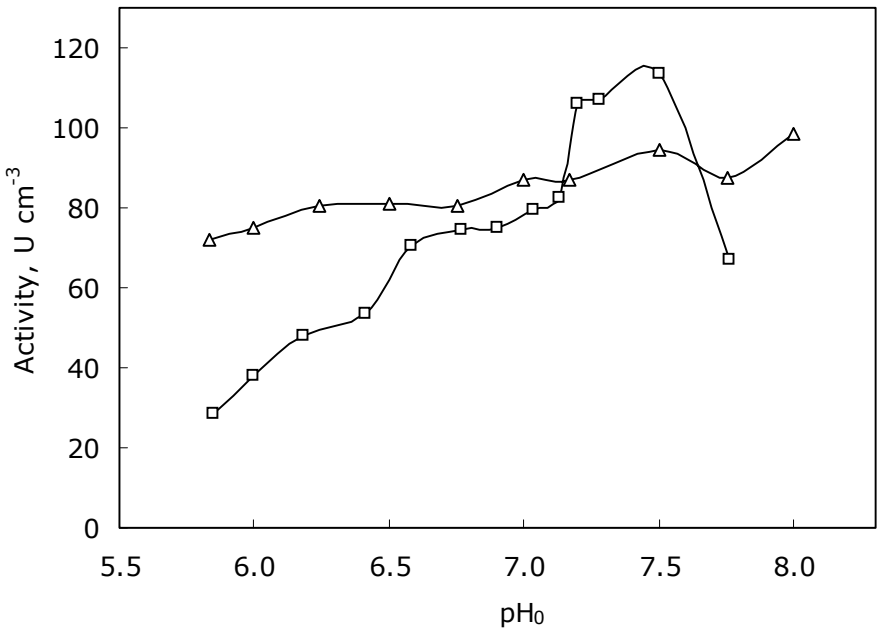

Figure 4.2 The variations in β-lactamase activity with the initial pH. V=33 cm^3, T=37°C, N=200 min^{-1}, t= 32 h, w/o buffer, (Δ); buffer, (□).

Thereafter, the effects of pH and temperature were investigated in the medium without buffer. As seen in Figure 4.3, T=37°C, and pH_0=7.5 were found to be the most favorable conditions for β-lactamase activity. These results are consistent with the pH and temperature range used in the literature for β-lactamase production by *Bacillus* species (Sargent et al.,1968; Sargantanis and Karim, 1996- 1998).

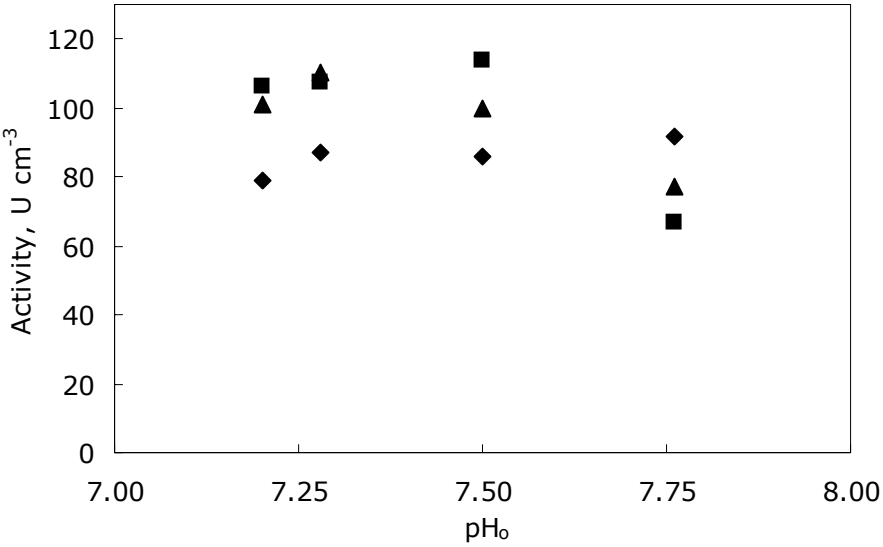

Figure 4.3 The variations in β-lactamase activity with the initial pH and temperature of the cultivation medium. at t=32 h, V=33 cm^3, N=200 min^{-1}, T (°C) : 32 ,(♦); 37, (■); 40, (▲).

4.2.2 Effect of Carbon Source Concentration

Glucose, being easily metabolized by microorganisms, is widely used in fermentation media. The effects of glucose concentration on β-lactamase production were investigated in the range of C_G^0=6.0, 7.0, 8.0, 9.0, 10.0, 11.0, and 12.0 kg m^{-3}, in the medium containing 7.1 kg m^{-3} $(NH_4)_2HPO_4$ and the salt solution at a cultivation temperature of 37°C with an initial pH of 7.5. As can be seen in Figure 4.4 the activity of β-lactamase did not change significantly in this range and $C_G°$=7 kg m^{-3} was selected as the initial glucose concentration to be used in the pilot-scale bioreactor experiments.

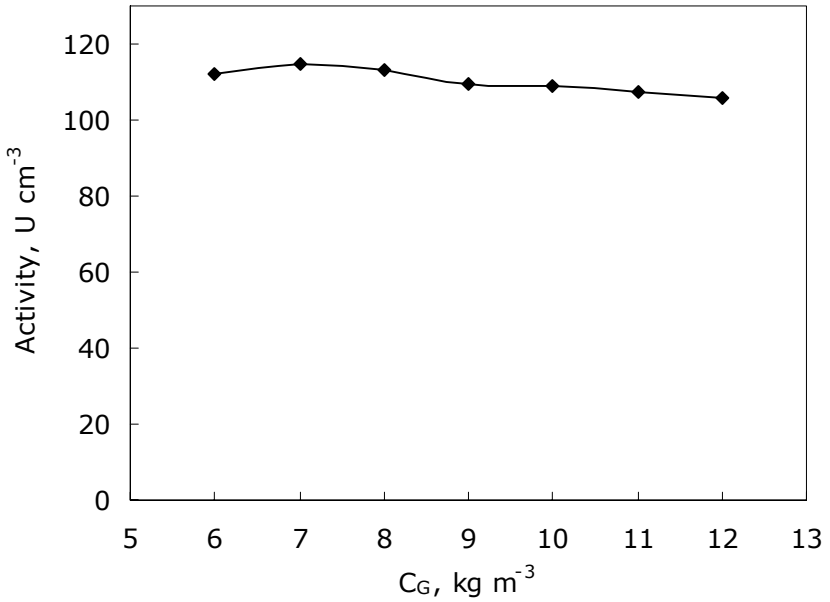

Figure 4.4 The variations in β-lactamase activity with the initial glucose concentration. t=32 h, V=33 cm^3, T=37°C, pH_0 =7.2, N=200 min^{-1}.

4.2.3 The Optimized Medium

As a result, among the investigated media, the highest β-lactamase activity was obtained at T=37°C and pH_0 =7.5 as 115 U cm^{-3}, in the medium containing 7.0 kg m^{-3} glucose, 7.1 kg m^{-3} $(NH_4)_2HPO_4$, and the salt solution which was 2 fold higher than the activity obtained in the RPM.

4.3 Effects of Oxygen Transfer

Using the optimized defined medium, T and pH conditions obtained in the laboratory scale bioreactors the effects of oxygen transfer on fermentation and oxygen transfer characteristics were investigated in the pilot scale bioreactor system by using three agitation rates N = 250, 500, 750 min^{-1} and three air inlet rates Q_0/V_R = 0.2, 0.5, 1 vvm. The effects of oxygen transfer were investigated at seven different conditions with the above values of the Q_0/V_R and N. These conditions were abbreviated as given in Table 4.1 according to the oxygen-transfer conditions applied. Throughout the bioprocess, dissolved oxygen, pH, glucose concentration, cell concentration, β-lactamase activity, amino acid and organic acid concentrations, liquid phase mass transfer coefficient, specific rates and yield coefficients were determined.

Table 4.1 Oxygen transfer conditions

#	Q_0/V_R, vvm	N, min^{-1}	Abbreviation
1	0.2	250	LimOT
2	0.5	250	LOT_1
3	0.2	500	LOT_2
4	0.5	500	MOT_1
5	0.2	750	MOT_2
6	1.0	500	HOT_1
7	0.5	750	HOT_2

4.3.1 Dissolved Oxygen Concentration and pH Profiles

The variations in dissolved oxygen concentration (C_O) and medium pH with the cultivation time, air inlet rate, and agitation rate are shown in Figure 4.5 and 4.6, respectively. C_O depends on the extent of the OTR to the media and the OUR of the cells. When the OTR was very low, i.e. at LimOT and to an extent at LOT_1 conditions the C_O exhibited a sudden drop at the early hours of the fermentation and at t= 1-27 h for LimOT and, at t=2-10.5 h for LOT_1 the transferred oxygen was totally consumed. When the OTR was higher, i.e., at LOT_2, MOT_1, and MOT_2 conditions, a decrease and/or an increase in the dissolved oxygen level with cultivation time was observed depending on the metabolic stage of the growth. Further, at HOT_1 and HOT_2 conditions, although the biomass concentration increased, C_O did not change considerably throughout the bioprocess as the OTR was high enough. Considering the C_O profiles, Q_0/V_R = 0.2 vvm and N =250 min^{-1} (LimOT) is regarded as "limited-oxygen transfer" condition; Q_0/V_R = 0.5 vvm and N =250 min^{-1} (LOT_1), and Q_0/V_R = 0.2 vvm and N =500 min^{-1} (LOT_2) are regarded as "low-oxygen transfer" conditions; Q_0/V_R = 0.5 vvm and N =500 min^{-1} (MOT_1), Q_0/V_R = 0.2 vvm and N =750 min^{-1} (MOT_2) are regarded as "medium oxygen transfer" conditions; and lastly Q_0/V_R = 1.0 vvm and N =500 min^{-1} (HOT_1) and Q_0/V_R = 0.5 vvm and N =750 min^{-1} (HOT_2) are regarded as "high-oxygen transfer" condition.

The initial pH value was pH_0=7.5 for all the conditions. The locus of pH versus time profiles were similar at LOT_2, MOT_1, MOT_2, HOT_1, and HOT_2 conditions, and pH has a tendency to decrease until t=10 h; thereafter, it

reached to the stationary phase. However, at LOT_1 and LimOT conditions the decrease rate of pH was higher than the other conditions. At LimOT condition where the lowest pH was observed, the pH of the fermentation broth decreased until t= 12 h; whereas, at t=12-19 h it was constant; and after t=19 h pH increased.

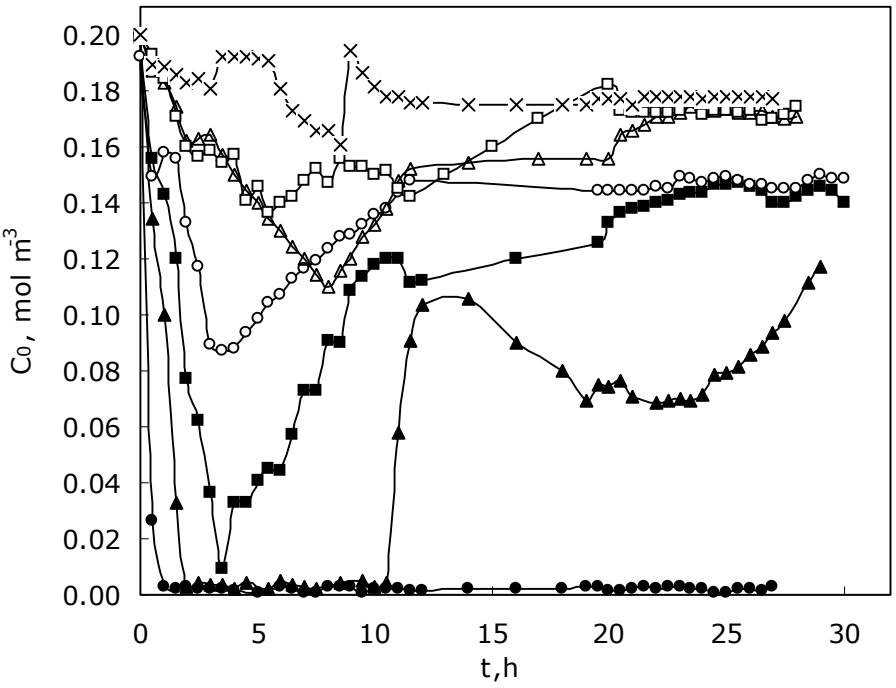

Figure 4.5 The variations in dissolved oxygen concentration with cultivation time. T=37^{0}C, C_0^*= 0.20 mol m^{-3}, V_R= 1.65 * 10^{-3} m^3. LimOT: (●); LOT_1:(▲); LOT_2: (■); MOT_1: (○); MOT_2: (Δ); HOT_1: (□); HOT_2: (x).

In the literature, Çelik and Çalık (2004) reported the variations in pH and dissolved oxygen profiles throughout the β-lactamase production process at 32^{0}C, pH_0 = 6.0, N=500 min^{-1}, and Q_0/V_R = 0.5 vvm in the semi-defined medium. In the above study, pH decreased until t=4.5 h to pH=5.8, thereafter it increased and reached a constant value of pH= 7.6. The C_O decreased suddenly at the early stage of the fermentation and at t= 4.5-7 h the transferred oxygen was totally consumed. Thereafter, the C_O gradually increased. The C_O profile obtained by Çelik and Çalık (2004) and C_O obtained in this work at MOT_1 condition (N=500 min^{-1}, and Q_0/V_R = 0.5 vvm) were similar; however, between

t=4.5-7 h because of the higher cell concentration obtained by Çelik and Çalık (2004) the transferred oxygen was totally consumed; whereas, in this study the dissolved oxygen concentration decreased until t=4 h and then increased.

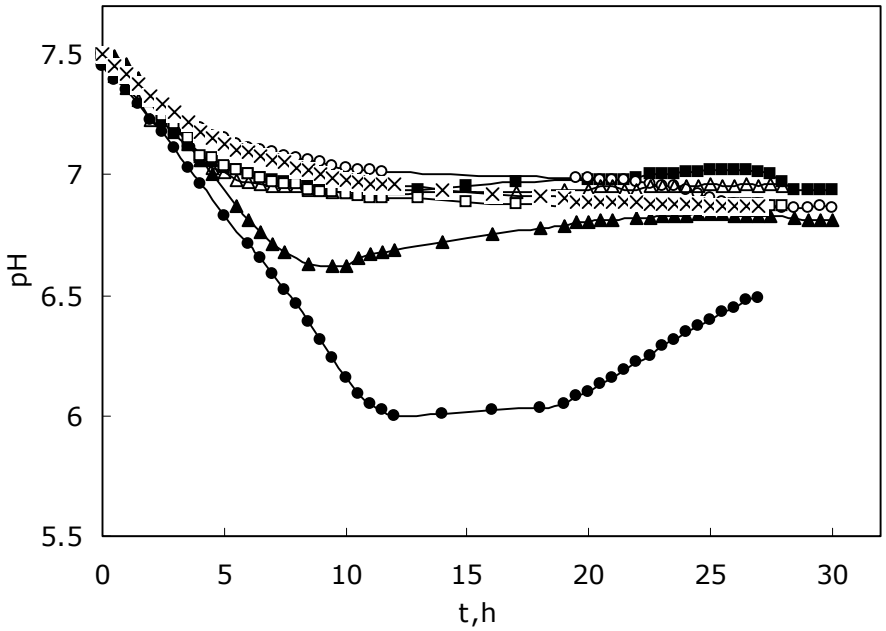

Figure 4.6 The variations in medium pH with cultivation time. C_G^0 = 7.0 kg m^{-3}, T=37^{0}C, V_R= 1.65 * 10^{-3} m^3. LimOT: (●); LOT_1:(▲); LOT_2: (■); MOT_1: (○); MOT_2: (Δ); HOT_1: (□); HOT_2: (x).

4.3.2 Glucose Concentration Profiles

Variations in the glucose concentration with the cultivation time, air inlet rate, and agitation rate are given in Figure 4.7. Glucose concentration (C_G^0 = 7.0 kg m^{-3}), decreased with the cultivation time, as expected. At the end of the bioprocesses, the lowest amount of glucose was attained at LimOT and MOT_1 conditions that correspond to the consumption of %91.5 of the initial glucose. However the rate of glucose consumption was the highest:

1. at t=0-2 h at LOT_1 condition,

2. at t= 2-5 h at LimOT condition;

3. at t= 5-11 h at HOT_2 condition;

4. at t= 11-20 h at LOT_2 condition;

5. at t= 20-28 h at MOT_1 condition.

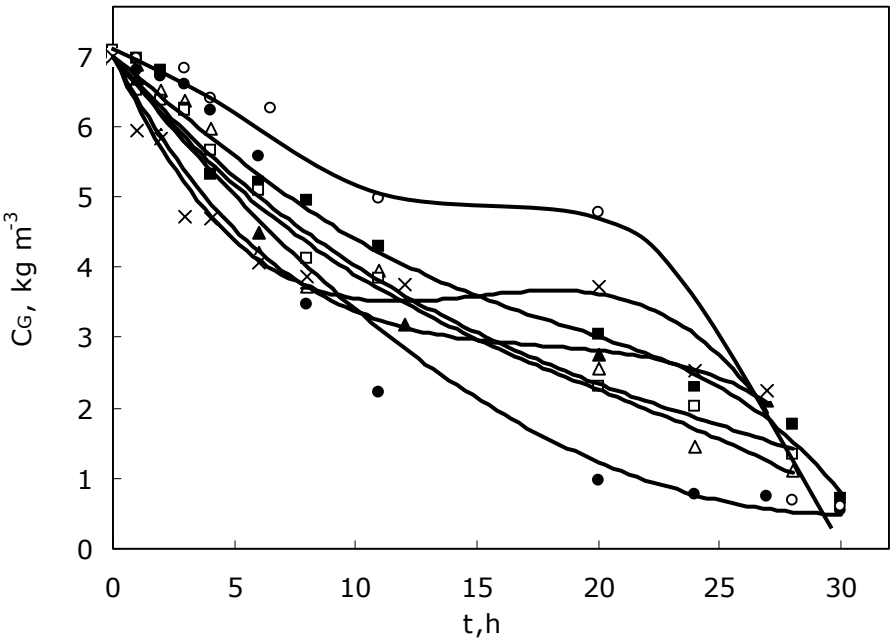

Figure 4.7 The variations in glucose concentration with cultivation time. C_G^0=7.0 kg m^{-3}, T=37°C, V_R= 1.65 * 10^{-3} m^3. LimOT: (●); LOT_1:(▲); LOT_2: (■); MOT_1: (○); MOT_2: (Δ); HOT_1: (□); HOT_2: (x).

4.3.3 Cell Concentration Profiles

The variations in the cell concentration with cultivation time and the oxygen transfer conditions applied are given in Figure 4.8. Cell concentration increased at a high rate between t=2-7 h, and then reached the stationary phase. The highest cell concentrations were obtained at MOT_2 and HOT_2 conditions as C_X= 0.67 kg m^{-3} and the lowest cell concentration was obtained at LimOT and HOT_1 as C_X= 0.54 kg m^{-3}.

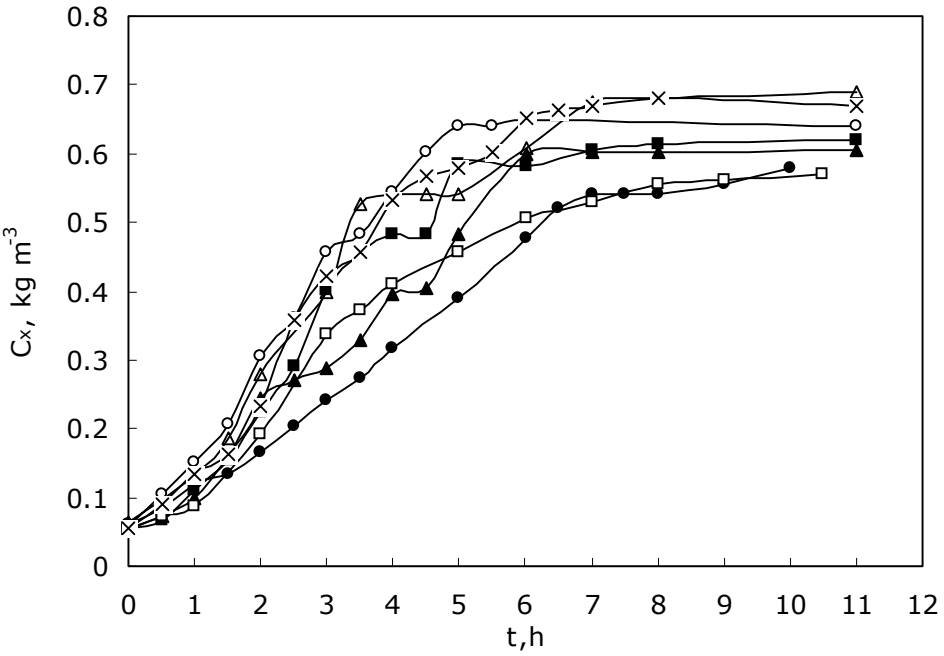

Figure 4.8 The variations in cell concentration with cultivation time. C_G^0=7.0 kg m^{-3} T=37°C, V_R= 1.65 * 10^{-3} m^3. LimOT: (●); LOT_1:(▲); LOT_2: (■); MOT_1: (○); MOT_2: (Δ); HOT_1: (□); HOT_2: (x).

4.3.4 Beta-lactamase Activity Profiles

The variations in β-lactamase activity with the cultivation time, air inlet rate and agitation rate are given in Figure 4.9. As can be seen from Figure 4.9 the lowest β-lactamase activity was obtained at LimOT condition where the lowest cell concentration was obtained. At MOT_1 condition β-lactamase activity was higher than the other conditions throughout the process but at t=24 h LOT_2 and MOT_1 gave all most the same β-lactamase activity values ca. A=90 U cm^{-3}. In the process the cultivation time in which the highest β-lactamase activity was obtained shifted 1.33-fold to an earlier cultivation time (t=24h) compared to the laboratory scale experiments (t=32h) with a cost of 22 % lower activity.

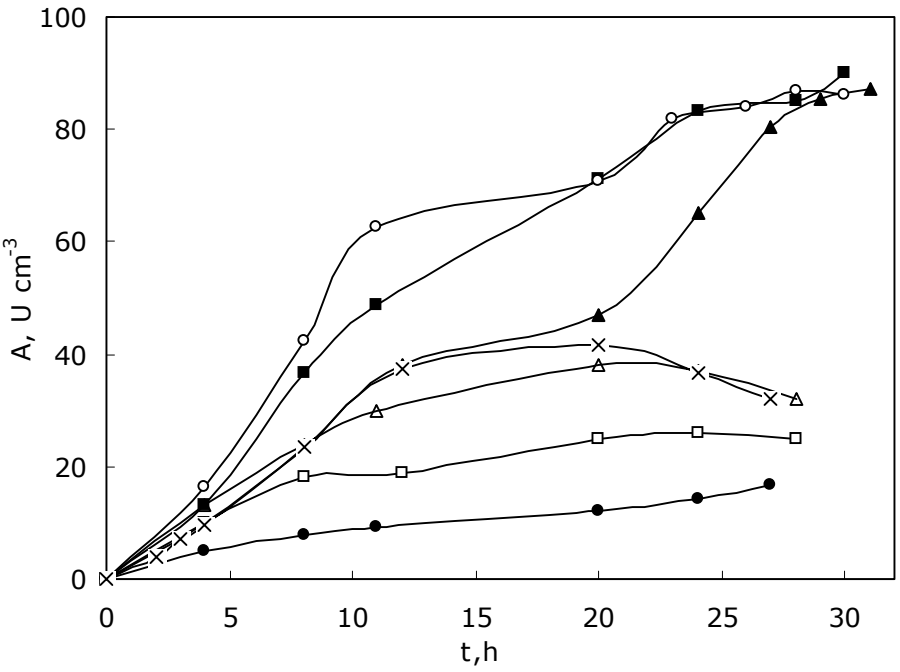

Figure 4.9 The variations in β-lactamase activity with cultivation time. C_G^0=7.0 kg m^{-3}, T=37°C, V_R= 1.65 * 10^{-3} m^3. LimOT: (●); LOT_1:(▲); LOT_2: (■); MOT_1: (○); MOT_2: (Δ); HOT_1: (□); HOT_2: (x).

4.3.5 Amino Acid Concentrations

The oxygen transfer conditions influenced the amino acids synthesis and their concentrations in the fermentation broth, as the synthesis of some of them might be the rate limiting step(s) in the metabolic reaction network in β-lactamase synthesis. For the production of proteins, regulation of the metabolic reaction network should cause good coupling of supply and demand for the amino acids (Çalık et al., 2000).

The variations in amino acid concentrations in the fermentation broth with cultivation time and for seven different oxygen transfer conditions applied were given in Table 4.2.a, 4.2.b, 4.2.c, 4.2.d, 4.2.e, 4.2.f, 4.2.g. At all the oxygen transfer conditions, generally aspartic acid and the asparagine were the amino acids detected in the broth.

At LimOT condition all the amino acids but glutamic acid, histidine, proline, tyrosine, valine, methionine, cystein, isoleucine and lysine were present

in the fermentation broth. Nevertheless, at LOT_1 condition besides these amino acids; phenlylalanine was not present in the fermentation broth; while at LOT_2 condition arginine, threonine, alanine, valine, methionine, cystein, ornithine, tyrptophan and lysine were not detected in the fermentation broth. At MOT_1 condition glutamic acid, threonine, alanine, tyrosine, isoleucine, leucine and lysine; at MOT_2 condition glutamic acid, glycine, threonine, alanine, tyrosine, ornithine, tyrptophan and lysine; at HOT_1 condition glutamic acid, threonine, alanine, tyrosine, isoleucine, leucine and lysine and lastly at HOT_2 condition glutamic acid, tyrosine, valine, methionine, cystein isoleucine and lysine were not present in the fermentation broth. In general the amino acid concentrations in the fermentation broth was low and considering all the amino acid profiles and oxygen transfer conditions, arginine concentration was the highest at LimOT condition obtained as 0.072 kg m^{-3} at t=3 h.

As it is seen from the Table 4.2.a, 4.2.b, 4.2.c, 4.2.d, 4.2.e, 4.2.f, and 4.2.g the total amino acid concentration excreted to the fermentation broth was maximum at LOT_2 condition at t=24 h as T_{AA} = 0.133 kg m^{-3} and minimum at HOT_1 condition at t=20 h as T_{AA} = 0.001 kg m^{-3}. At LimOT condition (Table 4.2.a) total amino acid concentration decreased sharply between t=3-5 h and then it was almost constant throughout the fermentation at 0.010 kg m^{-3}, nevertheless at LOT_1 condition (Table 4.2.b) it increased between t=3-11 and gave a maximum at t=11 h and then decreased until t=20 h and reached a constant value between t= 20-24 h. At MOT_1 condition (Table 4.2.c) total amino acid concentration decreased between t=3-11 h and then increased and gave a maximum at t= 20 h. In general at HOT_1 and HOT_2 conditions total amino acid concentrations were less than the other conditions and these conditions showed similar profiles that is, total amino acid concentration decreased between t=3-20 h and then showed a little increase between t= 20-24 h.

Table 4.2.a The variations in amino acid concentrations in the fermentation broth with the cultivation time at LimOT condition.

	Cultivation time, h				
C_{AA}, kg m^{-3}	3	5	11	20	24
Asn		0.003	0.002	0.003	0.004
Asp		0.004			0.007
Gln				0.001	
Ser				0.002	
Gly	0.006			0.003	
Arg	0.072				
Thr	0.003				
Ala	0.003				
Leu	0.003		0.003	0.003	0.003
Phe	0.007				
Trp	0.007				
Total	**0.101**	**0.007**	**0.005**	**0.012**	**0.014**

Table 4.2.b The variations in amino acid concentrations in the fermentation broth with the cultivation time at LOT_1 condition.

	Cultivation time, h				
C_{AA}, kg m^{-3}	3	5	11	20	24
Asn	0.001	0.002	0.002	0.002	0.010
Asp		0.001	0.005	0.002	0.007
Gln		0.001	0.003	0.002	0.001
Ser		0.001	0.002	0.002	
Gly	0.003	0.001	0.006	0.003	
His					
Arg			0.014		
Thr	0.001		0.010		
Ala			0.009		
Leu	0.004	0.006	0.007	0.006	0.006
Phe					
Trp		0.028	0.010	0.003	
Total	**0.009**	**0.040**	**0.068**	**0.020**	**0.024**

Table 4.2.c The variations in amino acid concentrations in the fermentation broth with the cultivation time at LOT_2 condition.

	Cultivation time, h				
C_{AA}, kg m^{-3}	3	5	11	20	24
Asn	0.003			0.006	0.006
Asp	0.003	0.006	0.006		0.022
Glu				0.007	0.013
Gln					0.003
Ser					0.002
Gly		0.002		0.003	
His					0.034
Pro		0.004			0.011
Tyr					0.006
Ile				0.004	0.023
Leu			0.003	0.005	0.010
Phe				0.003	0.003
Total	**0.006**	**0.012**	**0.009**	**0.028**	**0.133**

Table 4.2.d The variations in amino acid concentrations in the fermentation broth with the cultivation time at MOT_1 condition.

	Cultivation time, h				
C_{AA}, kg m^{-3}	3	5	11	20	24
Asn	0.009	0.002	0.001	0.003	0.002
Asp	0.003	0.002	0.003	0.025	0.004
Gln			0.001		
Ser	0.001	0.001	0.001		0.001
Gly		0.001	0.001		0.001
His	0.008				0.003
Arg		0.008			
Pro			0.007	0.018	
Val	0.003	0.003	0.003	0.005	0.003
Met	0.002	0.003	0.003	0.005	0.003
Cys	0.002	0.003	0.002	0.006	0.002
Phe	0.005	0.006		0.004	
Trp	0.002	0.001			
Total	**0.035**	**0.030**	**0.022**	**0.066**	**0..019**

Table 4.2.e The variations in amino acid concentrations in the fermentation broth with the cultivation time at MOT_2 condition.

	Cultivation time, h				
C_{AA}, kg m^{-3}	3	5	11	20	24
Asn	0.008	0.004			0.004
Asp	0.005				
Gln		0.001			
His		0.017		0.008	
Arg	0.028				
Pro		0.003			0.003
Val		0.006		0.001	
Met		0.006			
Cys		0.001			
Leu		0.004	0.002		0.003
Phe		0.004			
Total	**0.041**	**0.046**	**0.002**	**0.009**	**0.010**

Table 4.2.f The variations in amino acid concentrations in the fermentation broth with the cultivation time at HOT_1 condition.

	Cultivation time, h				
C_{AA}, kg m^{-3}	3	5	11	20	24
Asn	0.005		0.002		0.007
Asp		0.012			
Gly	0.001		0.002		
His			0.003		
Arg	0.018				
Thr		0.003	0.001		
Ala		0.004	0.001		
Pro	0.006				
Ile	0.001				0.002
Leu					0.001
Phe		0.001	0.002	0.001	0.002
Total	**0.031**	**0.020**	**0.011**	**0.001**	**0.012**

Table 4.2.g The variations in amino acid concentrations in the fermentation broth with the cultivation time at HOT_2 condition.

	Cultivation time, h				
C_{AA}, kg m^{-3}	3	5	11	20	24
Asn	0.002	0.001	0.001	0.003	0.003
Asp		0.002		0.003	0.002
Gln	0.001				
Gly	0.005				0.002
His		0.001			
Arg					
Thr	0.002				0.001
Ala	0.001				
Leu	0.007	0.007	0.008		0.007
Phe	0.004				
Trp	0.006		0.002		0.002
Total	**0.028**	**0.011**	**0.011**	**0.006**	**0.017**

4.3.6 Organic Acid Concentrations

Since oxygen acts as the driving force in the TCA cycle and the rate of the TCA cycle is influenced by the oxygen transfer conditions in the metabolic reaction network (Çalık et al., 2000), the synthesis of the TCA cycle organic acids, acetic acid and lactic acid are important for increasing the yield and the selectivity. At all the oxygen transfer conditions, generally acetic acid and lactic acid are the organic acids detected in the broth at high concentrations. The variations of organic acid concentrations with the cultivation time and oxygen-transfer conditions are shown in Table 4.3. At LimOT condition, at t=3, 5, 11, 20 h, the organic acid having the highest concentration was lactic acid in contrast to the other oxygen transfer conditions applied, as at all the others acetic acid was the main organic acid excreted to the fermentation broth. At LimOT condition at t=11 h lactic acid was excreted having the concentration of 1.464 kg m^{-3} which was the highest value obtained throughout the bioprocesses.

Table 4.3 The variations in organic acid concentrations in the fermentation broth with the cultivation time at LimOT, LOT_1, LOT_2 MOT_1, MOT_2, HOT_1, and HOT_2 conditions.

Condition	T (h)	C_{OA}, kg m^{-3}						
		Cit	αKG	Suc	Ac	Lac	But	Gluc
LimOT	3				0.267	0.325		
	5				0.507	1.112	0.003	
	11		0.009	0.020	0.344	1.464		
	20		0.176		0.899	1.436	0.002	
	24				1.290	0.968		
LOT_1	3				0.391	0.185		
	5				0.664	0.667	0.002	
	11			0.007	0.987	0.636		
	20			0.013	0.577	0.386		
	24			0.007	0.362	0.218		
LOT_2	3				0.339	0.041		
	5				0.620	0.035		
	11				0.667	0.012		
	20				0.405			
	24				0.241			
MOT_1	3				0.432	0.010		0.006
	5				0.553	0.017		0.009
	11	0.016			0.550	0.020	0.023	
	20				0.675	0.061	0.019	
	24				0.392	0.043	0.006	
MOT_2	3				0.607			
	5				0.858		0.006	
	11				1.248			
	20				0.548			0.002
	24				0.508		0.025	
HOT_1	3				0.642		0.006	
	5				0.647			0.001
	11				1.254		0.019	
	20				0.811		0.011	
	24				0.592		0.029	
HOT_2	3				0.616	0.049	0.030	
	5				0.719	0.009		0.004
	11				0.688		0.017	
	20				0.664	0.046	0.021	
	24				0.324	0.028		

The variations in total organic acid concentration with the cultivation time and the oxygen transfer conditions are given in Figure 4.10. As it is seen in the figure, the total organic acid concentration excreted to the fermentation broth was maximum at LimOT condition at t=20 h as T_{OA} = 2.513 kg m^{-3}, explaining the reason of the highest rate of decrease in the medium pH at these condition and minimum at HOT_2 condition at t=24 h as T_{OA} = 0.352 kg m^{-3}. Total organic acid concentrations as well as the non-detected organic acids can be seen in Table 4.4. As it is clear in Table 4.4 at LOT_2, MOT_1, MOT_2, HOT_1 and HOT_2 conditions, the TCA cycle organic acids α-ketoglutaric acid and succinic acid were not detected in the fermentation broth. Nevertheless, under LimOT condition α-ketoglutaric and succinic acids and under LOT_1 condition succinic acid were excreted to the fermentation broth. Under the lower range of oxygen transfer conditions, LimOT and LOT_1, due to the insufficient operation of TCA cycle α-ketoglutaric and succinic acids were excreted to the fermentation broth.

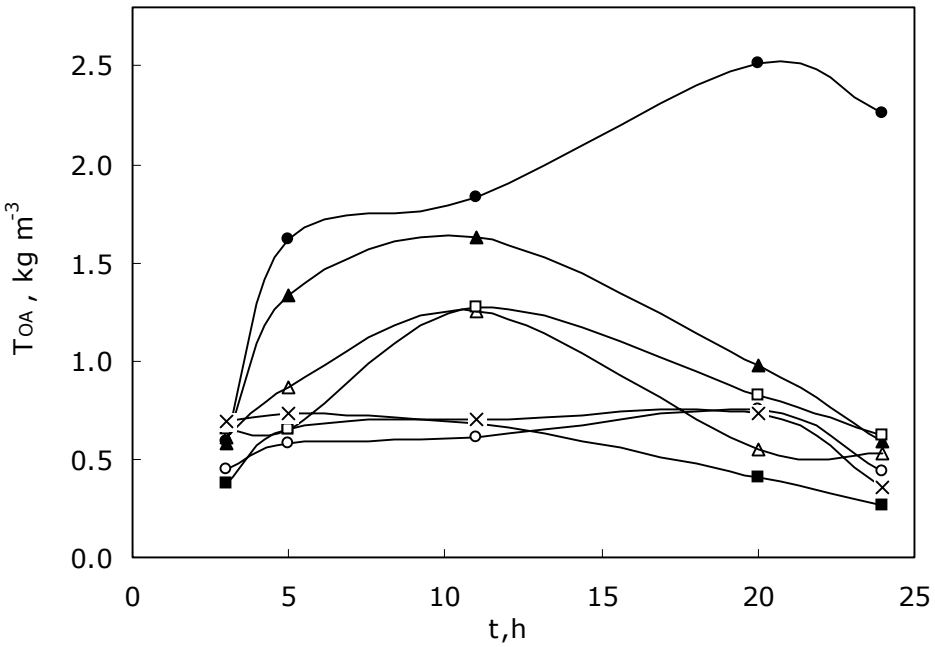

Figure 4.10 The variations in total organic acid concentration with cultivation time. C_G^0=7.0 kg m^{-3}, T=37°C, V_R= 1.65 * 10^{-3} m^3. LimOT: (●); LOT_1:(▲); LOT_2: (■); MOT_1: (○); MOT_2: (Δ); HOT_1: (□); HOT_2: (x).

Table 4.4 The variations of total organic acid concentration and non-excreted organic acids with the constant air inlet and agitation rates.

Oxygen-transfer condition	T_{OA} (kg m^{-3})	Non-excreted organic acids
LimOT	0.592-2.513	citric, pyruvic, gluconic acids
LOT_1	0.576-1.630	citric, pyruvic, α-KG, gluconic acids
LOT_2	0.268-0.679	citric, pyruvic, α-KG, gluconic, succinic acids
MOT_1	0.441-0.755	pyruvic, α-KG, succinic acids
MOT_2	0.533-1.248	citric, pyruvic, α-KG, lactic, succinic acids
HOT_1	0.621-1.273	citric, pyruvic, α-KG, lactic, succinic acids
HOT_2	0.352-0.732	citric, pyruvic, α-KG, succinic acids

4.3.7 Oxygen Transfer Characteristics

In β-lactamase production by *Bacillus licheniformis* in a defined medium, the Dynamic Method was applied to find the oxygen transfer parameters, i.e., oxygen uptake rate (OUR), r_0, and oxygen transfer coefficient, K_La, during the cultivation times corresponding to the characteristic regions of the batch bioprocess, for different oxygen transfer conditions applied. At t<0 h, the physical oxygen transfer coefficient K_La_o was measured in the medium in the absence of the microorganism. The variations in K_La, oxygen uptake rate, oxygen transfer rate and the enhancement factor E ($=K_La/K_La_o$) throughout the bioprocess are given in Table 4.5.a and 4.5.b. As dissolved oxygen concentration in the medium was very low between t=1-27 h at LimOT, between t=2-11 h at LOT_1, between t=1-8 h at LOT_2 conditions, the Dynamic Method could not be applied. For LimOT, LOT_1, and LOT_2 conditions the following assumption was used :

* $E=1$ and $K_La_0=K_La$,

to calculate the OTR. When mass transfer is accompanied by a chemical reaction, enhancement factor can be enhanced several-fold depending on the relative rates of mass transfer and chemical reaction; therefore, obtained OTR values can be considered as the lowest OTR values.

4.3.7.1 Volumetric Oxygen Transfer Coefficient

As can be seen from Table 4.5.a and Table 4.5.b, throughout the bioprocess in general K_La increased and then decreased at MOT_1 and MOT_2 conditions; however, at LOT_1, LOT_2, HOT_1, and HOT_2 it gradually increased with the residence time. K_La depends on agitation rate, temperature, rheological properties of the fermentation medium, and presence of fine particles in the mass transfer zone. Since temperature and agitation rate were kept constant throughout the bioprocess, the reason for the change in K_La could be the change in the viscosity of the medium due to the secreted metabolites and growth.

Average K_La value increased with the increase in the agitation and aeration rates as expected and when compared with the gas flow rate, the agitation rate was a more effective parameter for increasing the oxygen transfer coefficient. The highest oxygen transfer coefficient was obtained at HOT_2 condition as 0.044 s^{-1} at t=2 and t=20 h of the cultivation time.

In general the enhancement factors E were slightly higher than 1.0, showing that a slow reaction is accompanied by mass transfer as expected in most of the fermentation processes accomplished in stirred bioreactors and they did not show a significant difference at oxygen transfer conditions applied and changed in the range E= 1.0-2.1.

The K_La values were also calculated from the correlations (Eq 4.1) with the corresponding constants given in Table 2.5. The variations in oxygen transfer coefficients obtained from correlations with the average experimental values are given in Table 4.6. There is a fairly good agreement between the experimental and correlated values for coelescing bubbles (Eq 1-4) given by Moo-Young and Blanch (1981), within the agitation and air-inlet rate range used. Average experimental values were used for comparison because of the dynamic behavior of the fermentation media, which could not be correlated for the entire fermentation process.

$$K_L a = k\left(\frac{P_G}{V_R}\right)^{\beta} V_s^{\alpha} \qquad (4.1)$$

In the calculations, the power input P_G in aerated stirred liquid was calculated from the following correlation (Rose, 1981):

$$\log(P_G / P) = -192(D_I / D)^{4.38} \mathrm{Re}^{0.115} Fr^{1.95 D_I / D} Ae \qquad (4.2)$$

The power input in gas free stirred liquid was calculated from the Equation 4.5 given below (Nielsen and Villadsen, 1994):

$$P = N_p \rho_l N^3 D_I^{\ 5} \qquad (4.3)$$

The power number was obtained from Reynolds number versus Power number graph given in Figure 4.11 (Nielsen and Villadsen, 1994).

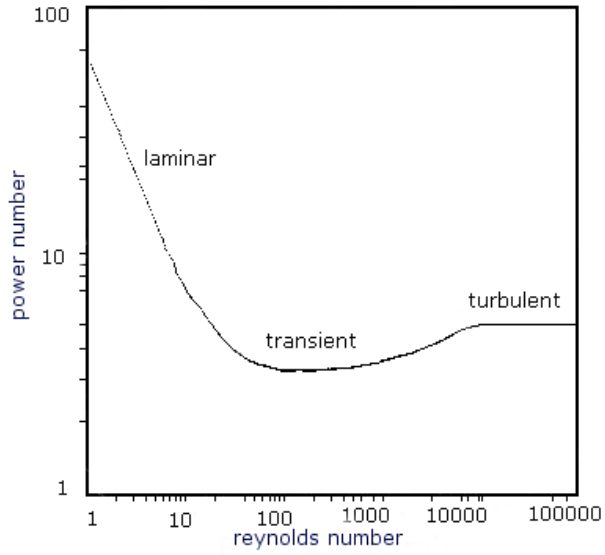

Figure 4.11 Correlation between the power number and the reynolds number for a bioreactor system with one-six bladed Rushton turbine impeller and baffles.

4.3.7.2 Oxygen Uptake Rate

Increase in substrate consumption rate, cell concentration, and cell production rate, increased the oxygen uptake rate (OUR), which depends on the metabolic functions of the cell.

As expected, at the early stage of the fermentation OUR tend to increase at all conditions, mainly as a result of increase in the cell production rate, the cell concentration and the substrate consumption rates. Generally, after t=11 h as the biomass production rate decreased, OUR also decreased. The highest OUR was observed at LOT_2 condition at t=5 h as $1.6*10^{-3}$ mol $m^{-3}s^{-1}$.

In order to compare mass transfer and biochemical reaction rates in the β-lactamase production process by *B. licheniformis* which was investigated under seven different constant oxygen transfer conditions, the maximum possible oxygen utilization rate ($OD=\mu_{max}C_X/Y_{X/O}$) and the maximum possible mass transfer rate ($OTR_{max}=K_La{C_O}^*$) were calculated throughout the bioprocess. A kind of Damköhler number, Da, defined as maximum possible oxygen utilization rate per maximum mass transfer rate (Çalık et al., 2000 and 2003); and effectiveness factor, η, defined as the oxygen uptake rate per maximum possible oxygen utilization rate values (Çalık et al., 2000 and 2003) can be seen in Table 4.5.a and 4.5.b.

It is clear in Table 4.5.a that, LimOT, LOT_1 and LOT_2 conditions, were mass-transfer limited conditions (Da>>1). While, at MOT_1, MOT_2, HOT_1, and HOT_2 conditions, at=2-8 h the mass-transfer resistance was more effective (Da>>1).

As it is apparent from Table 4.5.a and Table 4.5.b, the high effectiveness factor, η, values until t=5 h indicate that the cells are consuming oxygen with such a high rate that maximum possible oxygen utilization (OD) value is approached and thereafter the decrease in η indicates that the cells are consuming lower oxygen than the oxygen demand (OD).

Table 4.5.a The variations in oxygen transfer parameters with cultivation time at LimOT. LOT_1 and LOT_2 conditions

Condition	t (h)	K_La (s^{-1})	E K_La/K_La_0	OTR*10^3 (mol $m^{-3}s^{-1}$)	OTR_{max}*10^3 (mol $m^{-3}s^{-1}$)	OUR*10^3 (mol $m^{-3}s^{-1}$)	OD*10^3 (mol $m^{-3}s^{-1}$)	Da OD/OTR_{max}	η OUR/OD
	2*	0.007	1.000	1.379	1.400	1.379	4.105	2.932	0.336
	5*	0.007	1.000	1.393	1.400	1.393	8.071	5.765	0.173
	8*	0.007	1.000	1.379	1.400	1.379	77.445	55.318	0.018
LIMOT	11*	0.007	1.000	1.386	1.400	1.386			
	20*	0.007	1.000	1.393	1.400	1.393			
	24*	0.007	1.000	1.386	1.400	1.386			
	28*	0.007	1.000	1.400	1.400	1.400			
	2*	0.008	1.000	1.576	1.600	1.576	4.380	2.737	0.361
	5*	0.008	1.000	1.576	1.600	1.576	19.668	12.293	0.080
	8*	0.008	1.000	1.576	1.600	1.576			
LOT_1	11*	0.008	1.000	1.139	1.600	1.139			
	20	0.014	1.775	1.789	2.840	0.500			
	24	0.014	1.750	1.800	2.800	0.500			
	28	0.017	2.075	1.594	3.320	0.400			
	2*	0.010	1.000	1.220	2.000	1.300	1.983	0.991	0.656
	5*	0.010	1.000	1.596	2.000	1.600	32.725	16.363	0.049
	8*	0.010	1.000	1.092	2.000	1.000	63.440	31.720	0.016
LOT_2	11	0.013	1.300	1.043	2.600	1.000			
	20	0.014	1.410	0.948	2.820	0.800			
	24	0.016	1.630	0.919	3.260	0.700			
	28	0.021	2.100	1.218	4.200	0.700			

Table 4.5.b The variations in oxygen transfer parameters with the cultivation time at MOT_1. MOT_2. HOT_1 and HOT_2 conditions.

Condition	t (h)	K_La (s^{-1})	E K_La/K_La_0	OTR*10^5 (mol $m^{-3}s^{-1}$)	OTRmax*10^5 (mol $m^{-3}s^{-1}$)	OUR*10^5 (mol $m^{-3}s^{-1}$)	OD*10^5 (mol $m^{-3}s^{-1}$)	Da OD/OTR_{max}	η OUR/OD
	2	0.016	1.090	1.055	3.160	0.900	1.934	0.612	0.465
	5	0.018	1.228	1.808	3.560	1.100	18.304	5.142	0.060
	8	0.026	1.807	1.996	5.240	1.000			
MOT_1	11	0.026	1.807	1.483	5.240	0.900			
	20	0.020	1.379	1.112	4.000	0.900			
	24	0.022	1.517	1.162	4.400	0.900			
	28	0.022	1.517	1.214	4.400	0.900			
	2	0.020	1.058	0.752	4.000	1.000	2.427	0.607	0.412
	5	0.022	1.173	1.330	4.434	1.500	12.034	2.714	0.125
	8	0.023	1.217	2.070	4.600	1.300			
MOT_2	11	0.024	1.265	1.243	4.780	1.200			
	20	0.024	1.249	1.038	4.720	1.000			
	24	0.033	1.746	0.904	6.600	0.800			
	28	0.028	1.455	0.798	5.500	0.800			
	2	0.019	1.000	0.760	3.800	1.100	1.811	0.477	0.607
	5	0.019	1.000	1.028	3.800	0.800	6.379	1.679	0.125
	8	0.019	1.000	1.011	3.800	0.700	13.347	3.512	0.052
HOT_1	11	0.019	1.000	1.048	3.800	0.600			
	20	0.020	1.053	0.352	4.000	0.600			
	24	0.029	1.526	0.829	5.800	0.600			
	28	0.036	1.895	0.936	7.200	0.600			
	2	0.044	1.758	0.753	8.860	1.000	1.040	0.117	0.962
	5	0.035	1.389	0.294	7.000	1.200	36.192	5.170	0.033
HOT_2	8	0.030	1.198	1.045	6.040	0.900			
	11	0.029	1.151	0.638	5.800	0.900			
	20	0.044	1.746	1.021	8.800	0.900			

Table 4.6 The variations in oxygen transfer coefficients obtained from different correlations and the average experimental value.

Conditions	$K_La.\ s^{-1}$								
	Exp	Eq 1	Eq 2	Eq 3	Eq 4	Eq 5	Eq 6	Eq 7	Eq 8
LimOT	**0.007**	0.005	0.005	0.006	0.005	0.007	0.018	0.012	0.046
LOT_1	**0.011**	0.007	0.007	0.008	0.007	0.009	0.020	0.016	0.053
LOT_2	**0.016**	0.010	0.018	0.015	0.011	0.031	0.074	0.031	0.194
MOT_1	**0.021**	0.016	0.024	0.021	0.016	0.038	0.082	0.042	0.215
MOT_2	**0.025**	0.017	0.036	0.027	0.017	0.071	0.169	0.054	0.215
HOT_1	**0.023**	0.020	0.029	0.025	0.021	0.040	0.082	0.050	0.444
HOT_2	**0.036**	0.024	0.048	0.036	0.025	0.083	0.181	0.072	0.475

4.3.8 Specific Rates and Yield Coefficients

The variations in the specific growth rate, μ, the specific oxygen uptake rate, q_o, the specific substrate consumption rate, q_s, the specific product formation rate, q_P, and the yield coefficients with cultivation time are given in Table 4.7.a and 4.7.b. The variations in the specific growth rate with the cultivation time are given in Figure 4.12 and as can be seen from the figure at all the oxygen transfer conditions applied the specific growth rates decreased in the logarithmic growth phase, and in general at t=7 h μ=0 h^{-1}. The maximum specific growth rate of μ_{max}=1.04 h^{-1} was obtained at t=1 h at LOT_1 condition. The variations in specific substrate consumption, specific oxygen uptake and specific β-lactamase production rates with cultivation time are given in Figures 4.13. 4.14 and 4.15 respectively. As seen in Figure 4.13, the specific substrate consumption rates first decreased and then increased at all the conditions except, LimOT and HOT_1 at which they gradually decreased throughout the fermentation. The highest value of q_S was obtained at t=2 h of LOT_1 condition as 2.17 kg kg^{-1} h^{-1}; where the lowest value was obtained at t=28 h of LimOT and HOT_1 conditions as 0.07 kg kg^{-1} h^{-1}. However, the specific oxygen uptake rates decreased throughout the bioprocess due to the increased cell concentration and gave a maximum at LimOT condition at t=2 h as q_0=0.94 kg kg^{-1} h^{-1} and a minimum at LOT_1 condition at t=28 h as q_0=0.08 kg kg^{-1} h^{-1}. As can be seen in Figure 4.15, in the β-lactamase formation the specific production rate decreased throughout the process at all the oxygen transfer conditions applied but at LimOT and LOT_1 conditions after t=20 h the specific production rate again began to increase. The highest value of q_p was obtained at t=0.5 h at LOT_2 condition as $69.5*10^6$ U kg^{-1} h^{-1}.

The yield of cell on substrate and the yield of cell on oxygen decreased with the cultivation time at all the oxygen transfer conditions applied, however at LimOT condition they increased between t=2-5 h. The highest $Y_{X/S}$ value was obtained at MOT_1 condition at t=2 h as $Y_{X/S}$=0.72 kg kg^{-1} and the yield of cell on oxygen reached a maximum, $Y_{X/O}$=1.49 kg kg^{-1}, at t=2 h at MOT_1 condition. Nevertheless, the yield of substrate on oxygen showed a decrease and/or an increase throughout the fermentation and gave the highest value at HOT_2 condition at t=20 h as $Y_{S/O}$=8.07 kg kg^{-1}.

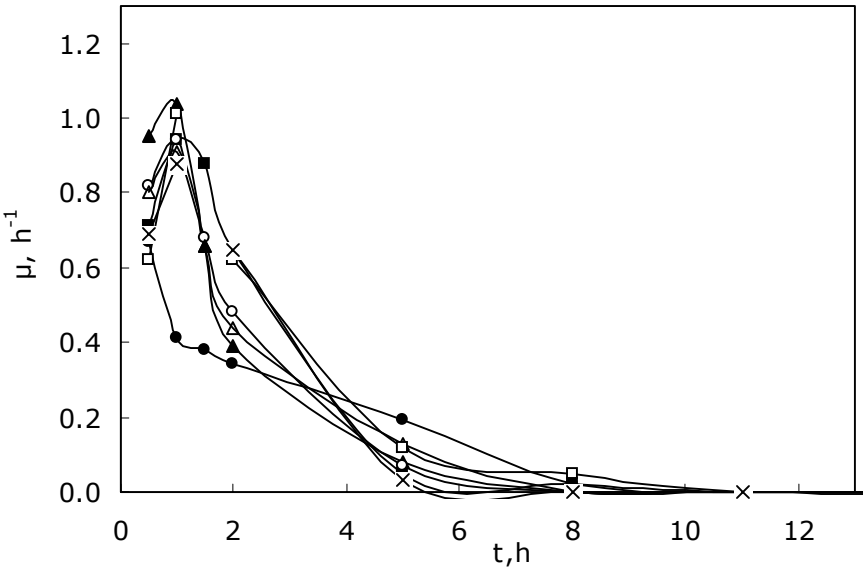

Figure 4.12 The variations in the specific growth rate with the cultivation time. C_G^0=7.0 kg m^{-3}, T=37°C, V_R= 1.65 * 10^{-3} m^3. LimOT: (●); LOT_1:(▲); LOT_2: (■); MOT_1: (○); MOT_2: (Δ); HOT_1: (□); HOT_2: (x).

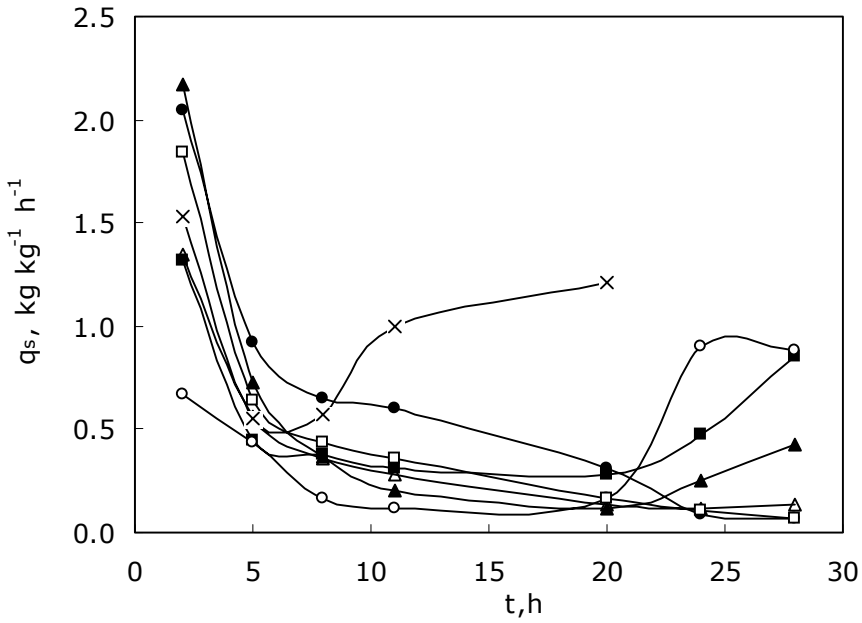

Figure 4.13 The variations in the specific substrate consumption rate with the cultivation time. C_G^0=7.0 kg m^{-3}, T=37°C, V_R= 1.65 * 10^{-3} m^3. LimOT: (●); LOT_1:(▲); LOT_2: (■); MOT_1: (○); MOT_2: (Δ); HOT_1: (□); HOT_2: (x).

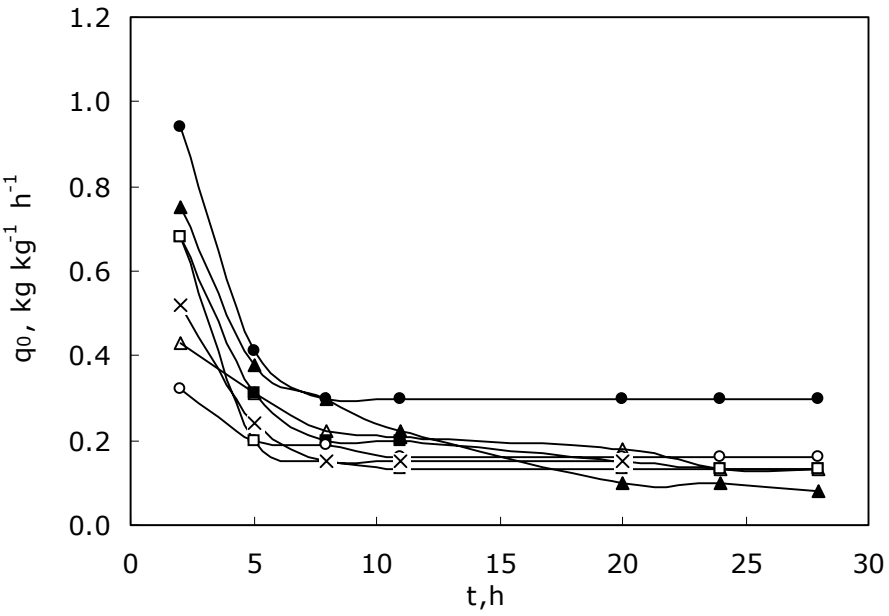

Figure 4.14 The variations in the specific oxygen uptake rate with the cultivation time. C_G^0=7.0 kg m^{-3}, T=37°C, V_R= 1.65 * 10^{-3} m^3, LimOT: (●); LOT_1:(▲); LOT_2: (■); MOT_1: (○); MOT_2: (Δ); HOT_1: (□); HOT_2: (x).

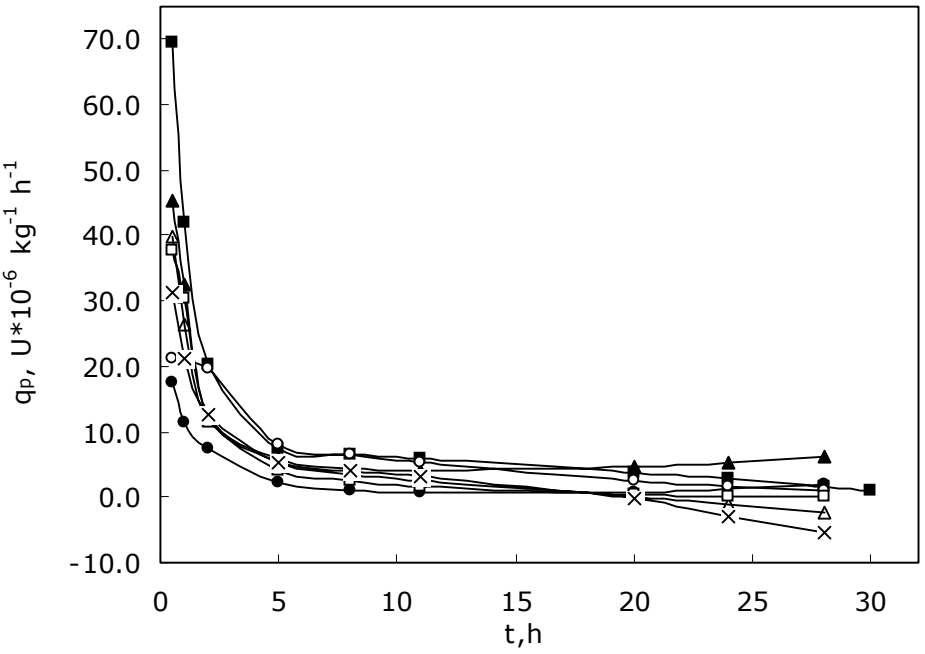

Figure 4.15 The variations in the specific β-lactamase production rate with the cultivation time. C_G^0=7.0 kg m^{-3}, T=37°C, V_R= 1.65 * 10^{-3} m^3. LimOT: (●); LOT_1:(▲); LOT_2: (■); MOT_1: (○); MOT_2: (Δ); HOT_1: (□); HOT_2: (x).

Table 4.7.a The variations in the specific rates and yield coefficients with the cultivation time at LimOT. LOT_1 and LOT_2 condition.

Condition	t (h)	C_x (kg m^{-3})	μ (h^{-1})	r_o (kg O_2 m^{-3} h^{-1})	q_0 (kg kg^{-1} h^{-1})	q_s (kg kg^{-1} h^{-1})	q_P*10^{-6} (U kg^{-1} h^{-1})	$Y_{x/o}$ (kg kg^{-1})	$Y_{x/s}$ (kg kg^{-1})	$Y_{s/o}$ (kg kg^{-1})
LimOT	2	0.17	0.34	0.16	0.94	2.04	7.47	0.36	0.17	2.17
	5	0.39	0.19	0.16	0.41	0.92	2.19	0.46	0.21	2.24
	8	0.54	0.02	0.16	0.30	0.65	1.04	0.07	0.03	2.17
	11	0.54	0.00	0.16	0.30	0.60	0.68	0.00	0.00	2.03
	20	0.54	0.00	0.16	0.30	0.31	0.69	0.00	0.00	1.05
	24	0.54	0.00	0.16	0.30	0.09	1.21	0.00	0.00	0.30
	28	0.54	0.00	0.16	0.30	0.07	2.04	0.00	0.00	0.24
LOT_1	2	0.24	0.39	0.18	0.75	2.17	12.7	0.52	0.18	2.89
	5	0.48	0.08	0.18	0.38	0.73	5.79	0.21	0.11	1.92
	8	0.60	0.00	0.18	0.30	0.37	4.32	0.00	0.00	1.23
	11	0.60	0.00	0.13	0.22	0.20	4.16	0.00	0.00	0.91
	20	0.60	0.00	0.06	0.10	0.12	4.63	0.00	0.00	1.20
	24	0.60	0.00	0.06	0.10	0.25	5.31	0.00	0.00	2.50
	28	0.60	0.00	0.05	0.08	0.43	6.28	0.00	0.00	5.38
LOT_2	2	0.22	0.65	0.15	0.68	1.32	20.36	0.95	0.49	1.94
	5	0.59	0.05	0.18	0.31	0.45	7.47	0.16	0.11	1.45
	8	0.61	0.02	0.12	0.20	0.38	6.52	0.10	0.05	1.90
	11	0.61	0.00	0.12	0.20	0.31	5.86	0.00	0.00	1.55
	20	0.61	0.00	0.09	0.15	0.28	3.90	0.00	0.00	1.87
	24	0.61	0.00	0.08	0.13	0.47	2.87	0.00	0.00	3.62
	28	0.61	0.00	0.08	0.13	0.85	1.75	0.00	0.00	6.54

Table 4.7.b The variations in the specific rates and yield coefficients with cultivation time at MOT_1. MOT_2. HOT_1 and HOT_2 conditions.

Condition	t (h)	C_x (kg m^{-3})	μ (h^{-1})	r_o (kg O_2 m^{-3} h^{-1})	q_0 (kg kg^{-1} h^{-1})	q_s (kg kg^{-1} h^{-1})	q_P*10^{-6} (U kg^{-1} h^{-1})	$Y_{x/o}$ (kg kg^{-1})	$Y_{x/s}$ (kg kg^{-1})	$Y_{s/o}$ (kg kg^{-1})
	2	0.31	0.48	0.10	0.32	0.67	19.64	1.49	0.72	2.08
	5	0.64	0.07	0.13	0.20	0.44	7.90	0.34	0.16	2.17
	8	0.64	0.00	0.12	0.19	0.16	6.43	0.00	0.00	0.85
MOT_1	11	0.64	0.00	0.10	0.16	0.12	5.24	0.00	0.00	0.77
	20	0.64	0.00	0.10	0.16	0.16	2.50	0.00	0.00	1.02
	24	0.64	0.00	0.10	0.16	0.90	1.69	0.00	0.00	5.76
	28	0.64	0.00	0.10	0.16	0.88	1.13	0.00	0.00	5.63
	2	0.28	0.44	0.12	0.43	1.35	11.84	1.02	0.33	3.14
	5	0.54	0.13	0.17	0.31	0.56	5.22	0.42	0.23	1.81
	8	0.67	0.00	0.15	0.22	0.36	3.39	0.00	0.00	1.64
MOT_2	11	0.67	0.00	0.14	0.21	0.28	2.61	0.00	0.00	1.33
	20	0.67	0.00	0.12	0.18	0.14	0.14	0.00	0.00	0.78
	24	0.67	0.00	0.09	0.13	0.12	-1.03	0.00	0.00	0.92
	28	0.67	0.00	0.09	0.13	0.14	-2.24	0.00	0.00	1.08
	2	0.19	0.62	0.13	0.68	1.84	12.56	0.91	0.34	2.71
	5	0.46	0.12	0.09	0.20	0.64	4.08	0.61	0.19	3.20
	8	0.55	0.05	0.08	0.15	0.44	2.50	0.34	0.11	2.93
HOT_1	11	0.55	0.00	0.07	0.13	0.36	1.72	0.00	0.00	2.77
	20	0.55	0.00	0.07	0.13	0.16	0.38	0.00	0.00	1.23
	24	0.55	0.00	0.07	0.13	0.11	0.17	0.00	0.00	0.85
	28	0.55	0.00	0.07	0.13	0.07	0.19	0.00	0.00	0.54
	2	0.23	0.65	0.12	0.52	1.53	12.63	1.25	0.42	2.94
	5	0.58	0.03	0.14	0.24	0.55	5.14	0.13	0.06	2.29
HOT_2	8	0.66	0.00	0.10	0.15	0.57	4.14	0.00	0.00	3.80
	11	0.66	0.00	0.10	0.15	1.00	3.27	0.00	0.00	6.67
	20	0.66	0.00	0.10	0.15	1.21	-0.32	0.00	0.00	8.07

4.4 Metabolic Flux Analysis

Effects of the oxygen transfer conditions on the intracellular reaction rate distributions were investigated at limited, low, medium and high oxygen transfer conditions by the metabolic flux analysis based on a detailed description of the stoichiometry of all relevant biorections involved in growth and product formation that include the glycolysis pathway, the gluconeogenesis pathway, the anaplerotic and the pentose phosphate pathway reactions; metabolic intermediates of the TCA cycle; the serine, alanine, aspartic acid, glutamic acid and aromatic family amino acids, and histidine biosynthesis pathways; and the biomass synthesis including DNA, lipids, cell components synthesis. The stoichiometric reactions of the network used in this study are given in Appendix G. The overall pathway was simplified by lumping some reactions into single ones without losing representation accuracy. The extensive analysis of the broth did not reveal any pools of metabolic by-products except SAP that was included in the model. The exact amino acid combination of β-lactamase (Ledent et al., 1997) and SAP (Jacobs, 1995) by *B.licheniformis* was used while formulating their chemical composition. Also, the following major assumptions are incorporated in the model:

1. All cells are assumed to show an identical behavior throughout the bioprocess;

2. Amino acid and organic acid excretions and transportation processes are assumed to function via passive transport mechanism;

3. Transportation of CO_2, NH_3 in the form NH_4^+, and phosphate from the cell to the broth and from the broth to the cell are also assumed to employ passive transport;

4. The enzyme secretion is assumed to function via passive transport mechanism;

5. Conversion of NADPH to NADH via the transhydrogenation reaction is reversible and not energy dependent.

The calculated accumulation rates of the metabolites, i.e., the organic acids, the amino acids, β-lactamase, SAP, and the cell were used in the model to find the intracellular flux distributions by using Equation 2.20 given in Chapter 2. LimOT, LOT_1, MOT_1 and HOT_2 conditions were chosen among limited, low, medium and high oxygen transfer conditions in order to determine the effects of oxygen on intracellular reaction rates. Considering biomass and β-lactamase concentration profiles, the bioprocess can be divided into 4 periods as depicted in Figure 4.16.

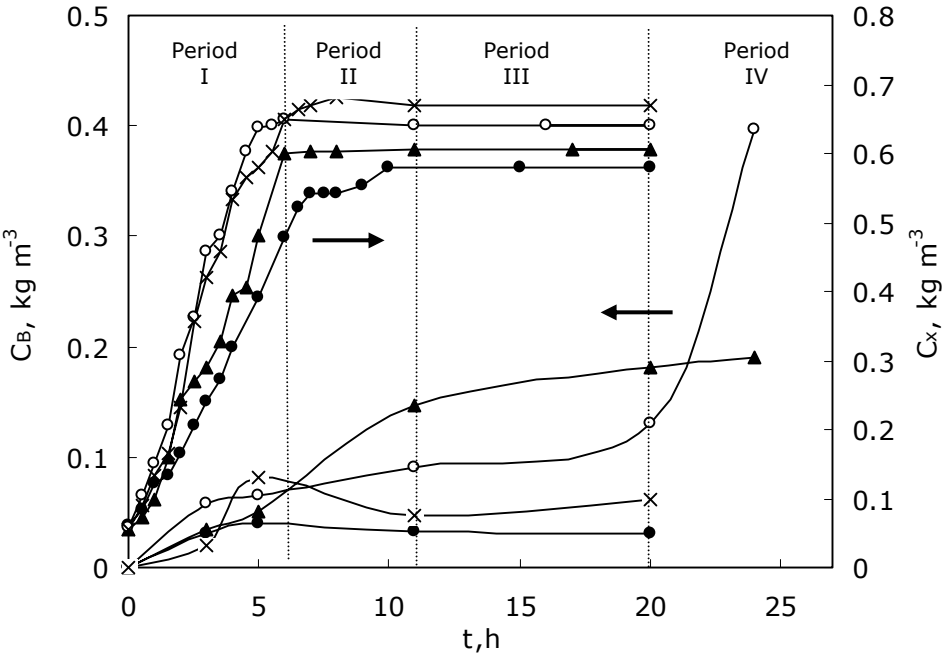

Figure 4.16 The variations of cell and beta-lactamase concentrations with the cultivation time. LimOT: (●); LOT_1:(▲); MOT_1: (○); HOT_2: (x).

Period I (0<t<6 h) is the exponential growth phase where the β-lactamase synthesis starts to increase, Period II (6<t<11 h) is the stationary phase where the β-lactamase synthesis was the highest in general, Period III (11<t<20) is the stationary phase for β-lactamase synthesis and Period IV (20<t<30 h) is the degradation period at HOT_2 condition, whereas at MOT_1 and LOT_1 again β-lactamase synthesis increased. The data of cultivation times of t_1=4 h, t_2=8 h, t_3=15 h, and t_4=22 h were used to obtain the intracellular metabolic flux distributions in Period I, II, III and IV respectively. The data obtained throughout β-lactamase fermentation were exploited, using a linear approach, to calculate

the specific growth rate and the uptake and the excretion rates of the metabolites, i.e., the organic acids and the amino acids, and the secretion rates of β-lactamase and SAP. The measured net output-rates of metabolites that are derived from the data points of the batch-bioreactor experiments were used in the model in order to calculate the intracellular flux distributions. The variations in SAP concentration the with cultivation time at LimOT, LOT_1, MOT_1 and HOT_2 conditions are given in Figure 4.17. At all the conditions, produced SAP was at low levels. At LOT_1 condition SAP was not observed in the fermentation broth. However, at LimOT and MOT_1 condition the concentration of SAP decreased with the cultivation time whereas the concentration of SAP in the HOT_2 condition stayed constant throughout the fermentation.

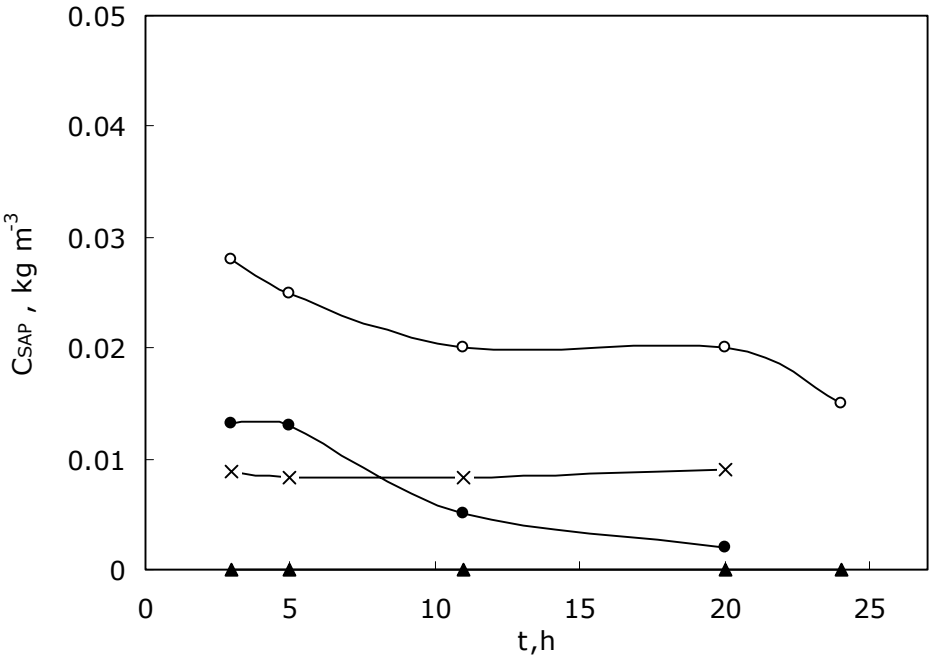

Figure 4.17 The variations of SAP concentration with the cultivation time. LimOT: (●); LOT_1:(▲); MOT_1: (○); HOT_2: (x).

4.4.1 Metabolic Flux Analysis for LimOT Condition

Metabolic flux distributions for the two periods of LimOT condition are given in Table 4.8. As seen in Table 4.8, the flux through β-lactamase synthesis (R149) and cell formation flux (R145) decreased and reached zero from period I to period III.

In period I the glycolysis pathway reactions were active; while the gluconeogenesis pathway reactions were inactive, as expected. However, in Period III, the reactions Pyr formation from PEP (R14) and AcCoA formation from Pyr(R16) were inactive in the glycolysis pathway. In this period, Pyr was produced mainly from the anapleoric reaction (R36) and from the Lac (R32). Similar to period I, in period III the gluconeogenesis pathway reactions were inactive.

In Period I at LimOT condition, the key intermediate R5P, synthesized for the nucleotides and biomass components, formation was achieved by branching at F6P through the interconversion reaction since the fluxes from G6P to both Glc (R2) and Gluc6P (R17) were inactive and ca. 12% of the glucose was directed to the formation of R5P from Xyl5P (R22). Nevertheless, in period III, R5P was produced using oxidative reactions (R20) and ca. 14% of the glucose was directed to the R5P formation by oxidative way.

In period I, Cit (R37), ICit (R38) and αKG (R39) formation reactions were inactive in the TCA cycle, while in period III the successful operation of TCA cycle was observed and glyoxylate shunt was inactive in both periods. As αKG is a branch point in the TCA cycle, the magnitude of the fluxes through the αKG formation reaction or the fluxes diverted from αKG influences the TCA cycle fluxes and consequently, the energy generation. Among the amino acid pathways the flux directed to glutamate from αKG (R73) is certainly important; in period I ca. 6% of the glucose was directed to the TCA cycle via αKG.

Glucose as the carbon source, ATP is generated in the glycolysis pathway by the substrate -level phosphorylation reactions (R10, R14), and in the TCA cycle by both substrate-level phosphorylation (R41) and oxidative phosphorylation (R122, R123) reactions. The total ATP generation rates were calculated from R10, R14, R33, R41, R101, R112, R122 and R123 and they were tabulated in Table 4.9. At LimOT condition, ATP generation rate slightly decreased with the cultivation time from period I to period III. Throughout the fermentation 24-53% and 40-76% of the ATP was produced by the substrate-level phosphorylation reactions (R10, R14, and R41) and by the oxidative phosphorylation reactions (R122, R123), respectively. In period III, according to the model ATP was not used as the maintenance energy, however in period I ca. 16% of the total ATP produced was used for maintenance (R147).

In period I the formation reactions of Lac (R31) and Ac (R33) were active while in period III they were inactive. Further, in Period III R32 catalysed by the enzyme lactate dehydrogenase was active as Lac was converted to Pyr. Indeed synthesis of the amino acids that are required for the biomass synthesis and building blocks of β-lactamase is important. For glutamic acid-family amino acids αKG, for aspartic acid-family amino acids OA, for alanine-family amino acids Pyr, for serine-family amino acids PG3, for aromatic-family amino acids PEP and E4P, and for histidine synthesis R5P are the branch points. Among the amino acid pathways the flux directed to glutamate is certainly important as mentioned above and according to the model, Glu is used for the biosynthesis of Ser (R48), Ala (R51), Val (R53), Leu (R54), Asp (R57), mDAP (R62, Ile (R66), Phe (R69), Tyr (R70), Gln (R74), Pro (R75) and ornithine (Orn; R76), while it is also produced from αKG (R73) via the catabolism reactions of Ala (R79), Pro (R90), Arg (R80), Val (R95) and His (R86) and by the biosynthesis reactions of Asn (R58), GMP (R98), CaP (R136), UDPNAG (R137). In period I, at the branch point of αKG in the TCA cycle, the flux through R40 was higher than the flux through R39 due to the additional αKG synthesis through the amino acid formation reactions of Ser (R48), Val (R53), Leu (R54) and Phe (R69). However, in period III the flux from the TCA cycle via αKG was diverted to Glu since the flux through R39 to R40 slightly decreased. The flux towards Asp from OA increased with the cultivation time and all the fluxes in the aspartic acid family amino acids were active in period I. However, in period III the formation reaction of AspSa (R59) through formation reaction of Met (R67) were inactive. The flux through the aromatic-family amino acids (R68), was higher in period III than in period I.

4.4.2 Metabolic Flux Analysis for LOT_1 Condition

Metabolic flux distributions for four periods of LOT_1 condition are given in Table 4.8. As seen in Table 4.8, the specific cell growth rate (R145) was the highest at period I and zero in period II, III and IV. However flux through β-lactamase synthesis (R149) was zero in period I and the highest at period II.

In period I the glycolysis pathway reactions were active; however in Period III the Pyr formation reaction (R14) and similar to period III at LimOT condition, in Period II and IV at LOT_1 condition both R14 and the AcCoA formation reaction from Pyr (R16) were inactive in the glycolysis pathway. However for all period gluconeogenesis pathway reactions were inactive.

In Period IV, the key intermediate R5P formation was achieved by branching at F6P through the interconversion reaction since the fluxes from G6P to both Glc (R2) and Gluc6P (R17) were inactive and ca. 10% of the glucose was directed to R5P through R22. Nevertheless, in period I, II, and III R5P was produced using oxidative reaction and in period I ca. 9% of the glucose, in period II ca. 61% of the glucose, and in period III ca. 28% of the glucose was directed to the R5P formation reaction.

The analysis of the TCA-cycle fluxes showed that, in period I, only the formation of Mal (R44) and OA (R45) reactions were active in the TCA cycle. However in period II only formation of SucCoA (R40) and Suc (R41) were inactive in the TCA cycle. In period III the successful operation of TCA cycle was observed while in period IV αKG (R39) and Suc (R41) formation reactions were inactive in the TCA cycle. In the process at LOT_1 condition, glyoxylate shunt was inactive in period I and period III, but in period II and IV it was active. Moreover in period II the reaction through Pyr synthesis from Mal (R35) was active, while in other periods anapleoric reactions (R35, R36) were inactive.

The total ATP generation rate decreased with the cultivation time at LOT_1 condition (Table 4.9). Throughout the fermentation 15-50% and 40-85% of the ATP was produced by the substrate-level phosphorylation reactions (R10, R14, and R41) and by the oxidative phosphorylation reactions (R122, R123), respectively. Furthermore the ATP consumption for maintenance (R147) increased from period I to II then decreased throughout the process at LOT_1 condition.

In period III and in period IV, at the branch point of αKG in the TCA cycle, the flux through R40 was slightly higher than the flux through R39 due to the additional αKG synthesis through the amino acid formation reactions. However in period II the flux from the TCA cycle via αKG was diverted to Glu since the flux through R39 to R40 decreased.

For the synthesis of Asp and further aspartic acid-group amino acids, the flux of the reaction that branched at OA towards Asp (R57) decreased from period I to period II then increased with cultivation time. In Period I and II the flux from AspSa through HSer (R64), Thr (R65), Ile (R66) and Met (R67) were active, while in period III and period IV these reactions were inactive. The fluxes through the aromatic-family amino acids (R68) were active in all periods.

Further, for the synthesis reaction of Ser from PG3 and Glu (R48) were active in all periods except period IV.

4.4.3 Metabolic Flux Analysis for MOT_1 Condition

Metabolic flux distributions for the four periods of MOT_1 condition are given in Table 4.8. As seen in Table 4.8, the specific cell growth rate (R145) was the highest at period I and it was zero in period II, III and IV. However flux through β-lactamase synthesis (R149) increased from period I to II and then decreased from period II to period III and then increased from period III to IV.

In period III, the glycolysis pathway reactions were active; however, in Period II, AcCoA formation reaction (R16) from Pyr, in period I, the Pyr formation reaction (R14) and in period IV, similar to period II and IV at LOT_1 condition, both R14 and R16 were inactive in the glycolysis pathway. Similar to LOT_1 condition, at MOT_1 condition gluconeogenesis pathway reactions were inactive in all period. Similar to period II at LOT_1 condition, the reaction through Pyr synthesis from Mal (R35) was active in period II at MOT_1 condition, while in period I, III and IV anapleoric reactions (R35, R36) were inactive.

In Period II and IV, the key intermediate R5P formation was achieved by interconversion reaction since the fluxes from G6P to both Glc (R2) and Gluc6P (R17) were inactive and in period II ca. 12% of glucose, in period IV ca. 20% of glucose was directed to R5P formation through R22. Nevertheless, in period I and III, R5P was produced by oxidative (R20) reaction and in period I ca. 25% of the glucose and in period III ca. 16% of the glucose was directed to R5P formation reaction.

In period I R40, and R41; in period II R39, R41, R42, and R45; and in period III R40-R45 were inactive in the TCA cycle. However in period IV, the successful operation of TCA cycle was observed. Moreover, the glyoxylate shunt was inactive in period III while it was active in period I, II and IV.

The total ATP generation rate increased with the cultivation time at MOT_1 condition (Table 4.9). Throughout the fermentation 33-53% and 34-58% of the ATP was produced by the substrate-level phosphorylation reactions (R10, R14, and R41) and by the oxidative phosphorylation reactions (R122, R123), respectively. In period II, III and IV, according to the model ATP was not used

as the maintenance energy, however in period I 58% of the total ATP produced was used for maintenance (R147).

In period II, at the branch point of αKG in the TCA cycle, the flux through R40 was higher than the flux through R39 due to the additional αKG synthesis through the amino acid formation reactions. However, in period I, III and IV the flux from the TCA cycle via αKG was diverted to Glu since the flux through R39 to R40 slightly decreased.

For the synthesis of Asp and further aspartic acid-group amino acids, the flux of the reaction that branched at OA towards Asp (R57) increased from period I to period II then decreased from period II to period III and then again increased from period III to IV. In period I, II and IV the flux from AspSa through Lys(R63), HSer (R64), Thr (R65), Ile (R66) and Met (R67) were active, while in period III these reactions were inactive. The fluxes through the aromatic-family amino acids (R68) and the synthesis reaction of Ser from PG3 and Glu (R48) were active in all periods.

4.4.4 Metabolic Flux Analysis for HOT_2 Condition

Metabolic flux distributions for the two periods of HOT_2 condition are given in Table 4.8. As seen in Table 4.8, the specific cell growth rate (R145) and the flux through β-lactamase synthesis decreased with cultivation time.

In period I Pyr formation reaction (R14) in the glycolysis pathway, in period III, similar to period IV at MOT_1 condition, in addition to R14, the AcCoA formation reaction (R16) from Pyr were inactive. Similar to LOT_1 and MOT_1 condition, in period I and in period III the gluconeogenesis pathway reactions were inactive.

In period III at HOT_2 condition, the key intermediate R5P formation was achieved by branching at F6P through the interconversion reaction and ca. 20% of the glucose was diverted to formation of R5P through R22. Nevertheless, in period I, R5P was produced using oxidative (R20) reaction and ca. 45% of the glucose was directed to R5P formation reaction.

In period I the reactions R37, R38, and R39; and in period III R40, and R41 were inactive in the TCA cycle. In the process, the glyoxylate shunt was inactive in period I while it is active in period III.

The total ATP generation rate slightly increased with the cultivation time at HOT_2 condition (Table 4.9). Throughout the fermentation 20-49% and 51-80% of the ATP was produced by the substrate-level phosphorylation reactions (R10, R14, and R41) and by the oxidative phosphorylation reactions (R122, R123), respectively. According to the model ATP was not used as the maintenance energy, in period III while in period I 37% of the total ATP produced was used for maintenance (R147).

In period I, at the branch point of αKG in the TCA cycle, the flux through R40 was higher than the flux through R39 due to the additional αKG synthesis through the amino acid formation reactions of Ser (R48), Ala (R51), Val(R53), Leu (R54), Phe (R69), Tyr (R70). However in period III, the flux from the TCA cycle via αKG was diverted to Glu since the flux through R39 to R40 decreased. The flux towards Asp from OA increased with the cultivation time and all the fluxes through the aspartic acid family amino acids were active throughout the bioprocess. Moreover, the flux through the aromatic-family amino acids (R68) and serine-family amino acids (R48) were higher in period III than in period I.

Metabolic flux analysis results show that with glucose as the carbon source, energy is generated first in the glycolysis pathway by the substrate level phosphorylation and then in the TCA cycle by the oxidative phosphorylation reactions. Although it is expected that ATP generation would be the highest at high oxygen transfer condition, the comparison of the ATP generation at LimOT, LOT_1, MOT_1, and HOT_2 showed a different profile that verifies the regulatory responses of cell in the metabolic reaction network.

Table 4.8 Metabolic flux distribution of β-lactamase fermentation of B.l*icheniformis* at LimOT, LOT_1, MOT_1, and HOT_2 conditions

	LimOT condition fluxes mmol g^{-1} DW h^{-1}		LOT_1 condition fluxes mmol g^{-1} DW h^{-1}				MOT_1 condition fluxes mmol g^{-1} DW h^{-1}				HOT_2 condition fluxes mmol g^{-1} DW h^{-1}	
R#	t=4	t=15	t=4	t=8	t=15	t=22	t=4	t=8	t=15	t=22	t=4	t=15
1	6.2500	2.7270	6.5500	2.0370	0.4630	0.9260	3.0900	3.8190	6.5500	10.7640	3.4600	9.9330
2	0.0000	0.0000	0.0000	0.0000	0.0000	0.0000	0.0000	0.0000	0.0000	0.0000	0.0000	0.0000
3	0.0000	0.0000	0.0000	0.0000	0.0000	0.0000	0.0000	0.0000	0.0000	0.0000	0.0000	0.0000
4	6.2060	2.3380	5.9250	0.7890	0.3340	0.9260	2.2900	3.819	5.5030	10.764	1.8850	9.9330
5	0.0000	0.0000	0.0000	0.0000	0.0000	0.0000	0.0000	0.0000	0.0000	0.0000	0.0000	0.0000
6	0.0000	0.0000	0.0000	0.0000	0.0000	0.0000	0.0000	0.0000	0.0000	0.0000	0.0000	0.0000
7	0.0000	0.0000	0.0000	0.0000	0.0000	0.0000	0.0000	0.0000	0.0000	0.0000	0.0000	0.0000
8	5.4300	2.3380	5.9100	1.3120	0.3340	0.8330	2.2740	3.3430	5..1770	8.6340	1.8480	7.9490
9	0.0000	0.0000	0.0000	0.0000	0.0000	0.0000	0.0000	0.0000	0.0000	0.0000	0.0000	0.0000
10	10.7470	4.2860	11.8670	3.0270	0.7100	1.4810	4.7040	6.3200	10.7040	17.2380	3.6580	15.8950
11	0.0000	0.0000	0.0000	0.0000	0.0000	0.0000	0.0000	0.0000	0.0000	0.0000	0.0000	0.0000
12	9.8190	4.2860	11.7990	2.6770	0.6360	1.4810	4.0420	6.2050	9.6900	15.0580	3.5190	13.9050
13	0.0000	0.0000	0.0000	0.0000	0.0000	0.0000	0.0000	0.0000	0.0000	0.0000	0.0000	0.0000
14	2.3110	0.0000	4.7860	0.0000	0.0000	0.0000	0.0000	1.4330	1.0930	0.0000	0.0000	0.0000

Table 4.8 Continued

	LimOT condition fluxes mmol g^{-1} DW h^{-1}		LOT_1 condition fluxes mmol g^{-1} DW h^{-1}				MOT_1 condition fluxes mmol g^{-1} DW h^{-1}				HOT_2 condition fluxes mmol g^{-1} DW h^{-1}	
R#	t=4	t=15	t=4	t=8	t=15	t=22	t=4	t=8	t=15	t=22	t=4	t=15
15	0.0000	0.0000	0.0000	0.0000	0.0000	0.0000	0.0000	0.0000	0.0000	0.0000	0.0000	0.0000
16	2.3070	0.0000	3.3930	0.0000	0.0940	0.0000	3.2620	0.0000	2.7660	0.0000	0.1130	0.0000
17	0.0000	0.3900	0.5980	1.2480	0.1290	0.0000	0.7710	0.0000	1.0470	0.0000	1.5620	0.0000
18	0.0000	0.0000	0.0000	0.0000	0.0000	0.0000	0.0000	0.0000	0.0000	0.0000	0.0000	0.0000
19	0.0000	0.0000	0.0000	0.0000	0.0000	0.0000	0.0000	0.0000	0.0000	0.0000	0.0000	0.0000
20	0.0000	0.3900	0.5980	1.2480	0.1290	0.0000	0.7710	0.0000	1.0470	0.0000	1.5620	0.0000
21	0.0000	0.0000	0.0000	0.5230	0.0000	0.0000	0.0000	0.0000	0.0000	0.0000	0.0000	0.0000
22	0.7510	0.0000	0.0000	0.0000	0.0000	0.0930	0.0000	0.4760	0.3260	2.1300	0.0290	1.9840
23	0.0000	0.3900	0.1160	0.4220	0.0430	0.0930	0.2380	0.0000	0.3490	0.0090	0.0000	0.0007
24	0.0610	0.0000	0.0000	0.0000	0.0000	0.0000	0.0000	0.0000	0.0000	0.0000	0.0000	0.0000
25	0.0000	0.3900	0.1160	0.4220	0.0430	0.0930	0.2380	0.0000	0.3490	0.0090	0.0000	0.0007
26	0.0610	0.0000	0.0000	0.0000	0.0000	0.0000	0.0000	0.0000	0.0000	0.0000	0.0000	0.0000
27	0.0000	0.0000	0.0000	0.1020	0.0000	0.0000	0.0000	0.0000	0.0000	0.0000	0.0000	0.0000
28	0.6900	0.3900	0.1160	0.0000	0.0430	0.1850	0.2380	0.4760	0.6750	2.1380	0.0290	1.9850

Table 4.8 Continued

	LimOT condition fluxes mmol g^{-1} DW h^{-1}		LOT_1 condition fluxes mmol g^{-1} DW h^{-1}				MOT_1 condition fluxes mmol g^{-1} DW h^{-1}				HOT_2 condition fluxes mmol g^{-1} DW h^{-1}	
R#	t=4	t=15	t=4	t=8	t=15	t=22	t=4	t=8	t=15	t=22	t=4	t=15
29	0.0000	0.3900	0.1120	0.4220	0.0430	0.0930	0.2340	0.0000	0.3490	0.0090	0.0000	0.0007
30	0.0680	0.0000	0.0000	0.0000	0.0000	0.0000	0.0000	0.0000	0.0000	0.0000	0.0020	0.0000
31	6.6480	0.0000	6.6870	0.0000	0.0000	0.0000	0.0070	0.0005	6.6870	0.0000	0.0000	0.0860
32	0.0000	0.0630	0.0000	0.0000	0.5140	0.0000	0.0000	0.0000	0.0000	0.0780	0.4190	0.0000
33	1.9950	0.0000	3.4140	0.0000	0.0000	0.0000	1.4150	0.0000	3.6010	0.0000	0.0000	0.0000
34	0.0000	3.4850	0.0000	0.0930	1.8110	0.9170	0.0000	4.2320	0.0000	12.0670	0.3360	8.8440
35	0.0000	0.0000	0.0000	0.5620	0.0000	0.0000	0.0000	5.8090	0.0000	0.0000	0.0000	0.0000
36	0.0000	0.8110	0.0000	0.0000	0.0000	0.0000	0.0000	0.0000	0.0000	0.0000	0.0000	0.0000
37	0.0000	1.7130	0.0000	0.9420	2.0150	0.5850	0.8500	2.3510	0.0090	7.8870	0.0000	5.9690
38	0.0000	1.7130	0.0000	0.9420	2.0150	0.5850	0.8500	2.3480	0.0090	7.8870	0.0000	5.9690
39	0.0000	1.7130	0.0000	0.1030	2.0150	0.0000	0.1980	0.0000	0.0090	1.8010	0.0000	0.0070
40	0.3480	1.7110	0.0000	0.0000	2.0310	0.0030	0.0000	0.3460	0.0000	1.6710	1.3330	0.0000
41	0.3480	0.9320	0.0000	0.0000	2.0310	0.0000	0.0000	0.0000	0.0000	1.6710	2.1020	0.0000
42	0.0000	0.0000	0.0000	0.0000	0.0000	0.2750	0.0000	0.0000	0.0000	0.0000	0.0000	0.0000

Table 4.8 Continued

	LimOT condition fluxes mmol g^{-1} DW h^{-1}		LOT_1 condition fluxes mmol g^{-1} DW h^{-1}				MOT_1 condition fluxes mmol g^{-1} DW h^{-1}				HOT_2 condition fluxes mmol g^{-1} DW h^{-1}	
R#	t=4	t=15	t=4	t=8	t=15	t=22	t=4	t=8	t=15	t=22	t=4	t=15
43	0.3480	1.7450	0.0000	0.8390	2.0220	0.5880	0.6530	2.7210	0.0000	7.7570	2.1020	5.9620
44	0.4520	6.8760	0.2830	0.8830	2.0230	0.8970	0.7980	3.4610	0.0000	7.8190	3.7110	5.9640
45	0.4520	6.8760	0.2830	1.1610	2.0230	1.4820	1.4500	0.0000	0.0000	13.9050	3.7110	11.9270
46	0.0000	0.0000	0.0000	0.8390	0.0000	0.5850	0.6530	2.3480	0.0000	6.0860	0.0000	5.9620
47	0.0000	0.0000	0.0000	0.8390	0.0000	0.5850	0.6530	2.3480	0.0000	6.0860	0.0000	5.9620
48	0.9290	0.0000	0.0670	0.3500	0.0750	0.0000	0.6620	0.1150	1.0140	2.1800	0.1390	1.9910
49	0.1540	0.0000	0.0000	0.0240	0.0000	0.0000	0.1250	0.0030	0.0000	0.0230	0.0580	0.0030
50	0.0620	0.0000	0.0370	0.0060	0.0000	0.0000	0.0540	0.0000	0.0000	0.0000	0.0270	0.0008
51	0.0000	0.0000	0.0860	0.0000	0.0000	0.0000	0.0000	0.0000	0.0000	0.0000	0.0630	0.0000
52	0.1990	1.8000	0.1500	1.5560	0.0000	0.0000	0.1480	0.0380	0.0190	0.1480	0.9200	1.0990
53	0.1120	0.0000	0.0640	0.0210	0.0000	0.0000	0.0710	0.0300	0.0000	0.0520	0.8310	0.0040
54	0.0870	1.8000	0.0860	1.5350	0.0000	0.0000	0.0770	0.0070	0.0190	0.0960	0.0880	1.0950
55	0.8060	0.0000	0.4790	0.3030	0.0860	0.0000	0.5290	0.4760	1.0240	2.1210	1.5890	1.9840
56	0.0240	0.0000	0.1890	0.0010	0.0000	0.0000	0.0000	0.3670	0.0000	0.0140	1.5340	0.0005

Table 4.8 Continued

	LimOT condition fluxes mmol g^{-1} DW h^{-1}		LOT_1 condition fluxes mmol g^{-1} DW h^{-1}				MOT_1 condition fluxes mmol g^{-1} DW h^{-1}				HOT_2 condition fluxes mmol g^{-1} DW h^{-1}	
R#	t=4	t=15	t=4	t=8	t=15	t=22	t=4	t=8	t=15	t=22	t=4	t=15
57	0.6750	4.3530	1.2610	0.2190	0.5430	0.9580	0.6000	4.6170	0.0190	10.4780	3.7110	8.7940
58	0.0990	0.0020	0.0450	0.0180	0.0000	0.0250	0.0000	0.0020	7.6120	0.0460	0.0370	0.0050
59	0.2460	0.0000	0.8200	0.1160	0.5450	0.8870	0.3570	4.2400	0.0000	10.3500	1.9520	8.7800
60	0.0950	0.0000	0.0510	0.0340	0.5450	0.8870	0.2320	4.2290	0.0000	10.1600	1.8330	8.7730
61	0.0950	0.0000	0.0510	0.0340	0.5450	0.8870	0.2320	4.2290	0.0000	10.1600	1.8330	8.7730
62	0.0950	0.0000	0.0510	0.0340	0.5450	0.8870	0.2320	4.2290	0.0000	10.1600	1.8330	8.7730
63	0.0950	0.0000	0.0510	0.0340	0.5450	0.8870	0.2320	4.2290	0.0000	10.1600	1.8330	8.7730
64	0.1500	0.0000	0.7690	0.0810	0.0000	0.0000	0.1250	0.0110	0.0000	0.1900	0.1190	0.0070
65	0.1120	0.0000	0.7470	0.0760	0.0000	0.0000	0.0940	0.0100	0.0000	0.1810	0.1000	0.0060
66	0.0770	0.0000	0.0430	0.0200	0.0000	0.0000	0.0490	0.0040	0.0000	0.0500	0.0500	0.0020
67	0.0380	0.0000	0.0220	0.0060	0.0000	0.0000	0.0310	0.0010	0.0000	0.0090	0.0190	0.0008
68	0.6220	0.7790	0.2270	0.3200	0.0860	0.2780	0.4720	0.4760	1.0240	2.1470	0.0280	1.9860
69	0.0180	0.0000	0.0270	0.0100	0.0000	0.0000	0.0360	0.0000	0.0000	0.0210	0.0050	0.0009
70	0.0000	0.7790	0.0210	0.0090	0.0000	0.2780	0.0230	0.3670	0.0000	0.0240	0.0230	0.0020

Table 4.8 Continued

	LimOT condition fluxes mmol g^{-1} DW h^{-1}		LOT_1 condition fluxes mmol g^{-1} DW h^{-1}				MOT_1 condition fluxes mmol g^{-1} DW h^{-1}				HOT_2 condition fluxes mmol g^{-1} DW h^{-1}	
R#	t=4	t=15	t=4	t=8	t=15	t=22	t=4	t=8	t=15	t=22	t=4	t=15
71	0.6040	0.0000	0.1790	0.3020	0.0860	0.0000	0.4130	0.1090	1.0240	2.1070	0.0000	1.9830
72	0.6040	0.0000	0.1790	0.3020	0.0860	0.0000	0.4130	0.1090	1.0240	2.1070	0.0000	1.9830
73	0.5740	4.3550	1.9500	0.5890	1.0190	1.8360	1.7380	8.8790	0.2080	21.2440	6.2310	17.5890
74	0.5150	4.3550	0.5260	0.0770	0.0000	0.0530	0.3480	0.3720	7.6200	0.1380	1.7510	0.0090
75	0.0580	0.0000	0.0320	0.0160	0.0000	0.0000	0.0360	0.0190	0.0000	0.0000	0.0380	0.0020
76	0.0150	4.3520	0.0540	0.0420	0.0010	0.0310	0.1030	0.0000	0.0000	0.0490	0.0560	0.0020
77	0.0000	4.3520	0.0450	0.0420	0.0010	0.0310	0.0930	0.0000	0.0000	0.0490	0.0510	0.0020
78	0.0000	4.3520	0.0450	0.0420	0.0010	0.0310	0.0930	0.0000	0.0000	0.0490	0.0510	0.0020
79	0.5440	0.0000	0.0000	0.2600	0.1110	0.0060	0.3120	0.1030	0.8520	2.0040	0.0000	1.9790
80	0.5660	4.3520	0.0000	0.0000	0.0160	0.0310	0.0000	0.0080	0.0000	0.0000	0.0000	0.0000
81	0.0000	0.0000	0.0000	0.0000	0.0000	0.0000	0.0090	0.0000	7.6020	0.0000	0.0000	0.0000
82	0.0000	0.0000	0.0000	0.0000	0.0000	0.0000	0.0000	0.0000	0.0000	0.0000	0.0000	0.0000
83	0.0000	0.0000	0.0000	0.0000	0.0000	0.0000	0.0000	0.0010	0.0000	0.0040	0.0000	0.0000
84	0.0000	0.0000	0.0000	0.0000	0.0000	0.0000	0.0000	0.0000	0.0000	0.0000	0.0000	0.0000

Table 4.8 Continued

	LimOT condition fluxes mmol g^{-1} DW h^{-1}		LOT_1 condition fluxes mmol g^{-1} DW h^{-1}				MOT_1 condition fluxes mmol g^{-1} DW h^{-1}				HOT_2 condition fluxes mmol g^{-1} DW h^{-1}	
R#	t=4	t=15	t=4	t=8	t=15	t=22	t=4	t=8	t=15	t=22	t=4	t=15
85	0.0000	0.0040	0.2250	0.0000	0.0110	0.0080	0.0000	0.0000	0.0220	0.0000	0.0000	0.0000
86	0.0000	0.0000	0.1750	0.0000	0.0000	0.0000	0.0320	0.3660	0.0000	0.0000	1.5190	0.0000
87	0.0000	0.0000	0.0000	0.0000	0.0000	0.0000	0.0000	0.0000	0.0000	0.0000	0.0000	0.0000
88	0.0000	1.8000	0.0000	1.4940	0.0010	0.0000	0.0000	0.0000	0.0000	0.0000	0.0000	1.1020
89	0.0000	0.0000	0.0000	0.0000	0.0000	0.0000	0.0000	0.0000	0.0000	0.0000	0.0000	0.0000
90	0.0000	0.0000	0.0000	0.0000	0.0000	0.0000	0.0000	0.0000	0.0000	0.0210	0.0000	0.0000
91	0.0000	0.0000	0.0000	0.0000	0.0000	0.0160	0.0000	0.0000	0.0000	0.0000	0.0000	0.0000
92	0.0000	0.0000	0.6760	0.0000	0.0160	0.0000	0.0000	0.0000	0.0100	0.0470	0.0000	0.0000
93	0.6430	0.0000	0.0000	0.3220	0.0930	0.0060	0.4080	0.1100	0.8520	2.0970	0.0180	1.9840
94	0.0000	0.7790	0.0000	0.0000	0.0000	0.2780	0.0000	0.3730	0.0000	0.0000	0.0000	0.0000
95	0.0000	0.0000	0.0000	0.0000	0.0000	0.0000	0.0000	0.0260	0.0000	0.0000	0.7690	0.0000
96	0.0690	0.0000	0.0420	0.0000	0.0000	0.0000	0.0450	0.0000	0.0000	0.0000	0.0210	0.0000
97	0.0920	0.0000	0.2310	0.0010	0.0000	0.0000	0.0450	0.3670	0.0000	0.0140	1.5550	0.0005
98	0.0570	0.0000	0.0350	0.0000	0.0000	0.0000	0.0370	0.0000	0.0000	0.0000	0.0180	0.0000

Table 4.8 Continued

	LimOT condition fluxes mmol g^{-1} DW h^{-1}		LOT_1 condition fluxes mmol g^{-1} DW h^{-1}				MOT_1 condition fluxes mmol g^{-1} DW h^{-1}				HOT_2 condition fluxes mmol g^{-1} DW h^{-1}	
R#	t=4	t=15	t=4	t=8	t=15	t=22	t=4	t=8	t=15	t=22	t=4	t=15
99	0.0570	0.0000	0.0350	0.0000	0.0000	0.0000	0.0370	0.0000	0.0000	0.0000	0.0180	0.0000
100	0.0870	0.0000	0.2280	0.0010	0.0000	0.0000	0.0410	0.3670	0.0000	0.0140	1.5540	0.0005
101	0.0000	0.0000	0.0000	0.0000	0.0000	0.0000	0.0000	0.0000	0.0000	0.0000	0.0000	0.0000
102	0.0050	0.0000	0.0030	0.0000	0.0000	0.0000	0.0030	0.0000	0.0000	0.0000	0.0020	0.0000
103	0.0050	0.0000	0.0030	0.0000	0.0000	0.0000	0.0030	0.0000	0.0000	0.0000	0.0020	0.0000
104	0.0350	0.0000	0.1960	0.0010	0.0000	0.0000	0.0070	0.3670	0.0000	0.0140	1.5380	0.0005
105	1.0980	4.3530	0.8590	0.3770	0.0880	0.0560	0.7520	0.8440	8.6360	2.2350	3.2780	1.9930
106	0.1100	0.0000	0.0680	0.0000	0.0000	0.0000	0.0720	0.0000	0.0000	0.0000	0.0340	0.0000
107	0.1100	0.0000	0.0680	0.0000	0.0000	0.0000	0.0720	0.0000	0.0000	0.0000	0.0340	0.0000
108	0.1050	0.0000	0.0650	0.0000	0.0000	0.0000	0.0690	0.0000	0.0000	0.0000	0.0320	0.0000
109	0.0490	0.0000	0.0300	0.0000	0.0000	0.0000	0.0320	0.0000	0.0000	0.0000	0.0150	0.0000
110	0.0050	0.0000	0.0030	0.0000	0.0000	0.0000	0.0030	0.0000	0.0000	0.0000	0.0020	0.0000
111	0.0000	0.0000	0.0000	0.0000	0.0000	0.0000	0.0000	0.0000	0.0000	0.0000	0.0000	0.0000
112	0.0050	0.0000	0.0030	0.0000	0.0000	0.0000	0.0030	0.0000	0.0000	0.0000	0.0020	0.0000

Table 4.8 Continued

	LimOT condition fluxes mmol g^{-1} DW h^{-1}		LOT_1 condition fluxes mmol g^{-1} DW h^{-1}				MOT_1 condition fluxes mmol g^{-1} DW h^{-1}				HOT_2 condition fluxes mmol g^{-1} DW h^{-1}	
R#	t=4	t=15	t=4	t=8	t=15	t=22	t=4	t=8	t=15	t=22	t=4	t=15
113	0.0050	0.0000	0.0030	0.0000	0.0000	0.0000	0.0030	0.0000	0.0030	0.0000	0.0020	0.0000
114	0.0050	0.0000	0.0030	0.0000	0.0000	0.0000	0.0030	0.0000	0.0030	0.0000	0.0020	0.0000
115	0.0000	0.0000	0.0000	0.0170	0.0000	0.0000	0.0340	0.0010	0.0000	0.0000	0.0000	0.0020
116	0.0380	0.0000	0.0220	0.0060	0.0000	0.0000	0.0310	0.0010	0.0220	0.0000	0.0190	0.0008
117	0.1610	0.0000	0.0990	0.0010	0.0000	0.0000	0.0570	0.0003	0.0990	0.0000	0.0570	0.0005
118	0.1610	0.0000	0.2740	0.0010	0.0000	0.0000	0.0900	0.3670	0.2740	0.0000	1.5760	0.0005
119	0.0510	0.0040	0.3490	0.0000	0.0110	0.0080	0.0000	0.0000	0.3490	0.0220	0.0210	0.0000
120	3.6360	4.4430	3.8020	0.0000	0.0000	3.8930	3.0270	12.2150	3.8020	0.0000	8.6590	40.2250
121	0.0000	0.0000	0.0000	0.0000	0.0000	0.0000	0.0000	0.0000	0.0000	0.0000	0.0000	0.0000
122	4.8520	12.8770	6.7350	7.5610	6.0220	0.2460	7.3930	0.0000	6.7350	7.8480	8.7980	0.4700
123	0.3480	3.5460	0.0000	2.3340	2.5690	1.4750	0.8260	6.9970	0.0000	0.0000	5.3980	15.8340
124	3.8690	7.9870	3.6880	3.7630	4.3940	1.3920	4.8940	4.3360	3.6880	4.8590	6.4940	9.0240
125	0.0000	0.0000	0.0000	0.0000	0.0000	0.0000	0.0000	0.0000	0.0000	0.0000	0.0000	0.0000
126	1.0090	4.3530	2.2700	0.9590	1.0780	1.8340	2.4760	9.3480	2.2700	1.2280	7.9070	19.5800

Table 4.8 Continued

	LimOT condition fluxes mmol g^{-1} DW h^{-1}		LOT_1 condition fluxes mmol g^{-1} DW h^{-1}				MOT_1 condition fluxes mmol g^{-1} DW h^{-1}				HOT_2 condition fluxes mmol g^{-1} DW h^{-1}	
R#	t=4	t=15	t=4	t=8	t=15	t=22	t=4	t=8	t=15	t=22	t=4	t=15
127	0.0000	0.0000	0.0000	0.0000	0.0000	0.0000	0.0000	0.0000	0.0000	0.0000	0.0000	0.0000
128	0.1000	0.0000	0.0590	0.0110	0.0000	0.0000	0.0850	0.0000	0.0000	0.0050	0.0460	0.0020
129	1.1330	4.3530	0.8800	0.3770	0.0880	0.0560	0.7740	0.8440	8.6360	2.2350	3.2890	1.9930
130	0.5570	0.0000	0.3430	0.0000	0.0000	0.0000	0.3640	0.0000	0.0000	0.0000	0.1710	0.0000
131	0.0000	0.0000	0.0000	0.0000	0.0000	0.0000	0.0000	0.0000	0.0000	0.0000	0.0000	0.0000
132	0.0340	0.0000	0.0210	0.0000	0.0000	0.0000	0.0220	0.0000	0.0000	0.0000	0.0100	0.0000
133	0.0060	0.0000	0.0040	0.0000	0.0000	0.0000	0.0040	0.0000	0.0000	0.0000	0.0020	0.0000
134	0.0060	0.0000	0.0040	0.0000	0.0000	0.0000	0.0040	0.0000	0.0000	0.0000	0.0020	0.0000
135	0.0670	0.0000	0.0410	0.0000	0.0000	0.0000	0.0440	0.0000	0.0000	0.0000	0.0210	0.0000
136	0.1100	4.3520	0.1130	0.0420	0.0010	0.0310	0.1650	0.0000	0.0000	0.0490	0.0850	0.0020
137	0.0180	0.0000	0.0110	0.0000	0.0000	0.0000	0.0120	0.0000	0.0000	0.0000	0.0060	0.0000
138	0.0070	0.0000	0.0040	0.0000	0.0000	0.0000	0.0050	0.0000	0.0000	0.0000	0.0020	0.0000
139	0.0060	0.0000	0.0040	0.0000	0.0000	0.0000	0.0040	0.0000	0.0000	0.0000	0.0020	0.0000
140	0.0060	0.0000	0.0040	0.0000	0.0000	0.0000	0.0040	0.0000	0.0000	0.0000	0.0020	0.0000

Table 4.8 Continued

	LimOT condition fluxes mmol g^{-1} DW h^{-1}		LOT_1 condition fluxes mmol g^{-1} DW h^{-1}				MOT_1 condition fluxes mmol g^{-1} DW h^{-1}				HOT_2 condition fluxes mmol g^{-1} DW h^{-1}	
R#	t=4	t=15	t=4	t=8	t=15	t=22	t=4	t=8	t=15	t=22	t=4	t=15
141	0.0060	0.0000	0.0040	0.0000	0.0000	0.0000	0.0040	0.0000	0.0000	0.0000	0.0020	0.0000
142	0.0440	0.0000	0.0270	0.0000	0.0000	0.0000	0.0290	0.0000	0.0000	0.0000	0.0140	0.0000
143	0.0000	0.0000	0.0000	0.0000	0.0000	0.0000	0.0000	0.0000	0.0000	0.0000	0.0000	0.0000
144	0.0040	0.0000	0.0030	0.0000	0.0000	0.0000	0.0030	0.0000	0.0000	0.0000	0.0010	0.0000
145	0.2600	0.0000	0.1600	0.0000	0.0000	0.0000	0.1700	0.0000	0.0000	0.0000	0.0800	0.0000
146	0.0000	0.0000	0.0000	0.0000	0.0000	0.0000	0.0000	0.0000	0.0000	0.0003	0.0000	0.0001
147	3.9800	0.0000	15.6840	16.0800	14.3970	0.0000	8.326	0.0000	0.0000	0.0000	10.6580	0.0000
148	0.2230	0.0000	0.9770	0.0000	0.5350	0.0620	0.0000	6.9680	0.0270	4.4590	0.0000	2.8360
149	0.0005	0.0000	0.0000	0.0010	0.0000	0.0000	0.0000	0.0003	0.0000	0.0030	0.0020	0.0001

Table 4.9 ATP generation throughout the fermentation.

LimOT	**Period I**		**Period III**	
mmol g^{-1} DW h^{-1}	ATP		ATP	
R#		ATP%		ATP%
10	10.747	42.21	4.286	19.80
14	2.311	9.08	0.000	0.00
33	1.995	7.84	0.000	0.00
41	0.348	1.37	0.932	4.31
101	0.000	0.00	0.000	0.00
112	0.005	0.02	0.000	0.00
122	9.704	38.12	12.877	59.50
123	0.348	1.37	3.546	16.39
Total	**25.458**	**100**	**21.641**	**100**

LOT1	**Period I**		**Period II**		**Period III**		**Perıod IV**	
mmol g^{-1} DW h^{-1}	ATP		ATP		ATP		ATP	
R#		ATP%		ATP%		ATP%		ATP%
10	11.867	35.38	3.027	14.78	0.710	4.09	1.481	42.95
14	4.786	14.27	0.000	0.00	0.000	0.00	0.000	0.00
33	3.414	10.18	0.000	0.00	0.000	0.00	0.000	0.00
41	0.000	0.00	0.000	0.00	2.031	11.70	0.000	0.00
101	0.000	0.00	0.000	0.00	0.000	0.00	0.000	0.00
112	0.003	0.01	0.003	0.01	0.000	0.00	0.000	0.00
122	13.470	40.16	15.122	73.82	12.044	69.40	0.492	14.27
123	0.000	0.00	2.334	11.39	2.569	14.80	1.475	42.78
Total	**33.540**	**100**	**20.486**	**100**	**17.354**	**100**	**3.448**	**100**

MOT1	**Period I**		**Period II**		**Period III**		**Period IV**	
mmol g^{-1} DW h^{-1}	ATP		ATP		ATP		ATP	
R#		ATP%		ATP%		ATP%		ATP%
10	4.704	32.80	6.320	42.85	10.704	46.05	17.238	45.16
14	0.000	0.00	1.433	9.72	1.093	4.70	0.000	0.00
33	1.415	9.87	0.000	0.00	3.601	15.49	0.000	0.00
41	0.000	0.00	0.000	0.00	0.000	0.00	1.671	4.38
101	0.000	0.00	0.000	0.00	0.000	0.00	0.000	0.00
112	0.003	0.02	0.000	0.00	0.000	0.00	0.000	0.00
122	7.393	51.55	0.000	0.00	7.848	33.76	1.430	3.75
123	0.826	5.76	6.997	47.44	0.000	0.00	17.832	46.72
Total	**14.341**	**100**	**14.750**	**100**	**23.246**	**100**	**38.171**	**100**

HOT2	**Period I**		**Period III**	
mmol g^{-1} DW h^{-1}	ATP		ATP	
R#		ATP%		ATP%
10	3.658	12.72	15.895	48.65
14	0.000	0.00	0.000	0.00
33	0.000	0.00	0.000	0.00
41	2.102	7.31	0.000	0.00
101	0.000	0.00	0.000	0.00
112	0.002	0.01	0.000	0.00
122	17.596	61.19	0.940	2.88
123	5.398	18.77	15.834	48.47
Total	**28.756**	**100**	**32.669**	**100**

CHAPTER 5

CONCLUSION

This study focuses on, the effects of oxygen transfer on β-lactamase production by *Bacillus licheniformis* on a defined medium. In order to clarify the oxygen transfer effects on the production of β-lactamase, firstly a glucose based defined medium was designed and using this medium, the effects of the bioreactor operation parameters, i.e., pH and temperature, on β-lactamase activity and cell formation were investigated in laboratory scale bioreactors. Thereafter, using the optimized medium the effects of oxygen transfer on cell generation, substrate consumption, product (β-lactamase) and by-products formation were investigated in the pilot scale bioreactor. Finally, the influence of oxygen transfer conditions on the intracellular reaction rates in β-lactamase production by *B.licheniformis* under well-defined batch bioreactor conditions was investigated using metabolic flux analysis to evaluate the effects of oxygen on the metabolism. In this context the following conclusions were drawn:

1. In order to design a defined medium firstly yeast extract was omitted from the medium found in the study of Çalık and Çelik (2004), and medium, that contained (kg m^{-3}): glucose, 8; $(NH_4)_2HPO_4$, 4.7 and the salt solution in which the β-lactamase activity was obtained as 60 U cm^{-3} was considered as the starting point for medium design experiments and the medium named as reference production medium (RPM).

2. The effect of $(NH_4)_2HPO_4$ concentration was investigated within the range corresponding to initial nitrogen concentration of 0.0 – 4.0 kg m^{-3} on β- lactamase activity at 37°C with an initial pH of 7.2. The highest β-lactamase activity was obtained at C_N^0 = 7.1 kg m^{-3} as A=76 U cm^{-3}.

3. The effect of pH control on β-lactamase production was investigated in the initial pH range of 5.8-8.0, in media with NaH_2PO_4 - Na_2HPO_4 buffer, and without buffer (the uncontrolled-pH operation).

Uncontrolled-pH operation was found to be more favorable for β-lactamase production. Furthermore, the effects of pH and temperature were investigated in the medium without buffer. T=37°C, and pH=7.5 were found to be the favorable condition for β-lactamase production.

4. The effects of glucose concentration on β-lactamase production were investigated in the range of $C_G°$=6.0, 7.0, 8.0, 9.0, 10.0, 11.0, and 12.0 kg m^{-3}, in the medium containing 7.1 kg m^{-3} $(NH_4)_2HPO_4$ and the salt solution at a cultivation temperature of T=37°C with an initial pH of 7.5. The activity of β-lactamase did not change significantly in this range and $C_G°$=7 kg m^{-3} was selected as an initial glucose concentration.

5. As a result of the medium design experiments, the highest β-lactamase activity was obtained as 115 U cm^{-3}, in the medium containing 7.0 kg m^{-3} glucose, 7.1 kg m^{-3} $(NH_4)_2HPO_4$, and the salt solution at pH=7.5, T= 37°C, N=200 min^{-1}, V=33 cm^3, which was 2-fold higher than the activity obtained in the RPM.

6. Using the optimized defined medium, T and pH obtained in the laboratory scale experiments the effects of oxygen transfer on fermentation and oxygen transfer characteristics were investigated in the pilot scale bioreactor system at seven oxygen transfer conditions. Throughout the bioprocess, dissolved oxygen, pH, glucose, cell, amino acid and organic acid concentrations, β-lactamase activity, liquid phase mass transfer coefficient, specific growth rate, and yield coefficients were determined.

7. Considering the C_O profiles, Q_0/V_R = 0.2 vvm and N =250 min^{-1} (LimOT) is regarded as "limited-oxygen transfer" condition; Q_0/V_R = 0.5 vvm and N =250 min^{-1} (LOT_1), and Q_0/V_R = 0.2 vvm and N =500 min^{-1} (LOT_2) are regarded as "low-oxygen transfer" conditions; Q_0/V_R = 0.5 vvm and N =500 min^{-1} (MOT_1), Q_0/V_R = 0.2 vvm and N =750 min^{-1} (MOT_2) are regarded as "medium oxygen transfer" conditions; and lastly Q_0/V_R = 1 vvm and N =500 min^{-1} (HOT_1) and Q_0/V_R = 0.5 vvm and N =750 min^{-1} (HOT_2) are regarded as "high-oxygen transfer" condition.

8. At LimOT and to an extent at LOT_1 conditions the C_O exhibited sudden drop at the early hours of the fermentation and at t= 1-27 h for LimOT and, at t=2-10.5 h for LOT_1 the transferred oxygen was totally consumed. When the OTR was higher, i.e., at LOT_2, MOT_1, and MOT_2 conditions, a decrease and/or an increase in the dissolved oxygen level with cultivation time was observed depending on the metabolic stage of the growth. Further, at HOT_1 and HOT_2 conditions, although the biomass concentration increased, DO concentration did not change considerably throughout the bioprocess as the OTR was high enough.

9. The locus of pH *vs* time profiles were similar at LOT_2, MOT_1, MOT_2, HOT_1, and HOT_2 conditions, and pH has a tendency to decrease until t=10 h; thereafter, it reached to the stationary phase. However, at LOT_1 and LimOT conditions the decrease rate of pH was higher than the other conditions. At LimOT condition where the lowest pH was observed, the pH of the fermentation broth decreased until t= 12 h; at t=12-19 h it was constant; and after t=19 h pH increased.

10. At all the oxygen transfer conditions applied, glucose concentration (C_G^0 = 7.0 kg m^{-3}), decreased with the cultivation time, as expected. At the end of the bioprocess, the lowest amount of glucose was attained at LimOT and MOT_1 conditions that correspond to the consumption of %91.5 of the initial glucose.

11. At all the conditions, cell concentration increased at a high rate between t=2-7 h, and then reached the stationary phase. The highest cell concentrations were obtained at MOT_2 and HOT_2 conditions as C_X= 0.67 kg m^{-3} and the lowest cell concentration was obtained at LimOT and HOT_1 as C_X= 0.54 kg m^{-3}.

12. Because of the inappropriate oxygen transfer the lowest β-lactamase activity was obtained at LimOT condition where the lowest cell concentration was obtained. At MOT_1 condition β-lactamase activity was higher than the other conditions throughout the process but at t=24 h LOT_2 and MOT_1 gave all most the same β-lactamase activity values ca. A=90 U cm^{-3}. In the process the cultivation time in which the highest β-lactamase activity was

obtained shifted 1.33-fold to an earlier cultivation time (t=24h) compared to the laboratory scale experiments (t=32h) with a cost of 22 % lower activity.

13. In general the amino acid concentrations in the fermentation broth was low and considering all the amino acid profiles and oxygen transfer conditions, arginine concentration was the highest at LimOT condition obtained as 0.072 kg m^{-3} at t=3 h. At all the oxygen transfer conditions, generally aspartic acid and the asparagine were the amino acids detected in the broth. The total amino acid concentration excreted to the fermentation broth was maximum at LOT_2 condition at t=24 h as T_{OA} = 0.133 kg m^{-3} and minimum at HOT_1 condition at t=20 h as T_{OA} = 0.001 kg m^{-3}.

14. At all the oxygen transfer conditions, acetic acid and lactic acid are the organic acids detected in the broth at high concentrations. At LimOT condition at t=11 h lactic acid was excreted having the concentration of 1.464 kg m^{-3} which was the highest value obtained throughout the bioprocess. Moreover, the total organic acid concentration excreted to the fermentation broth was maximum at LimOT condition at t=20 h as T_{OA} = 2.513 kg m^{-3}, explaining the reason of the highest rate of decrease in the medium pH at this condition. Under the lower range of oxygen transfer conditions, LimOT and LOT_1, due to the insufficient operation of TCA cycle α-ketoglutaric and succinic acid were excreted to the fermentation broth.

15. Average K_La, increased with the increase in the agitation and aeration rates and its values varied between 0.007-0.044 s^{-1}. There is a fairly good agreement between the experimental and correlated values for coelescing bubbles (Eq 1-4) given by Moo-Young and Blanch (1981), within the agitation and air-inlet rate range used. Because of the dynamic behavior of the fermentation media, K_La could not be correlated for the entire fermentation process.

16. In general the enhancement factors E were slightly higher than 1.0, showing that a slow reaction is accompanied by mass transfer and they did not show a significant difference at the oxygen transfer conditions applied and changed in the range between E= 1.0-2.1.

17. LimOT, LOT_1 and LOT_2 conditions, were the mass-transfer limited conditions (Da>>1). While, at MOT_1, MOT_2, HOT_1, and HOT_2 conditions, at=2-8 h mass-transfer resistance was more effective (Da>>1).

    The high effectiveness factor, η, values until t=5 h indicate that the cells are consuming oxygen with such a high rate that maximum possible oxygen utilization (OD) value is approached and thereafter the decrease in η indicates that the cells are consuming lower oxygen than the oxygen demand (OD).

18. At all the oxygen transfer conditions applied the specific growth rates decreased in the logarithmic growth phase and at stationary phase they reached a constant value $\mu=0\ h^{-1}$. The maximum specific growth rate of $\mu_{max}=1.04\ h^{-1}$ was obtained at t=1 h at LOT_1 condition.

19. The specific substrate consumption rates first decreased and then increased all the conditions except, LimOT and HOT_1 at which they gradually decreased throughout the fermentation. The highest value of q_S was obtained at t=2 h of LOT_1 condition as 2.17 kg kg^{-1} h^{-1}; where the lowest value was obtained at t=28 h of LimOT and HOT_1 conditions as 0.07 kg kg^{-1} h^{-1}.

20. The specific oxygen uptake rates decreased throughout the bioprocess due to the increased cell concentration and gave a maximum at LimOT condition at t=2 h as $q_0=0.94$ kg kg^{-1} h^{-1} and a minimum at LOT_1 condition at t=28 h as $q_0=0.08$ kg kg^{-1} h^{-1}.

21. In the β-lactamase formation the specific production rate decreased throughout the process at all the oxygen transfer conditions applied but at LimOT and LOT_1 conditions after t=20 h the specific

production rate again began to increase. The highest value of q_p was obtained at t=0.5 h at LOT_2 condition as $69.5*10^6$ U $kg^{-1}h^{-1}$.

22. The yield of cell on substrate and the yield of cell on oxygen decreased with the cultivation time at all the oxygen transfer conditions applied however at LimOT condition they increased between t=2-5 h. The highest $Y_{X/S}$ value was obtained at MOT_1 condition at t=2 h as $Y_{X/S}$=0.72 kg kg^{-1} and the yield of cell on oxygen reached a maximum, $Y_{X/O}$=1.49 kg kg^{-1}, at t=2 h at MOT_1 condition. The yield of substrate on oxygen showed a decrease and/or an increase throughout the fermentation and gave the highest value at HOT_2 condition at t=20 h as $Y_{S/O}$=8.07 kg kg^{-1}. Moreover at HOT_2 condition the $Y_{S/O}$ values increased with the cultivation time after t=5 h, indicating the increase in the efficiency of energy metabolism.

23. Because product and by-product formations in the bioprocess for β-lactamase production are dependent on the oxygen transfer rate, well-defined perturbations were achieved by the four different oxygen transfer conditions., i.e., limited-, low-, medium-, and high-oxygen transfer rates, and an in-depth insight was provided by applying metabolic flux analysis. The change in the oxygen transfer rate influenced the fluxes of the central pathways and consequently, the formation of the key intermediates including the amino acids, and consequently β-lactamase production throughout the bioprocess.

24. The only carbon source in the defined medium was glucose that enters into the carbon mechanism in the glycolysis pathway. The fluxes through glycolysis pathway were active at all the oxygen transfer conditions. However, in period I at LimOT and LOT_1 and in period III at MOT_1 conditions; and in period III at LOT_1 and in period I at MOT_1 conditions the Pyr formation reaction (R14), and in period II at MOT_1 the AcCoA formation reaction (R16) from Pyr and in period III at LimOT, in period II and IV at LOT_1 condition, in period IV at MOT_1 and in period III at HOT_2 conditions both R14 and R16 were inactive in the glycolysis pathway. Moreover, the

gluconeogenesis pathway reactions were inactive at all the conditions.

25. The key intermediate R5P formation was achieved by branching at F6P through the interconversion reactions since the fluxes from G6P to both Glc (R2) and Gluc6P (R17) were inactive in period I at LimOT, in period IV at LOT_1, in period II and IV at MOT_1 and in period III at HOT_2 conditions. Nevertheless, in period III at LimOT, in period I, II and III at LOT_1, in period I and III at MOT_1 and in period I at HOT_2 conditions R5P was produced using the oxidative reaction.

26. Because NADH and $FADH_2$ are generated in the TCA cycle and transfer their electrons to the molecular oxygen during the ATP generation by the oxidative phosphorylation and are then regenerated in the TCA cycle, the rate of the TCA cycle was strongly dependent on the oxygen transfer conditions. The successful operation of TCA cycle was observed in period III at LimOT and LOT_1 conditions and in period IV at MOT_1 conditons. The flux of the anaplerotic reaction either R35 or R36 that connects the TCA cycle respectively, from either Mal or OA to the gluconeogenesis pathway via Pyr was influenced by the oxygen transfer rate. In Period II at LimOT condition Pyr was produced by the reaction R36. Nevertheless, in period II at LOT_1 and MOT_1 conditions, the connection of the TCA cycle to Pyr was achieved via OA through the reaction R35.

27. The total ATP generation was the highest in period IV at MOT_1 condition, while the ATP requirements for the transport, translocation, and maintenance of the gradients stated in the model as the hydrolysis of ATP (R147), was the highest at LOT_1 condition.

28. The maximum β-lactamase concentration and activity were obtained experimentally at MOT_1 condition; however the metabolic flux analysis showed that the β-lactamase synthesis flux (R149) was the highest in Period I at HOT_2 condition, in period II at LOT_1 condition and in period IV of MOT_1 condition. Amongst the highest β-lactamase flux was obtained in period IV at MOT_1 condition. On the

bases of the results the following oxygen transfer strategy can be proposed:

In the bioreactor based on the periods of the bioprocess for the exponentional growth phase the high-oxygen transfer, for the stationary phase low–oxygen transfer, and for the β-lactamase synthesis period the medium-oxygen transfer conditions can be applied to fine tune bioreactor performance.

REFERENCES

Atkinson, B. and Mavituna, F., 1991. Biochemical Engineering and Biotechnology Handbook, 2nd ed., Macmillan Publishers Ltd., England.

Bailey, J.E. and Ollis D.F., 1986. Biochemical Engineering Fundamentals, 2nd ed., McGraw-Hill Inc., New York.

Bernstein, A., Nickerson, K.W., Day, R.A, 1967. Thermal Penicillinase Expression and Temperature Dependence of Penicillinase Production Inducible and Constitutive Strains of *Bacillus cereus*, Archives of Biochemistry and Biophysics, 119, 50-54.

Çalık, P., Çalık, G., Özdamar, T.H., 1998. Oxygen Transfer Effects in Serine Alkaline Protease Fermentation by *Bacillus licheniformis*: Use of Citric Acid as the Carbon Source, Enzyme and Microbial Technology, 23(7-8), 451-461.

Çalık, P., Çalık, G., Takaç, S., Özdamar, T.H., 1999. Metabolic Flux Analysis for Serine Alkaline Protease Fermentation by *Bacillus licheniformis* in a Defined Medium: Effects of the Oxygen Transfer Rate, Biotechnology and Bioengineering, 64, 151-167.

Çalık, P., Çalık, G., Özdamar, T.H., 2000. Oxygen Transfer Strategy and its Regulation Effects in Serine Alkaline Protease Production by *Bacillus licheniformis*, Biotechnology and Bioengineering, 69, 301-311.

Çalık, P., Özdamar, T.H., 2001. Effects of Carbon Sources on Metabolic Capacity of *Bacillus Licheniformis* for Serine Alkaline Protease, Neutral Protease and α-Amylase Production, Biochemical Engineering Journal., 8(1), 61-8.

Çalık, P., Özdamar, T.H., 2002. Bioreaction Network Flux Analysis for Industrial Microorganisms:A Review, Reviews in Chemical Engineering, 18(6), 553-596.

Çalık, P., Bilir, E., Çalık, G., Özdamar, T. H., 2002. Influence of pH Conditions on Metabolic Regulations in Serine Alkaline Protease Production, Enzyme and Microbial Technology, 31(5), 685–697.

Çalık, P., Bilir, E., Çalık, G., Özdamar, T.H., 2003a. Bioreactor Operation Parameters as Tools for Metabolic Regulations in Fermentation Processes: Influence of pH Conditions, Chemical Engineering Science, 58, 759-766.

Çalık, P., Tomlin, G., Oliver, S.G., Özdamar, T.H., 2003b. Overexpression of Serine Alkaline Protease in Bacillus licheniformis and its Impact on the Metabolic Reaction Network, Enzyme and Microbial Technology, 32(6), 706-720.

Çelik, E., 2003. Bioprocess Design Parameters for Beta-Lactamase Production by *Bacillus* Species, MS Thesis, METU, Ankara.

Çelik, E., Çalık, P., 2004. Bioprocess Parameters and Oxygen Transfer Characteristics in β-Lactamase Production by *Bacillus* Species, Biotechnology Progress, 20(2), 491-499.

Çalık, P., Tomlin, G., Oliver, S.G., and Özdamar, T.H., 2003. Overexpression of Serine Alkaline Protease in Bacillus licheniformis and its Impact on the Metabolic Reaction Network, Enzyme and Microbial Technology, 32(6), 706-720.

Cohen, A., 1983. The PICO TAG System: a New Method to Analyze Primary and Secondary Amino Acids with One Picomole Sensitivity, Biotechniques, Sept/Oct, 273-275.

Collins, J.R., 1979. The *Bacillus licheniformis* β-Lactamase System, In: Hamilton-Miller M.T. and Smith J.T. (ed.), Beta-Lactamases, Academic Press, Inc., (London), Ltd., London.

Doran, P.M., 1995. Bioprocess Engineering Principles, Academic Press Ltd., San Diego.

Faber, K., 2000. Biotransformations in Organic Chemistry, 4th ed., Springer, Germany.

Godfrey, T. and West, S.,1996. Industrial Enzymology, 2nd ed., Macmillan Press Ltd., London.

Hemila, H., Pokkinen, M., Palva, I., 1992. Improving the Production of *E. coli* Beta-Lactamase in *Bacillus subtilis* - The Effect of Glucose, Ph and Temperature on the Production Level, Journal of Biotechnology, 26, 245-256.

Jacobs, M., 1995. Expression of the Subtilisin Carlsberg-Encoding Gene in Bacillus *licheniformis* and Bacillus *subtilis*, Gene.; 152, 69-74.

Kuennen, R.W., Simone, M.J., Kreishman, G.P., 1980. The Temperature Dependence of the Production of Penicillinase in *Bacillus cereus* 569/H., Bioelectrochemistry and Bioenergetics, 7, 659-670.

Kushner, D.J. and Breuil, C., 1977. Archives of Microbiology, 112, 219-223.

Laskin, A.I. and Lechevalier, H.A., 1973. Handbok of Microbiology, volume 1, CRC Press, USA.

Ledent, P., Duez, C., Vanhove, M., Lejeune, A., Fonze,E., Charlier, P., Rhazi-Filali, F., Thamm,I., Guillaume,G., Samyn,B., Devreese,B., Van Beeumen, J., Lamotte-Brasseur, J., Frere, J.M., 1997. Unexpected Influence of a C-

Terminal-Fused His-tag on the Processing of an Enzyme and on the Kinetic and Folding Parameters, FEBS Lett, 413 (2), 194-196.

Lehninger, A.L., Nelson, D.L., Cox, M.M., 1993. Principles of Biochemistry, 2nd edition, Worth publishers Inc., New York.

Leisola, M., Jokela, J., Pastinen, O., Turunen, O., Schoemaker, H., 2001. Industrial Use of Enzymes in UNESCO Encyclopedia of Life Support Systems.

Matagne, A., Dubus A., Galleni M., Frère, J.M., 1999. The β-lactamase cycle: a tale of selective pressure and bacterial ingenuity, Nat. Prod. Rep., 16, 1–19.

Mehta, R.J. and Nash, C.H., 1978. Journal of Antibiotics, 31, 239-240.

Miller, G.L., 1959. Use of Dinitrosalicyclic Acid Reagent for Determination of Reduced Sugar, Analytical Chemistry, 31, 426-428.

Moses, V. and Cape, R.E., 1991. Biotechnology: The Science and The Business, Harwood Academic Publishers, Switzerland.

Moser, A., 1988. Bioprocess Technology, Springer-Verlag , New York.

Nielsen, J. and Villadsen, J., 1994. Bioreaction Engineering Principles, Plenum Press, New York.

Nielsen, J., Pedersen, H., Carlsen, M., 1999. Identification of Enzymes and Quantification of Metabolic Fluxes in the Wild Type and in a Recombinant *Aspergillus oryzae* Strain, Appl. Environ. Microbial, 65, 11-19.

Nielsen, J., Schmidt K, Norregaard, L.C., Pedersen, B., Meissner, A., Duus, J., Villadsen, J., 1999. Quantification of Intracellular Metabolic Fluxes from Fractional Enrichment and ^{13}C-^{13}C Coupling Constraints on the Isotopomer Distribution in Labeled Biomass Components, Metabolic Eng., 2, 166-179.

Pollock, M.R., 1957. Activity and Specificity of Inducers of Penicillinase Production in *Bacillus cereus*, Strain NRRL-569, Biochemical Journal, 66(3), 419-428.

Pollock, M.R., 1960. Penicillinase. In: Boyer P.D., Lardy H., Myrback K., The Enzymes, 2nd ed., Academic Press, New York.

Pollock M.R., 1965. Purification and Properties of Penicillinases from Two Strains of *Bacillus licheniformis*: a Chemical, Physicochemical and Physiological Comparison, Biochemical Journal, 94, 666-675.

Priest F.G., 1993. Sytematics and Ecology of *Bacillus*. In: Sonenshein, A.L., Hoch, J.A. and Losick, R. (eds.), *Bacillus subtilis* and Other Gram-Positive Bacteria: Biochemistry, Phsiology, and Molecular Genetics, American Society for Microbiology, Washington D.C.

Rainer, B.W., 1990. Determination Methods of the Volumetric Oxygen Transfer K_La in Bioreactors, Chem. Biochem. Eng. Q., 4(4), 185-186.

Rose, L. M., 1981. Mass Transfer in Gas Liquid Slurry Reactors, Chemical Reactor Design in Practice, Elsevier, Amsterdam.

Sargantanis, I.G. and Karim, M.N., 1996. Effect of Oxygen Limitation on Beta-lactamase Production, Biotechnology Progress, 12(6), 786-792.

Sargantanis, I.G. and Karim, M.N., 1998. Adaptive Pole Placement Control Algorithm for DO-Control in Beta-lactamase Production, Biotechnology and Bioengineering, 60(1), 1-9.

Sargent, M.G., Ghosh, B.K., Lampen, J.O., 1968. Characteristics of Penicillinase Release by Washed Cells of *Bacillus licheniformis*, Journal of Bacteriology, 96(4), 1231-1239.

Shuler, M.L. and Kargi, F., 1992. Bioprocess Engineering: Basic Concepts, Prentice Hall Inc., New Jersey.

Tang, X., Cai, T., Wang, P.G., 2003. Synthsis of Beta-Lactamses Activated Nitric Oxide Donors, Bioorganic and Medicinal Chemistry Letters, 13, 1687-1690.

Todar, K., 2000. Nutrition and Growth of Bacteria, University of Wisconins-Madison.

Wase, D.A.J., Patel, Y.R., 1987. Effects of Changes in Agitation Rate on Steady-State Penicillinase Titers in Continuously-Cultivated *Bacillus cereus*, Journal of Chemical Technology and Biotechnology, 38, 277-282.

White J.S. and White D.C., 1997. Source Book of Enzymes, CRC Press, New York.

APPENDIX A

Calibration of Bacillus *licheniformis* Concentration

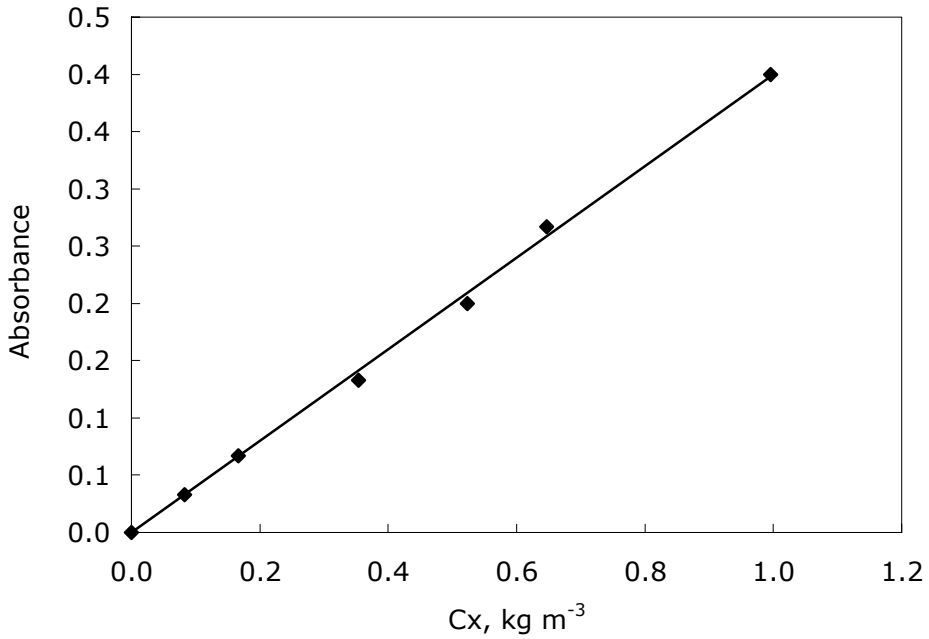

Figure A.1 Calibration curve for *Bacillus licheniformis* concentration

Slope of the calibration curve, m=2.49 1/kg m^{-3} (λ=600 nm)

$$Cx = \frac{Absorbance}{2.49} \times DilutionRatio$$

APPENDIX B

Calibration of Beta-Lactamase Activity

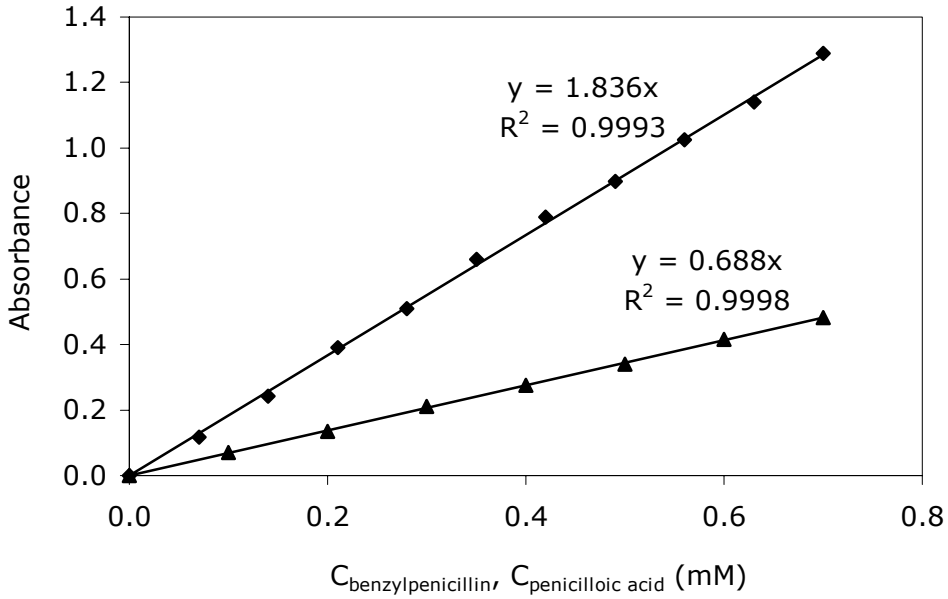

Figure A.2 Calibration Curve of the benzylpenicillin and penicilloic acid in 0.1 M phosphate buffer, pH=7.0, T=30°C, λ=232nm. Benzylpenicillin, (♦); Penicilloic acid, (▲).

One unit of β-lactamase activity was defined as the amount of enzyme that could hydrolyze 1μmol of benzylpenicillin at 30°C and pH 7.0 in one minute. The product of the hydrolysis reaction, penicilloic acid, also gives an absorbance at 232nm, therefore, the difference of the slopes is taken, m_1-m_2=1.148 mM^{-1}. The activity, U cm^{-3} is given by (Çelik, 2003),

$$A = \frac{C_{A0} m_1 - A_\lambda}{(m_1 - m_2) mM^{-1}} x \frac{1U}{10^{-3} mmol} x \frac{1l}{10^3 cm^3} x DilutionRatio$$

APPENDIX C

Calibration of Beta-Lactamase Concentration

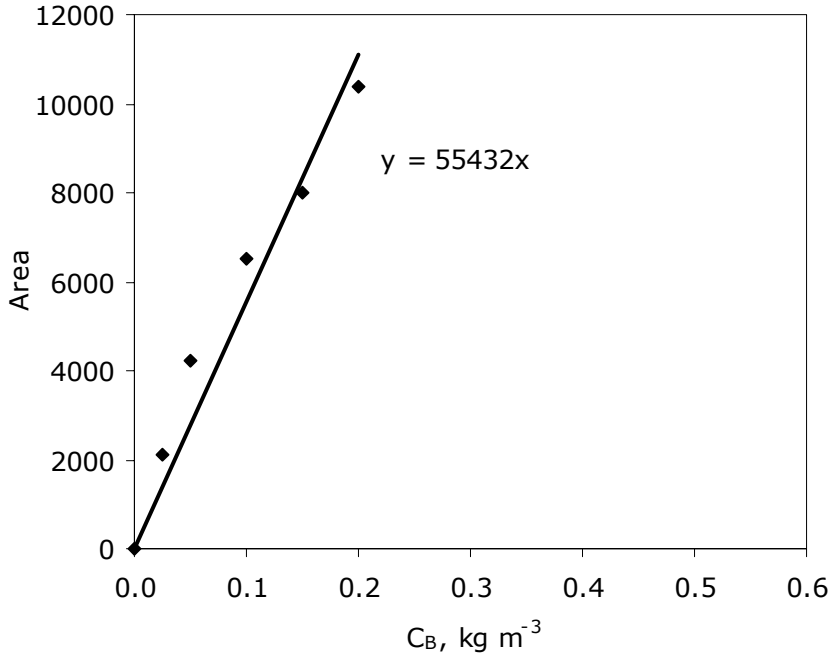

Figure C.1 Calibration curve for beta-lactamase concentration

$$C_B = \frac{Area}{55432} \times DilutionRatio$$

APPENDIX D

Calibration of Serine Alkaline Protease Concentration

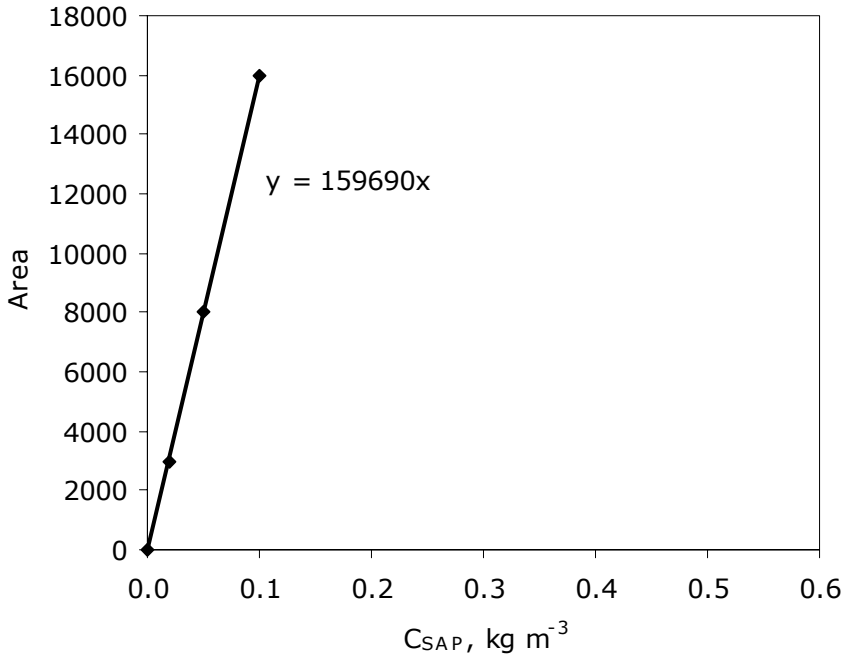

Figure D.1 Calibration curve for serine alkaline protease concentration

$$C_{SAP} = \frac{Area}{159690} \times DilutionRatio$$

APPENDIX E

Calibration of Reduced Sugar Concentration

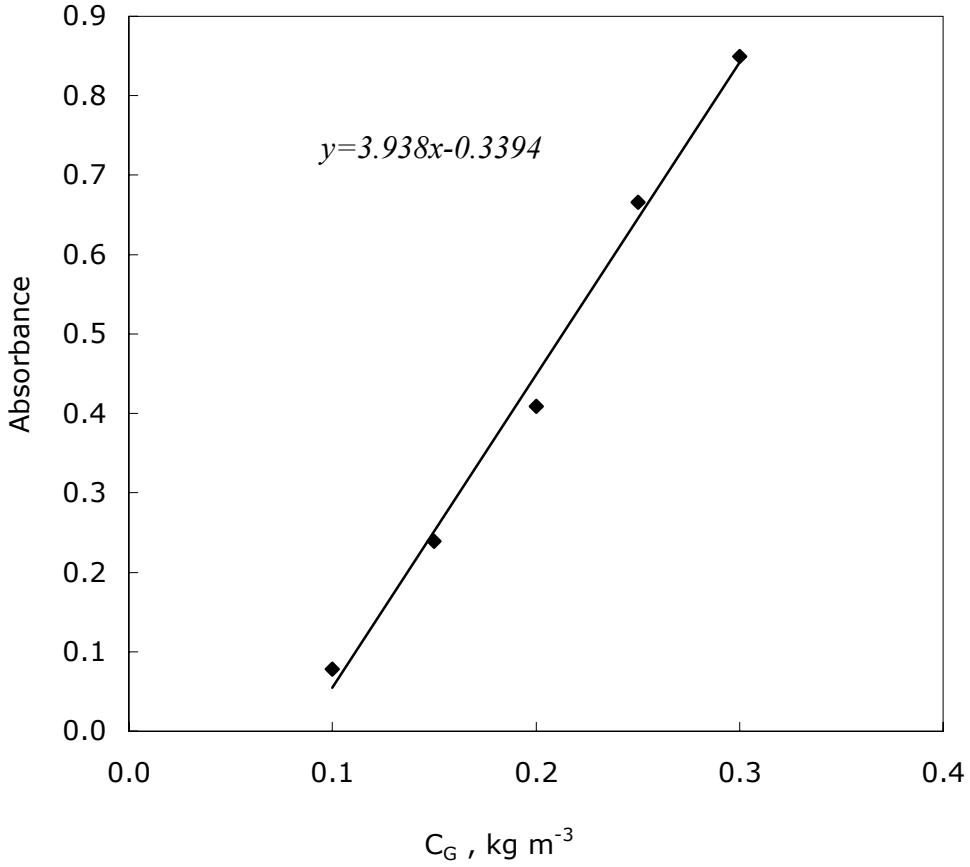

Figure E.3 Calibration Curve of the DNS solution

$$C_G = \left(\frac{Absorbance + 0.3394}{3.938} \right) \times DilutionRatio$$

APPENDIX F

Preparation of DNS Solution

1. a) 880 cm^3 of 1 % (m/v) DNS solution is prepared by dissolving 8.8 g dinitrosalisilyc acid in 880 cm^3 distilled water.

   b) After addition of 225 g ROCHELLE salt (sodium potassium tartarate), the solution is mixed.

   c) 300 cm^3 of 4.5 % NaOH, prepared by dissolving 13.5 g NaOH in 300 cm^3 distilled water, is added to this solution.

2. a) 22 cm^3 10 % NaOH, is prepared by dissolving 2.2 g NaOH in 22 cm^3 distilled water.

   b) 10 g christalized phenol and 100 cm^3 distilled water are added to the solution.

   c) 60 cm^3 is taken from this alkali-phenol mixture, 6.9 g $NaHCO_3$ is added and mixed.

The solution obtained from the first step is mixed with that from the second step and then they are stirred until ROCHELLE salt is dissolved. The prepared solution is kept in dark-colored bottle at 4°C and it should be used after 48 h.

APPENDIX G

Metabolic Reactions for Bacillus *licheniformis*

Glycolysis and Gluconeogenesis Pathway

1. Glc + PEP → G6P + Pyr
2. G6P → Glc + Pi
3. F6P → G6P
4. G6P → F6P
5. Frc + PEP → F6P + Pyr
6. Man + PEP → Man6P + Pyr
7. Man6P → F6P
8. F6P + ATP → 2T3P + ADP
9. 2T3P → F6P + Pi
10. T3P + ADP + Pi → PG3 + ATP + NADH
11. PG3 + ATP + NADH → T3P + ADP + Pi
12. PG3 → PEP
13. PEP → PG3
14. PEP + ADP → Pyr + ATP
15. Pyr + 2ATP → PEP + 2ADP
16. Pyr → AcCoA + CO_2 + NADH

Pentose Phosphate Pathway

17. G6P → Gluc6P + NADPH
18. Glc → Gluc + NADH
19. Gluc + ATP → Gluc6P + ADP
20. Gluc6P → R5P + CO_2 + NADPH
21. R5P → Xyl5P
22. Xyl5P → R5P
23. R5P → Rib5P
24. Rib5P → R5P
25. Xyl5P + Rib5P → S7P + T3P
26. S7P + T3P → Xyl5P + Rib5P
27. Xyl5P + E4P → F6P + T3P

28. F6P + T3P → Xyl5P + E4P
29. T3P + S7P → F6P + E4P
30. F6P + E4P → T3P + S7P

Branches from Glycolysis

31. Pyr + NADH → Lac
32. Lac → Pyr + NADH
33. AcCoA + ADP + Pi → Ac + ATP
34. Ac + ATP → AcCoA + ADP + Pi

Anapleoric Reactions

35. Mal → Pyr + CO_2 + NADPH
36. OA → Pyr + CO_2

TCA Cycle

37. AcCoA + OA → Cit
38. Cit → ICit
39. ICit → αKG + CO_2 + NADPH
40. αKG → SucCoA + CO_2 + NADH
41. SucCoA + Pi + ADP → Suc + ATP + CoA
42. Suc + ATP → SucCoA + ADP + Pi
43. Suc → Fum + $FADH_2$
44. Fum → Mal
45. Mal → OA + NADH
46. ICit → Glx + Suc
47. Glx + AcCoA → Mal

Biosynthesis of Serine Family Amino Acids

48. PG3 + Glu → Ser + αKG + NADH + Pi
49. Ser + THF → Gly + MetTHF
50. Ser + AcCoA + H_2S → Cys + Ac

Biosynthesis of Alanine Family Amino Acids

51. Pyr + Glu → Ala + αKG
52. 2Pyr + NADPH → KVal
53. KVal + Glu → Val + αKG
54. KVal + AcCoA + Glu → Leu + αKG + NADH + CO_2

Biosynthesis of Histidine

55. R5P + ATP → PRPP + AMP
56. PRPP + ATP + Gln → His + PRAIC + αKG + 2PPi + 2NADH + Pi

Biosynthesis of Aspartic Acid Family Amino Acids

57. OA + Glu → Asp + αKG
58. Asp + Gln + ATP → Asn + Glu + AMP + PPi
59. Asp + ATP + NADPH → AspSa + ADP + Pi
60. AspSa + Pyr → DC
61. DC + NADPH → Tet
62. Tet + AcCoA + Glu → Ac + αKG + mDAP
63. mDAP → Lys + CO_2
64. AspSa + NADPH → HSer
65. HSer + ATP → Thr + ADP + Pi
66. Thr + Pyr + NADPH + Glu → Ile + αKG + NH_3 + CO_2
67. AcCoA + Cys + HSer + H_2S + MTHF → Met + Pyr + 2Ac + NH_3 + THF

Biosynthesis of Aromatic Amino Acids

68. 2PEP + E4P + ATP + NADPH → Chor + ADP + 4Pi
69. Chor + Glu → Phe + αKG + CO_2
70. Chor + Glu → Tyr + αKG + NADH + CO_2
71. Chor + NH3 + PRPP → Pyr + IGP + CO_2 + PPi
72. IGP + Ser → Trp + T3P

Biosynthesis of Glutamic Acid Family Amino Acids

73. αKG + NH3 + NADPH → Glu
74. Glu + ATP + NH3 → Gln + ADP + Pi
75. Glu + ATP + 2 NADPH → Pro + ADP + Pi
76. 2Glu + AcCoA + ATP + NADPH → Orn + αKG + Ac + ADP + Pi
77. Orn + CaP → Citr + Pi
78. Citr + Asp + ATP → Arg + Fum + AMP + PPi

Catabolism of the amino acids

79. αKG + Ala → Pyr + Glu
80. Arg + αKG → 2Glu + NH_3 + NADPH + CO_2
81. Asn → Asp + NH_3
82. Asp → Fum + NH_3

83. Cys $\rightarrow$ Pyr + NH_3 + H_2S
84. Gln + αKG + NADPH $\rightarrow$ 2Glu
85. Gly + MetTHF $\rightarrow$ Ser + THF
86. His + THF $\rightarrow$ Glu + MeTHF
87. Ile + αKG $\rightarrow$ Glu + $FADH_2$ + 2NADH + CO_2 + SucCoA + AcCoA
88. Leu + αKG + ATP $\rightarrow$ Glu + $FADH_2$ + NADH + 2AcCoA + ADP + Pi
89. Phe $\rightarrow$ Tyr + NADPH
90. Pro $\rightarrow$ Glu + NADPH
91. Ser $\rightarrow$ Pyr + NH_3
92. Thr $\rightarrow$ Gly + NADH + AcCoA
93. Trp + NADPH $\rightarrow$ AcCoA + Ala
94. Tyr + αKG + SucCoA $\rightarrow$ Glu + Fum + AcCoA + Succ + CO_2
95. Val + αKG $\rightarrow$ Glu + $FADH_2$ + 3NADH + $2CO_2$ + SucCoA

Biosynthesis of Nucleotides

96. PRPP + 2Gln + Asp + $2H_2O$ + CO_2 + Gly + 4ATP + F10THF $\rightarrow$ 2Glu + PPi + 4ADP + 4Pi + THF + PRAIC + Fum
97. PRAIC + F10THF $\rightarrow$ IMP + THF
98. IMP + Gln + ATP $\rightarrow$ NADH + GMP + Glu + AMP + PPi
99. GMP + ATP $\rightarrow$ GDP + ADP
100. ATP + GDP $\rightarrow$ ADP + GTP
101. GTP + ADP $\rightarrow$ ATP + GDP
102. NADPH + ATP $\rightarrow$ dATP
103. NADPH + GDP + ATP $\rightarrow$ ADP + dGTP
104. IMP + GTP + Asp $\rightarrow$ GDP + Pi + Fum + AMP
105. AMP + ATP $\rightarrow$ 2ADP
106. PRPP + Asp + CaP $\rightarrow$ UMP + NADH + PPi + Pi + CO_2
107. UMP + ATP $\rightarrow$ UDP + ADP
108. UDP + ATP $\rightarrow$ ADP + UTP
109. UTP + NH_3 + ATP $\rightarrow$ CTP + ADP + Pi
110. ATP + NADPH + CDP $\rightarrow$ dCTP + ADP
111. CDP + ATP $\rightarrow$ CTP + ADP
112. CTP + ADP $\rightarrow$ CDP + ATP
113. UDP + MetTHF + 2ATP + NADPH $\rightarrow$ dTTP + DHF + 2ADP + PPi

Biosynthesis and interconversion of one-carbon units

114. DHF + NADPH $\rightarrow$ THF

115. MetTHF + CO_2 + NH_3 + NADH → Gly + THF
116. MetTHF + NADPH → MTHF
117. MetTHF → MeTHF + NADPH
118. MeTHF → F10THF
119. Gly + THF → MetTHF + NH_3 + NADH + CO_2

Transhydrogenation reaction

120. NADH → NADPH
121. NADPH → NADH

Electron Transprt System (P/O=2)

122. NADH + 2ADP + 2Pi → 2ATP
123. $FADH_2$ + ADP + Pi → ATP

Transport Reactions

124. CO_2 → exp
125. imp → CO_2
126. imp → NH_3
127. NH_3 → exp
128. 2ATP + 4 NADPH → AMP + ADP + H_2S + PPi + Pi
129. PPi → 2Pi
130. imp → Pi
131. Pi → exp

Biosynthesis of Fatty Acids

132. T3P + NADPH → GL3P
133. 7AcCoA + 6ATP + 12NADPH → C14:0 + 6ADP + 6Pi
134. 7AcCoA + 6ATP + 11NADPH → C14:1 + 6ADP + 6Pi
135. 8.2AcCoA + 7.2ATP + 14 NADPH → 7.2PI + 7.2ADP + PA
136. 2ATP + CO_2 + Gln → CaP + Glu + 2ADP + Pi

Other Biomass Components

137. F6P + Gln + AcCoA + UTP → UDPNAG + Glu + Ppi
138. PEP + NADPH + UGPNAG → UDPNAM + Pi
139. R5P + PEP + CTP → CMPKDO + PPi + 2Pi
140. Ser + CTP + ATP → CDPEtN + ADP + PPi + CO_2
141. S7P + ATP → ADPHep + PPi
142. G6P → G1P

143. G1P → G6P

144. UTP + G1P → UDPGlc + PPi

Biomass Synthesis

145. 0.5352Ala + 0.28Arg + 0.22Asn + 0.22Asp + 0.09Cys + 0.09His + 0.25Gln + 0.25Glu + 0.58Gly + 0.27Ile + 0.42Leu + 0.32Lys + 0.14Met + 0.0593Orn + 0.17Phe + 0.2Pro + 0.377Ser + 0.05Trp + 0.13Tyr + 0.24Thr + 0.4Val + 0.2GTP + 0.13UTP + 0.12CTP + 0.22DATP + 0.02DCTP + 0.02DGTP + 0.02DTTP + 0.129GL3P + 0.0235C140 + 0.0235C141 + 0.259PA + 0.0433UDPNAG + 0.0276UDPNAM + 0.0235CMPKDO + 0.0235CDPETN + 0.0157UDPGLC + 0.02354ADPHEP + 0.154G1P + 41.139ATP → Biomass + 41.139ADP + 41.139Pi

Serine Alkaline Protease Synthesis

146. (0.145Ala + 0.0146Arg + 0.0657Asn + 0.0328Asp + 0.0255Gln + 0.0182Glu + 0.127Gly + 0.0182His + 0.0365Ile + 0.0584Leu + 0.0328Lys + 0.0182Met + 0.0146Phe + 0.0365Pro + 0.116Ser + 0.0729Thr + 0.0036Trp + 0.0474Tyr + 0.113Val) x 274 + 5.5ATP → SAP + 5.5ADP + 5.5Pi

Maintenance

147. ATP → ADP + Pi

148. Pyr + CO_2 → OA

β-Lactamase Synthesis

149. 24Ala + 14Arg + 13Asn + 23Asp + 8Gln + 21Glu + 16Gly + 1His + 14Ile + 27Leu + 24Lys + 4Met + 7Phe + 11Pro + 11Ser + 23Thr + 3Trp + 6Tyr + 15Val + 5.5ATP → β-lactamase + 5.5ADP + 5.5Pi